Simulation of Localized Surface Plasmon Resonances via DNOs and IIOs

by

Xin Tong
B.A. (Central Unicersity of Finance and Economics) 2011
M.S. (Illinois Institute of Technology) 2014

THESIS

Submitted in partial fulfillment of the requirements
for the degree of Doctor of Philosophy in Mathematics
in the Graduate College of the
University of Illinois at Chicago, 2020

Chicago, Illinois

Defense Committee:
Prof. David P. Nicholls, Chair and Advisor
Prof. Jerry Bona
Prof. Gerard Awanou
Prof. Mimi Dai
Prof. Fred Hickernell, Illinois Institute of Technology

To myself,

ACKNOWLEDGMENTS

TABLE OF CONTENTS

LIST OF FIGURES

SUMMARY

This thesis focuses on simulating scattering returns of electromagnetic radiation from bounded obstacles and the Localized Surface Plasmon Resonances. We present High–Order Perturbation of Surfaces algorithms for the simulation of such configurations, formulated with Dirichlet–Neumann Operators and Impedance–Impedance Operators. With an implementation of these approaches we demonstrate the stable, robust, and highly accurate properties of our algorithms. We also demonstrate the validity and utility of our approaches with a sequence of numerical experiments. Moreover, we show how our formulation delivers a straightforward proof of existence, uniqueness, and analyticity of solutions.

CONTRIBUTIONS OF AUTHORS

The boundary formulation via Dirichlet–Neumann Operator, and its related algorithms and numerical experiments, were previously published as D. P. Nicholls and X. Tong, "High-Order Perturbation of Surfaces Algorithms for the Simulation of Localized Surface Plasmon Resonances in Two Dimensions," Journal of Scientific Computing, Volume 76, Issue 3, 1370-1395, 2018.

Under the supervision and guidance of Professor David Nicholls, Xin Tong carried out most of the research and numerical simulations presented in this thesis.

CHAPTER 1

INTRODUCTION

Simulating scattering returns of electromagnetic radiation from bounded obstacles is important to scientists and engineers. In the field of plasmonics (1; 2; 3; 4) such crucial applications as surface enhanced Raman scattering biosensing (5), imaging (6), and cancer therapy (7) are important examples. Due to the very strong plasmonic effect (the field enhancement can be several orders of magnitude) and its quite sensitive nature (the enhancement is only seen over a range of tens of nanometers in incident radiation for gold and silver particles), such simulations must be very robust and of high accuracy for many applications of interest.

In this thesis we focus upon the Localized Surface Plasmon Resonances (LSPRs), which can be induced in gold and silver nanorods with visible light, and how they change as the shapes of these rods are varied analytically away from perfectly cylindrical.

All of the classical numerical algorithms have been utilized for the simulation of this problem, for instance, Finite Difference Methods (8; 9), Finite Element Methods (10; 11), Discontinous Galerkin Methods (12), Spectral Element Methods (13), and Spectral Methods (14; 15; 16), but it can be argued (17; 18) that such volumetric approaches are greatly disadvantaged with an unnecessarily large number of unknowns for these piecewise homogeneous problems. Interfacial methods based upon Integral Equations (19) are a natural alternative, but these also face difficulties. One challenge is that an Integral Equation solver will return the scattering returns only for a specified geometric set-up. For instance, if this shape is changed then the solver must

1

be run again. Another difficulty is the dense and non-symmetric positive definite systems of linear equations which must be inverted with each simulation.

A "High Order Perturbation of Surfaces" (HOPS) approach (17; 18) can effectively address these concerns. More specifically, we consider the Method of Field Expansions (FE), which was introduced to calculate the solution to low-order by Rayleigh (20) and Rice (21). The high-order version of FE was first investigated by Bruno and Reitich (22; 23; 24; 25) and later enhanced and stabilized by the Nicholls and Reitich (26; 27), resulting in the Method of Transformed Field Expansions (TFE). These formulations maintain the advantageous properties of classical Integral Equation formulations (e.g., surface formulation and exact enforcement of far–field conditions) while avoiding the shortcomings stated above. For a description of the TFE approach to the bounded obstacle geometry see (28).

Our new approach is quite closely related to the work of Bruno and Reitich (25) who studied the same problem in the three–dimensional context of nanospheres. The current contribution differs in a number of ways beginning with its two–dimensional character which requires the study of different Hankel functions. In addition we utilize a formulation in terms of either Dirichlet–Neumann Operators (DNOs) first described in (29) or Impedance–Impedance Operators (IIOs), which permits the immediate simulation by other classical HOPS methods, (22; 23; 24; 25) or the stabilized TFE approach (27; 28; 30). The IIO formulation is considered to avoid the "Dirichlet eigenvalues" as advocated by Gillman, Barnett, and Martinsson (31).

The rest of this thesis is organized as follows: in Chapter 1 we present the governing equations with transparent boundary conditions, in Chapter 2 we give two boundary formulations

then present our HOPS algorithms, in Chapter 3 we prove the analyticity of Solutions in terms

of IIOs, in Chapter 4 we discuss numerical results and LSPR simulations. We end with con-

cluding remarks in Chapter 5.

1.1 <u>Governing Equations</u>

We consider a y–invariant obstacle of bounded cross–section as displayed in Figure 1. In this

thesis, we assume a dielectric material of refractive index n^u (e.g., air or water) occupies the

unbounded exterior, and a metal of refractive index n^w (e.g., gold or silver) fills the bounded

interior; however, our formulation can accommodate arbitrary materials in either domain. The

interface between these two domains is described in polar coordinates, $\{x = r\cos(\theta), z = r\sin(\theta)\}$, by the graph $r = \bar{g} + g(\theta)$ so that the exterior domain is specified by

$$S^u := \{r > \bar{g} + g(\theta)\},$$

while the interior domain is given by

$$S^w := \{r < \bar{g} + g(\theta)\}.$$

The superscripts are chosen to conform to the notation of previous work (18; 29; 32). Ob-

viously, the cylindrical geometry demands that the interface be 2π–periodic, $g(\theta + 2\pi) = g(\theta)$.

The structure is illuminated by monochromatic plane-wave incident radiation of frequency ω
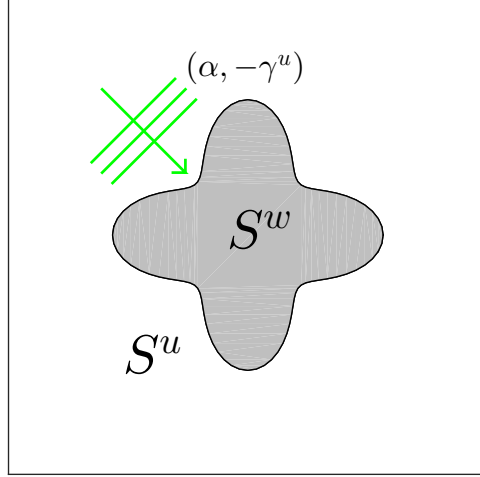
Figure 1. Plot of the cross–section of a metallic nanorod (occupying S^w) shaped by

$r = \bar{g} + \varepsilon \cos(4\theta)$ ($\varepsilon = \bar{g}/5$) housed in a dielectric (occupying S^u) under plane–wave

illumination with wavenumber $(\alpha, -\gamma^u)$.

and wavenumber $k^u = n^u \omega/c_0 = \omega/c^u$ (c_0 is the speed of light), aligned with the corrugations

of the obstacle. We consider the reduced incident fields of incidence angle ϕ, and

$$\mathbf{E}^{\mathrm{inc}} = \mathbf{A}e^{i\alpha x - i\gamma^u z} = \mathbf{A}e^{ir(\alpha \cos(\theta) - i\gamma^u \sin(\theta))},$$

$$\mathbf{H}^{\mathrm{inc}}(x, z) = \mathbf{B}e^{i\alpha x - i\gamma^u z} = \mathbf{B}e^{ir(\alpha \cos(\theta) - i\gamma^u \sin(\theta))},$$

$$\alpha = k^u \sin(\phi), \quad \gamma^u = k^u \cos(\phi),$$

where time dependence of the form $\exp(-i\omega t)$ has been factored out. The geometry demands that the reduced electric and magnetic fields, $\{\mathbf{E}, \mathbf{H}\}$, be 2π–periodic in θ. To close the problem, we specify that the scattered radiation is "outgoing" in S^u and bounded in S^w.

It is well–known (see, e.g., (33)) that in this two–dimensional setting, the time–harmonic Maxwell equations decouple into two scalar Helmholtz problems which govern the transverse electric (TE) and transverse magnetic (TM) polarizations. We define the invariant (y) directions of the scattered (electric or magnetic) fields by $\{u(r, \theta), w(r, \theta)\}$ in S^u and S^w, respectively, and the incident radiation in the outer domain by $u^{\text{inc}}(r, \theta)$.

All of these developments lead us to seek outgoing/bounded, 2π–periodic solutions of

$$\Delta u + (k^u)^2 u = 0, \qquad\qquad r > \bar{g} + g(\theta), \qquad\qquad (1.1a)$$

$$\Delta w + (k^w)^2 w = 0, \qquad\qquad r < \bar{g} + g(\theta), \qquad\qquad (1.1b)$$

$$u - w = \zeta, \qquad\qquad r = \bar{g} + g(\theta), \qquad\qquad (1.1c)$$

$$\partial_N u - \tau^2 \partial_N w = \psi, \qquad\qquad r = \bar{g} + g(\theta), \qquad\qquad (1.1d)$$

where the Dirichlet and Neumann data are

$$\zeta(\theta) := \left[-u^{\text{inc}}\right]_{r=\bar{g}+g(\theta)} = -e^{ik^u(\bar{g}+g(\theta))\sin(\phi-\theta)}, \qquad\qquad (1.1e)$$

$$\psi(\theta) := \left[-\partial_N u^{\text{inc}}\right]_{r=\bar{g}+g(\theta)} = \left\{(\bar{g} + g(\theta))ik^u \sin(\phi - \theta) + \left(\frac{g'(\theta)}{\bar{g} + g(\theta)}\right) \cos(\phi - \theta)\right\} \xi(\theta). \quad (1.1f)$$

In these

$$\partial_N = \hat{r}(\bar{g} + g)\partial_r - \hat{\theta}\left(\frac{g'}{\bar{g} + g}\right)\partial_\theta,$$

for unit vectors in the radial ($\hat{r}$) and angular ($\hat{\theta}$) directions, and

$$\tau^2 = \begin{cases} 1, & \text{TE}, \\ \\ (k^u/k^w)^2 = (n^u/n^w)^2, & \text{TM}, \end{cases}$$

where $\gamma^w = k^w \cos(\phi)$. The case of TM polarization is of extraordinary importance in the study of SPRs (1) and thus we concentrate our attention on the TM case from here.

1.2 Transparent Boundary Conditions

Regarding the Outgoing Wave Condition (OWC), commonly known as the Sommerfeld Radiation Condition (19), and Boundedness Boundary Condition (BBC), we introduce the circles $\{r = R^o\}$ and $\{r = R_i\}$, where

$$R^o > \bar{g} + |g|_{L^\infty}, \quad 0 < R_i < \bar{g} - |g|_{L^\infty},$$

define the domains

$$S^o := \{r > R^o\}, \quad S_i := \{r < R_i\}.$$
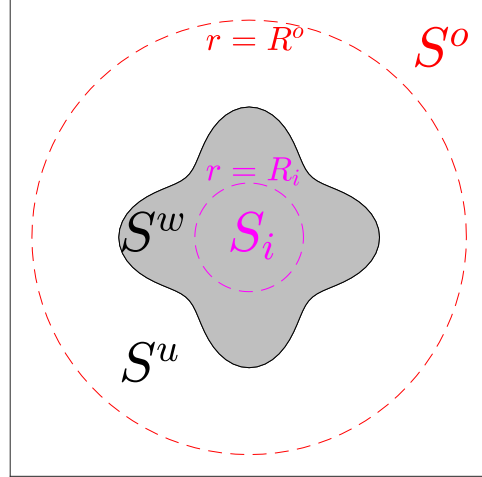
Figure 2. Plot of the domain with artificial boundaries

Note that we can find periodic solutions of the relevant Helmholtz problems on these domains given generic Dirichlet data, say $\underline{u}(\theta)$ and $\underline{w}(\theta)$. For this we use the exact solutions (19)

$$u(r,\theta) = \sum_{p=-\infty}^{\infty} \hat{\underline{u}}_p \frac{H_p(k^u r)}{H_p(k^u R^o)} e^{ip\theta}, \quad w(r,\theta) = \sum_{p=-\infty}^{\infty} \hat{\underline{w}}_p \frac{J_p(k^w r)}{J_p(k^w R_i)} e^{ip\theta}, \tag{1.2}$$

where, J_p is the p–th Bessel function and H_p is the p–th Hankel function of the first kind. We note that

$$u(R^o,\theta) = \sum_{p=-\infty}^{\infty} \hat{\underline{u}}_p e^{ip\theta}, \quad w(R_i,\theta) = \sum_{p=-\infty}^{\infty} \hat{\underline{w}}_p e^{ip\theta}.$$

With these formulas we can compute the *outward–pointing* Neumann data at the artificial boundaries

$$-\partial_r u(R^o, \theta) = \sum_{p=-\infty}^{\infty} -k^u \hat{\xi}_p \frac{H_p'(k^u R^o)}{H_p(k^u R^o)} e^{ip\theta} =: T^{(u)} \left[\underline{u}(\theta)\right],$$

$$\partial_r w(R_i, \theta) = \sum_{p=-\infty}^{\infty} k^w \hat{\mu}_p \frac{J_p'(k^w R_i)}{J_p(k^w R_i)} e^{ip\theta} =: T^{(w)} \left[\underline{w}(\theta)\right].$$

These define the order–one Fourier multipliers $\{T^{(u)}, T^{(w)}\}$.

With the operator $T^{(u)}$ it is not difficult to see that periodic, outward propagating solutions to the Helmholtz equation

$$\Delta u + (k^u)^2\, u = 0, \quad r > \bar{g} + g(\theta),$$

equivalently solve

$$\Delta u + (k^u)^2\, u = 0, \qquad\qquad \bar{g} + g(\theta) < r < R^o, \qquad\qquad (1.3a)$$

$$\partial_r u + T_u\left[u\right] = 0, \qquad\qquad r = R^o. \qquad\qquad (1.3b)$$

Similarly, one can show that periodic, bounded solutions to the Helmholtz equation

$$\Delta w + (k^w)^2\, w = 0, \quad r < \bar{g} + g(\theta),$$

equivalently solve

$$\Delta w + (k^w)^2 \, w = 0, \qquad\qquad R_i < r < \bar{g} + g(\theta), \qquad\qquad (1.4\text{a})$$

$$\partial_r w - T^{(w)} \, [w] = 0, \qquad\qquad r = R_i. \qquad\qquad (1.4\text{b})$$

Now solving (Equation 1.1) is equivalent to seek outgoing/bounded, 2π–periodic solutions of

$$\Delta u + (k^u)^2 u = 0, \qquad\qquad \bar{g} + g(\theta) < r < R^o, \qquad\qquad (1.5\text{a})$$

$$\Delta w + (k^w)^2 w = 0, \qquad\qquad R_i < r < \bar{g} + g(\theta), \qquad\qquad (1.5\text{b})$$

$$u - w = \zeta, \qquad\qquad r = \bar{g} + g(\theta), \qquad\qquad (1.5\text{c})$$

$$\partial_{\mathbf{N}} u - \tau^2 \partial_{\mathbf{N}} w = \psi, \qquad\qquad r = \bar{g} + g(\theta), \qquad\qquad (1.5\text{d})$$

$$\partial_r u + T^{(u)} \, [u] = 0, \qquad\qquad r = R^o, \qquad\qquad (1.5\text{e})$$

$$\partial_r w - T^{(w)} \, [w] = 0, \qquad\qquad r = R_i. \qquad\qquad (1.5\text{f})$$

We will apply a Non–Overlapping Domain Decomposition Method (34; 35). That is the domain $\{R_i < r < R^o\}$ consists of an exterior domain, $\{\bar{g} + g(\theta) < r < R^o\}$, and an interior domain, $\{R_i < r < \bar{g} + g(\theta)\}$. Next, the boundary conditions at the interface, (Equation 1.5c) and (Equation 1.5d), should be specified for each domain.

1.3   Boundary Formulations

We follow (29; 36; 37) to reduce the degrees of freedom to the surface unknowns. Define the (outer and inner) Dirichlet traces

$$U(\theta) := u(\bar{g} + g(\theta), \theta), \quad W(\theta) := w(\bar{g} + g(\theta), \theta),$$

and their exterior (outer and inner) Neumann counterparts

$$\tilde{U}(\theta) := -(\partial_N u)(\bar{g} + g(\theta), \theta), \quad \tilde{W}(\theta) := (\partial_N w)(\bar{g} + g(\theta), \theta).$$

From these we could recover the scattered field at any point with a suitable integral formula (38). Then, the governing equations reduce to the boundary conditions

$$U - W = \zeta, \quad -\tilde{U} - \tau^2 \tilde{W} = \psi. \tag{1.6}$$

Now we have two equations for four unknowns, however, the pairs $\{U, \tilde{U}\}$ and $\{W, \tilde{W}\}$ are clearly related, and we make this clear through the Dirichlet–Neumann operators (DNOs). For this we make the following definitions.

Definition 1.3.1 (Exterior Problem via DNO)**.** Given a sufficiently smooth deformation $g(\theta)$, the unique periodic solution of

$$\Delta u + (k^u)^2 \, u = 0, \qquad\qquad \bar{g} + g(\theta) < r < R^o, \qquad\qquad (1.7a)$$

$$u = U, \qquad\qquad r = \bar{g} + g(\theta), \qquad\qquad (1.7b)$$

$$\partial_r u + T^{(u)} \, [u] = 0, \qquad\qquad r = R^o, \qquad\qquad (1.7c)$$

defines the Dirichlet–Neumann Operator

$$G^{(u)} \, [U] = G^{(u)}(R^o, \bar{g}, g) \, [U] := \tilde{U}. \qquad\qquad (1.7d)$$

An analogous definition can be made on the interior domain, $\{R_i < r < \bar{g} + g(\theta)\}$, however, care is required. It is well known (19) that the governing Helmholtz equation, (Equation 1.1b), is not uniquely solvable at a "Dirichlet eigenvalue". For example, in the case $g \equiv 0$ the exact solution is given by (Equation 1.2) with R_i replaced by $\bar{g}$. It is easy to see that one will not be able to uniquely solve the Dirichlet problem when $J_p(k^w \bar{g}) = 0$ for *any* $p \in \mathbf{Z}$. Such configurations, and their generalizations to $g \not\equiv 0$, are the Dirichlet eigenvalues we must avoid. By contrast, the exterior problem has no such obstruction and can always be shown to be uniquely solvable (19).

Definition 1.3.2 (Interior Problem via DNO). Given a sufficiently smooth deformation $g(\theta)$, if we are not at a Dirichlet eigenvalue of the Laplacian on $\{r < \bar{g} + g(\theta)\}$, the unique periodic solution of

$$\Delta w + (k^w)^2 \, w = 0, \qquad\qquad R_i < r < \bar{g} + g(\theta), \qquad\qquad (1.8a)$$

$$w = W, \qquad\qquad r = \bar{g} + g(\theta), \qquad\qquad (1.8b)$$

$$\partial_r w - T^{(w)}\,[w] = 0, \qquad\qquad r = R_i, \qquad\qquad (1.8c)$$

defines the Dirichlet–Neumann Operator

$$G^{(w)}\,[W] = G^{(w)}(R_i, \bar{g}, g)\,[W] := \tilde{W}. \qquad\qquad (1.8d)$$

In terms of these operators the boundary conditions, (Equation 1.6), become

$$U - W = \zeta, \quad -G^{(u)}[U] - \tau^2 G^{(w)}[W] = \psi.$$

The first of these can be used to eliminate W,

$$W = U - \zeta,$$

so that the latter equation becomes

$$-G^{(u)}[U] - \tau^2 G^{(w)}[U - \zeta] = \psi,$$

or

$$(G^{(u)} + \tau^2 G^{(w)})U = -\psi + \tau^2 G^{(w)}[\zeta]. \tag{1.9}$$

Next, we introduce the "Impedance–Impedance Operators (IIOs)" as advocated by Gillman,

Barnett, and Martinsson (31) which can be constructed to avoid the "Dirichlet eigenvalues" on

a given domain. For convenience, we rewrite (Equation 1.1d)

$$\tau^u \partial_N u - \tau^w \partial_N w = \tau^u \psi, \tag{1.10}$$

where

$$\tau^m = \begin{cases} 1, & \text{TE}, \\ 1/\epsilon^{(m)}, & \text{TM}, \end{cases}, \quad m \in \{u, w\}.$$

To motivate our particular choices we focus upon the boundary conditions (Equation 1.1c)

and (Equation 1.1d) and operate upon this pair by the linear operator

$$P = \begin{pmatrix} Y & -I \\ Z & -I \end{pmatrix},$$

where I is the identity, and Y and Z are unequal operators to be specified. In the work of Despres (39; 40) these were chosen to be $\pm i\eta$ for a constant $\eta \in \mathbf{R}^+$, however, other choices are also possible. The resulting boundary conditions are

$$[-\tau^u \partial_N u + Yu] + [\tau^w \partial_N w - Yw] = [-\tau^u \psi + Y\zeta] \,, \tag{1.11a}$$

$$[-\tau^u \partial_N u + Zu] + [\tau^w \partial_N w - Zw] = [-\tau^u \psi + Z\zeta] \,, \tag{1.11b}$$

which inspire the following definitions for impedances

$$I^{(u)} := [-\tau^u \partial_N u + Yu]_{r=\bar{g}+g} \,, \quad I^{(w)} := [\tau^w \partial_N w - Zw]_{r=\bar{g}+g} \,,$$

their "conjugates"

$$\tilde{I}^{(u)} := [-\tau^u \partial_N u + Zu]_{r=\bar{g}+g} \,, \quad \tilde{I}^{(w)} := [\tau^w \partial_N w - Yw]_{r=\bar{g}+g} \,,$$

and the interfacial data

$$\xi := [-\tau^u \psi + Y\zeta] \,, \quad \nu := [-\tau^u \psi + Z\zeta] \,. \tag{1.12}$$

Through an integral formula these quantities can deliver the scattered field at *any* point (38; 41), thus, the governing equations reduce to the boundary conditions

$$I^{(u)} + \tilde{I}^{(w)} = \xi \,, \quad \tilde{I}^{(u)} + I^{(w)} = \nu \,. \tag{1.13}$$

Again, we have two equations for four unknowns, however, the pairs $\{I^{(u)}, \tilde{I}^{(u)}\}$ and $\{I^{(w)}, \tilde{I}^{(w)}\}$ are not independent and we make this explicit through the introduction of IIOs.

Definition 1.3.3 (Exterior Problem via IIO). Given a sufficiently smooth deformation $g(\theta)$, the unique periodic solution of

$$\Delta u + (k^u)^2\, u = 0, \qquad\qquad \bar{g} + g(\theta) < r < R^o, \qquad (1.14a)$$

$$-\tau^u \partial_N u + Y u = I^{(u)}, \qquad\qquad r = \bar{g} + g(\theta), \qquad (1.14b)$$

$$\partial_r u + T^{(u)}\,[u] = 0, \qquad\qquad r = R^o, \qquad (1.14c)$$

defines the Impedance–Impedance Operator

$$Q\left[I^{(u)}\right] = Q(R^o, \bar{g}, g)\left[I^{(u)}\right] := \tilde{I}^{(u)}. \qquad (1.14d)$$

A similar definition will presently be made on the interior domain, $\{R_i < r < \bar{g} + g(\theta)\}$, however, care is required. It is still an open question whether the Helmholtz equation, (Equation 1.1b), subject to impedance boundary conditions is uniquely solvable. Obviously we avoid these configurations and make an attempt in Appendix B to describe conditions on $\{\epsilon^{(w)}, R_i, \bar{g}, Z\}$ for which a unique solution exists. By contrast, the exterior problem for a dielectric (so that $\epsilon^{(u)} \in \mathbf{R}$) has no such obstruction and can always be shown to be uniquely solvable (41).

Definition 1.3.4 (Interior Problem via IIO)**.** Given a sufficiently smooth deformation $g(\theta)$, if it exists, the unique periodic solution of

$$\Delta w + (k^w)^2\, w = 0, \qquad\qquad R_i < r < \bar{g} + g(\theta), \qquad\qquad (1.15\text{a})$$

$$\tau^w \partial_N w - Zw = I^{(w)}, \qquad\qquad r = \bar{g} + g(\theta), \qquad\qquad (1.15\text{b})$$

$$\partial_r w - T^{(w)}\,[w] = 0, \qquad\qquad r = R_i, \qquad\qquad (1.15\text{c})$$

defines the Impedance–Impedance Operator

$$S\left[I^{(w)}\right] = S(R_i, \bar{g}, g)\left[I^{(w)}\right] := \tilde{I}^{(w)}. \qquad\qquad (1.15\text{d})$$

In terms of these operators the boundary conditions, (Equation 1.13), become

$$I^{(u)} + S[I^{(w)}] = \xi, \quad Q[I^{(u)}] + I^{(w)} = \nu,$$

or

$$\begin{pmatrix} I & S \\ Q & I \end{pmatrix} \begin{pmatrix} I^{(u)} \\ I^{(w)} \end{pmatrix} = \begin{pmatrix} \xi \\ \nu \end{pmatrix}. \qquad\qquad (1.16)$$

For later use, we write this more compactly as

$$\mathbf{AV} = \mathbf{R}, \qquad\qquad (1.17)$$

where

$$\mathbf{A} = \begin{pmatrix} I & S \\ Q & I \end{pmatrix}, \quad \mathbf{V} = \begin{pmatrix} I^{(u)} \\ I^{(w)} \end{pmatrix}, \quad \mathbf{R} = \begin{pmatrix} \xi \\ \nu \end{pmatrix}. \tag{1.18}$$

<center>**CHAPTER 2**</center>

<center>**HIGH–ORDER PERTURBATION OF SURFACES METHODS**</center>

Our approach to simulate solutions to (Equation 1.1) is perturbative in nature and based upon the assumption that $g(\theta) = \varepsilon f(\theta)$. We first investigate the purely cylindrical configuration, $g \equiv 0$, where if the "Fröhlich condition" is satisfied, an LSPR is excited.

2.1 The Trivial Configuration: LSPR Condition

In this section, we show how our formulation delivers the classical solution for plane wave scattering by a cylindrical obstacle. This is the case $g \equiv 0$, and (Equation 1.9) becomes

$$(G_0^{(u)} + \tau^2 G_0^{(w)})[U] = -\psi_0 + \tau^2 G_0^{(w)}[\zeta_0]. \tag{2.1}$$

In this trivial configuration, the solutions to (Equation 1.7) and (Equation 1.8) are,

$$u(r,\theta) = \sum_{p=-\infty}^{\infty} \hat{U}_p \frac{H_p(k^u r)}{H_p(k^u \bar{g})} e^{ip\theta}, \quad w(r,\theta) = \sum_{p=-\infty}^{\infty} \hat{W}_p \frac{J_p(k^w r)}{J_p(k^w \bar{g})} e^{ip\theta}, \tag{2.2}$$

respectively. From these we find for (Equation 1.7d)

$$G_0^{(u)}[U] = \sum_{p=-\infty}^{\infty} \hat{U}_p (-k^u \bar{g}) \frac{H_p'(k^u \bar{g})}{H_p(k^u \bar{g})} e^{ip\theta} =: -(k^u \bar{g}) \frac{H_D'(k^u \bar{g})}{H_D(k^u \bar{g})} U,$$

<center>18</center>

and for (Equation 1.8d)

$$G_0^{(w)}[W] = \sum_{p=-\infty}^{\infty} \hat{W}_p(k^w\bar{g}) \frac{J_p'(k^w\bar{g})}{J_p(k^w\bar{g})} e^{ip\theta} =: (k^w\bar{g}) \frac{J_D'(k^w\bar{g})}{J_D(k^w\bar{g})} W,$$

which define the order–one Fourier multipliers

$$G_0^{(u)} = -(k^u\bar{g}) \frac{H_D'(k^u\bar{g})}{H_D(k^u\bar{g})}, \quad G_0^{(w)} = (k^w\bar{g}) \frac{J_D'(k^w\bar{g})}{J_D(k^w\bar{g})},$$

respectively.

Returning to (Equation 2.1), using the solution (Equation 2.2), we find the coefficients at each wavenumber

$$\hat{U}_p = \frac{-(\hat{\psi}_0)_p + \tau^2(k^w\bar{g}) \frac{J_p'(k^w\bar{g})}{J_p(k^w\bar{g})} (\hat{\zeta}_0)_p}{-(k^u\bar{g}) \frac{H_p'(k^u\bar{g})}{H_p(k^u\bar{g})} + \tau^2(k^w\bar{g}) \frac{J_p'(k^w\bar{g})}{J_p(k^w\bar{g})}}$$

$$= \frac{H_p(k^u\bar{g}) J_p(k^w\bar{g})(\hat{\psi}_0)_p - \tau^2(k^w\bar{g}) H_p(k^u\bar{g}) J_p'(k^w\bar{g})(\hat{\zeta}_0)_p}{(k^u\bar{g}) J_p(k^w\bar{g}) H_p'(k^u\bar{g}) - \tau^2(k^w\bar{g}) H_p(k^u\bar{g}) J_p'(k^w\bar{g})}.$$

It is clear that the solvability of this system depends on the denominator

$$\tilde{\Delta}_p := -\tau^2(k^w\bar{g}) H_p(k^u\bar{g}) J_p'(k^w\bar{g}) + (k^u\bar{g}) H_p'(k^u\bar{g}) J_p(k^w\bar{g}). \tag{2.3}$$

We study this in the "small radius" (quasistatic) limit (2), $|k^u \bar{g}| \ll 1$ and $|k^w \bar{g}| \ll 1$. For a positive integer p,

$$J_p(z) \sim \frac{z^p}{2^p p!}, \qquad\qquad z \to 0,$$

$$H_p(z) \sim iY_p(z) \sim \frac{i(p-1)!}{\pi} \frac{2^p}{z^p}, \qquad\qquad z \to 0,$$

$$J_p'(z) \sim \frac{z^{p-1}}{2^p(p-1)!}, \qquad\qquad z \to 0,$$

$$H_p'(z) \sim iY_p'(z) \sim -\frac{ip!}{\pi} \frac{2^p}{z^{p+1}}, \qquad\qquad z \to 0,$$

so that

$$\tilde{\Delta}_p \sim -\tau^2 k^w \bar{g} \left(\frac{i(p-1)!}{\pi} \frac{2^p}{(k^u\bar{g})^p} \right) \left(\frac{(k^w\bar{g})^{p-1}}{2^p(p-1)!} \right) + k^u \bar{g} \left(-\frac{ip!}{\pi} \frac{2^p}{(k^u\bar{g})^{p+1}} \right) \left(\frac{(k^w\bar{g})^p}{2^p p!} \right)$$

$$= -\frac{i}{\pi}(\tau^2 + 1) \left(\frac{k^w}{k^u} \right)^p .$$

This demonstrates that, in the small radius limit, $\tilde{\Delta}_p \approx 0$ if $\tau^2 = -1$, or

$$\epsilon^{(u)} = -\text{Re}\left\{\epsilon^{(w)}\right\} - i\text{Im}\left\{\epsilon^{(w)}\right\},$$

where we have used $\tau^2 = \epsilon^{(u)}/\epsilon^{(w)}$. Since $\epsilon^{(u)}$ is real this can never be exactly satisfied, however, if the Fröhlich condition

$$\epsilon^{(u)} = -\text{Re}\left\{\epsilon^{(w)}\right\}, \tag{2.4}$$

is verified then it can "almost" be true.

We can repeat this calculation in terms of the IIO formulation in the following way. We consider (Equation 1.16) in the case $g \equiv 0$

$$\begin{pmatrix} I & S_0 \\ Q_0 & I \end{pmatrix} \begin{pmatrix} I^{(u)} \\ I^{(w)} \end{pmatrix} = \begin{pmatrix} \xi_0 \\ \nu_0 \end{pmatrix}. \tag{2.5}$$

In this trivial configuration, the solutions to (Equation 1.14) and (Equation 1.15) are,

$$u(r, \theta) = \sum_{p=-\infty}^{\infty} \frac{\left(\widehat{I^{(u)}}\right)_p}{-\tau^u(k^u\bar{g})H_p'(k^u\bar{g}) + \hat{Y}_p H_p(k^u\bar{g})} H_p(k^u r) e^{ip\theta}, \tag{2.6a}$$

$$w(r, \theta) = \sum_{p=-\infty}^{\infty} \frac{\left(\widehat{I^{(w)}}\right)_p}{\tau^w(k^w\bar{g})J_p'(k^w\bar{g}) - \hat{Z}_p J_p(k^w\bar{g})} J_p(k^w r) e^{ip\theta}, \tag{2.6b}$$

respectively. From these we find for (Equation 1.14d)

$$Q_0[I^{(u)}] = \sum_{p=-\infty}^{\infty} (\widehat{Q_0})_p \left(\widehat{I^{(u)}}\right)_p e^{ip\theta} = \sum_{p=-\infty}^{\infty} \left(\frac{-\tau^u(k^u\bar{g})H_p'(k^u\bar{g}) + \hat{Z}_p H_p(k^u\bar{g})}{-\tau^u(k^u\bar{g})H_p'(k^u\bar{g}) + \hat{Y}_p H_p(k^u\bar{g})}\right) \left(\widehat{I^{(u)}}\right)_p e^{ip\theta}$$

$$=: \left(\frac{-\tau^u(k^u\bar{g})H_D'(k^u\bar{g}) + ZH_D(k^u\bar{g})}{-\tau^u(k^u\bar{g})H_D'(k^u\bar{g}) + YH_D(k^u\bar{g})}\right) I^{(u)},$$

and for (Equation 1.15d)

$$S_0[I^{(w)}] = \sum_{p=-\infty}^{\infty} (\widehat{S_0})_p \left(\widehat{I^{(w)}}\right)_p e^{ip\theta} = \sum_{p=-\infty}^{\infty} \left(\frac{\tau^w(k^w\bar{g})J_p'(k^w\bar{g}) - \hat{Y}_p J_p(k^w\bar{g})}{\tau^w(k^w\bar{g})J_p'(k^w\bar{g}) - \hat{Z}_p J_p(k^w\bar{g})}\right) \left(\widehat{I^{(w)}}\right)_p e^{ip\theta}$$

$$=: \left(\frac{\tau^w(k^w\bar{g})J_D'(k^w\bar{g}) - YJ_D(k^w\bar{g})}{\tau^w(k^w\bar{g})J_D'(k^w\bar{g}) - ZJ_D(k^w\bar{g})}\right) I^{(w)},$$

which define the order–one Fourier multipliers

$$Q_0 = \left(\frac{-\tau^u(k^u \bar{g}) H'_D(k^u \bar{g}) + Z H_D(k^u \bar{g})}{-\tau^u(k^u \bar{g}) H'_D(k^u \bar{g}) + Y H_D(k^u \bar{g})} \right), \quad S_0 = \left(\frac{\tau^w(k^w \bar{g}) J'_D(k^w \bar{g}) - Y J_D(k^w \bar{g})}{\tau^w(k^w \bar{g}) J'_D(k^w \bar{g}) - Z J_D(k^w \bar{g})} \right), \quad (2.7)$$

respectively.

Returning to (Equation 2.5) we find the solution at each wavenumber is given by

$$\begin{pmatrix} \left(\widehat{I^{(u)}} \right)_p \\ \left(\widehat{I^{(w)}} \right)_p \end{pmatrix} = \frac{1}{1 - \widehat{(S_0)}_p \widehat{(Q_0)}_p} \begin{pmatrix} 1 & -\widehat{(S_0)}_p \\ -\widehat{(Q_0)}_p & 1 \end{pmatrix} \begin{pmatrix} \widehat{(\xi_0)}_p \\ \widehat{(\nu_0)}_p \end{pmatrix}. \qquad (2.8)$$

It is clear that the solvability of this system hinges on

$$1 - \widehat{(S_0)}_p \widehat{(Q_0)}_p,$$

which is equivalent to the $\tilde{\Delta}_p$ in (Equation 2.3).

2.2 The Non–Trivial Configurations

The exact solution to the trivial configuration and its scientific applications have been explored in depth. Our current interest is the non–trivial case where $g \not\equiv 0$, and we use a High–Order Perturbation of Surfaces (HOPS) scheme to simulate the scattering returns. In the rest of this Chapter, we will present our algorithms via Impedance–Impedance operators. (See Appendix A for DNOs.)

Assume $g(\theta) = \varepsilon f(\theta)$. For ε sufficiently small and f sufficiently smooth the operators, $\{Q, S\}$, and data, $\{\xi, \nu\}$, as we will show in Chapter 3, are analytic in ε so that the following Taylor series are strongly convergent

$$\{Q, S, \xi, \nu\} = \{Q, S, \xi, \nu\}(\varepsilon f) = \sum_{n=0}^{\infty} \{Q_n, S_n, \xi_n, \nu_n\}\varepsilon^n. \tag{2.9}$$

Given formulas for $\{Q_n, S_n\}$ it is relatively easy to identify recursive formulas for the $\{I_n^{(u)}, I_n^{(w)}\}$. We write (Equation 1.16) as

$$\begin{pmatrix} I & \sum_{n=0}^{\infty} S_n \varepsilon^n \\ \sum_{n=0}^{\infty} Q_n \varepsilon^n & I \end{pmatrix} \begin{pmatrix} \sum_{m=0}^{\infty} I_m^{(u)} \varepsilon^m \\ \sum_{m=0}^{\infty} I_m^{(w)} \varepsilon^m \end{pmatrix} = \begin{pmatrix} \sum_{n=0}^{\infty} \xi_n \varepsilon^n \\ \sum_{n=0}^{\infty} \nu_n \varepsilon^n \end{pmatrix},$$

and equate at order $\mathcal{O}(\varepsilon^n)$,

$$\begin{pmatrix} I & S_0 \\ Q_0 & I \end{pmatrix} \begin{pmatrix} I_n^{(u)} \\ I_n^{(w)} \end{pmatrix} = \begin{pmatrix} \xi_n \\ \nu_n \end{pmatrix} - \sum_{m=0}^{n-1} \begin{pmatrix} 0 & S_{n-m} \\ Q_{n-m} & 0 \end{pmatrix} \begin{pmatrix} I_m^{(u)} \\ I_m^{(w)} \end{pmatrix}. \tag{2.10}$$

At order zero we recover the trivial shape calculation, (Equation 2.5), from the previous section. The higher order corrections, $\{I_n^{(u)}, I_n^{(w)}\}$, can be recovered from (Equation 2.10). At every perturbation order we must invert the same linear operator,

$$\begin{pmatrix} I & S_0 \\ Q_0 & I \end{pmatrix},$$

which renders the algorithm extremely computationally efficient.

All that remains is to specify forms for the data, $\{\xi_n, \nu_n\}$, and operators, $\{Q_n, S_n\}$. The date $\{\xi_n, \nu_n\}$ is related to the incident radiation, $\{\zeta, \psi\}$, provided in (Equation 1.1e) and (Equation 1.1f). It is easy to show that

$$\zeta_n(\theta) = -e^{\bar{g}(i\alpha \cos\theta - i\gamma^u \sin\theta)}(i\alpha \cos\theta - i\gamma^u \sin\theta)^n F_n,$$

$$\psi_n(\theta) = \bar{g}(i\alpha \cos\theta - i\gamma^u \sin\theta)\zeta_n(\theta)$$
$$+ \left[f(i\alpha \cos\theta - i\gamma^u \sin\theta) - (f')(-i\alpha \sin\theta - i\gamma^u \cos\theta)\right]\zeta_{n-1}(\theta),$$

where

$$F_n = F_n(\theta) := \frac{(f(\theta))^n}{n!}.$$

Then the data (Equation 1.12) can be computed as

$$\xi_n = -\tau^u \psi_n + Y\zeta_n, \quad \nu_n = -\tau^u \psi_n + Z\zeta_n.$$

Remark 2.2.1. We focus on linear operators Y and Z which are independent of ε thus the perturbation order n.

For the operators, $\{Q_n, S_n\}$, we appeal to the method of Field Expansions and the method of Transformed Field Expansions (22; 23; 24; 26; 27) which we now present for completeness.

2.3 The Method of Field Expansions

The method of Field Expansions begins with the supposition that the scattered fields, $\{u, w\}$, depend analytically upon ε. Focusing upon the Exterior Problem via IIO (Equation 1.14), for the field u in the outer domain, $\{r > \bar{g} + \varepsilon f(\theta)\}$, this implies that

$$u = u(r, \theta; \varepsilon) = \sum_{n=0}^{\infty} u_n(r, \theta) \varepsilon^n.$$

Upon insertion of this into (Equation 1.14) one finds that the u_n must be 2π–periodic, outward–propagating solutions of the boundary value problem

$$\Delta u_n + \left(k^u\right)^2 u_n = 0, \qquad\qquad \bar{g} < r < R^o, \qquad (2.11a)$$

$$-\tau^u \bar{g} \partial_r u_n + Y u_n = \delta_{n,0} I_n^{(u)} + L_n^{\text{FE,ex}}, \qquad\qquad r = \bar{g}, \qquad (2.11b)$$

$$\partial_r u_n + T^{(u)}[u_n] = 0, \qquad\qquad r = R^o, \qquad (2.11c)$$

where $\delta_{n,\ell}$ is the Kronecker delta function, and

$$\begin{aligned}
L_n^{\text{FE,ex}} =& \frac{f}{\bar{g}} \delta_{n,1} I_{n-1}^{(u)} + \tau^u \left\{ \bar{g} \sum_{m=0}^{n-1} \partial_r^{n-m+1} u_m F_{n-m} + 2f \sum_{m=0}^{n-1} \partial_r^{n-m} u_m F_{n-m-1} \right. \\
&\left. + \frac{f^2}{\bar{g}} \sum_{m=0}^{n-2} \partial_r^{n-m-1} u_m F_{n-m-2} - \frac{f'}{\bar{g}} \sum_{m=0}^{n-1} \partial_\theta \partial_r^{n-m-1} u_m F_{n-m-1} \right\} \\
&- Y \sum_{m=0}^{n-1} \partial_r^{n-m} u_m F_{n-m} - \frac{f}{\bar{g}} Y \sum_{m=0}^{n-1} \partial_r^{n-m-1} u_m F_{n-m-1}.
\end{aligned}$$

The exact solutions (Equation 2.6a) are

$$u_n(r,\theta) = \sum_{p=-\infty}^{\infty} \frac{\hat{u}_{n,p}}{-\tau^u(k^u\bar{g})H_p'(k^u\bar{g}) + \hat{Y}_p H_p(k^u\bar{g})} H_p(k^u r)e^{ip\theta},$$

and the $\hat{u}_{n,p}$ are determined recursively from the boundary conditions, (Equation 2.11b), beginning, at order zero, with

$$\hat{u}_{0,p} = \left(\widehat{I^{(u)}}\right)_p.$$

From this the exterior IIO Q, (Equation 1.14d), can be computed from

$$Q[I^{(u)}] = (-\tau^u \partial_N u + (Zu))(\bar{g} + g(\theta), \theta)$$

$$= \left\{-\tau^u\left(\bar{g} + \varepsilon f, -\varepsilon f'\right) \cdot \left(\partial_r u, \frac{1}{\bar{g} + \varepsilon f}\partial_\theta u\right) + Zu\right\}(\bar{g} + \varepsilon f(\theta), \theta)$$

$$= \tau^u \sum_{n=0}^{\infty} \sum_{p=-\infty}^{\infty} \left\{-k^u(\bar{g} + \varepsilon f)\frac{H_p'(k^u(\bar{g} + \varepsilon f))}{-\tau^u(k^u\bar{g})H_p'(k^u\bar{g}) + \hat{Y}_p H_p(k^u\bar{g})}\right.$$

$$\left. + \frac{\varepsilon f'}{(\bar{g} + \varepsilon f)}(ip)\frac{H_p(k^u(\bar{g} + \varepsilon f))}{-\tau^u(k^u\bar{g})H_p'(k^u\bar{g}) + \hat{Y}_p H_p(k^u\bar{g})}\right\} \hat{u}_{n,p} e^{ip\theta}\varepsilon^n$$

$$+ \sum_{n=0}^{\infty} \sum_{p=-\infty}^{\infty} \hat{Z}_p \frac{H_p(k^u(\bar{g} + \varepsilon f))}{-\tau^u(k^u\bar{g})H_p'(k^u\bar{g}) + \hat{Y}_p H_p(k^u\bar{g})} \hat{u}_{n,p} e^{ip\theta}\varepsilon^n.$$

Expanding the Hankel functions $H'_p(k^u(\bar{g} + \varepsilon f))$ and $H_p(k^u(\bar{g} + \varepsilon f))$ in power series in ε, and equating at like powers of ε, this results in

$$
\begin{aligned}
Q_n(f)[I^{(u)}] = &-\frac{f}{\bar{g}} Q_{n-1}(f)[I^{(u)}] \\
&+ \tau^u \left(-k^u \bar{g} \sum_{\ell=0}^{n} \sum_{p=-\infty}^{\infty} \hat{u}_{\ell,p} \frac{(k^u f)^{n-\ell}}{(n-\ell)!} \frac{H_p^{(n+1-\ell)}(k^u \bar{g})}{-\tau^u(k^u \bar{g}) H'_p(k^u \bar{g}) + \hat{Y}_p H_p(k^u \bar{g})} e^{ip\theta} \right. \\
&- 2k^u f \sum_{\ell=0}^{n-1} \sum_{p=-\infty}^{\infty} \hat{u}_{\ell,p} \frac{(k^u f)^{n-1-\ell}}{(n-1-\ell)!} \frac{H_p^{(n-\ell)}(k^u \bar{g})}{-\tau^u(k^u \bar{g}) H'_p(k^u \bar{g}) + \hat{Y}_p H_p(k^u \bar{g})} e^{ip\theta} \\
&- \frac{k^u}{\bar{g}} f^2 \sum_{\ell=0}^{n-2} \sum_{p=-\infty}^{\infty} \hat{u}_{\ell,p} \frac{(k^u f)^{n-2-\ell}}{(n-2-\ell)!} \frac{H_p^{(n-1-\ell)}(k^u \bar{g})}{-\tau^u(k^u \bar{g}) H'_p(k^u \bar{g}) + \hat{Y}_p H_p(k^u \bar{g})} e^{ip\theta} \\
&+ \frac{f'}{\bar{g}} \sum_{\ell=0}^{n-1} \sum_{p=-\infty}^{\infty} \hat{u}_{\ell,p} \frac{(k^u f)^{n-1-\ell}}{(n-1-\ell)!} \frac{H_p^{(n-1-\ell)}(k^u \bar{g})}{-\tau^u(k^u \bar{g}) H'_p(k^u \bar{g}) + \hat{Y}_p H_p(k^u \bar{g})} (ip) e^{ip\theta} \right) \\
&+ \sum_{\ell=0}^{n} \sum_{p=-\infty}^{\infty} \hat{Z}_p \hat{u}_{\ell,p} \frac{(k^u f)^{n-\ell}}{(n-\ell)!} \frac{H_p^{(n-\ell)}(k^u \bar{g})}{-\tau^u(k^u \bar{g}) H'_p(k^u \bar{g}) + \hat{Y}_p H_p(k^u \bar{g})} e^{ip\theta} \\
&+ \frac{f}{\bar{g}} \sum_{\ell=0}^{n-1} \sum_{p=-\infty}^{\infty} \hat{Z}_p \hat{u}_{\ell,p} \frac{(k^u f)^{n-1-\ell}}{(n-1-\ell)!} \frac{H_p^{(n-1-\ell)}(k^u \bar{g})}{-\tau^u(k^u \bar{g}) H'_p(k^u \bar{g}) + \hat{Y}_p H_p(k^u \bar{g})} e^{ip\theta},
\end{aligned}
$$

where the superscript in parentheses denotes derivative.

Similar considerations hold for the IIO S. Focusing on the Interior Problem via IIO (Equation 1.15), we write the field w in the inner domain, $\{r < \bar{g} + \varepsilon f(\theta)\}$, as

$$
w = w(r, \theta; \varepsilon) = \sum_{n=0}^{\infty} w_n(r, \theta) \varepsilon^n.
$$

Inserting this into (Equation 1.15), the w_n must be 2π–periodic, bounded solutions of the boundary value problem

$$\Delta w_n + (k^w)^2\, w_n = 0, \qquad\qquad R_i < r < \bar{g}, \qquad (2.12a)$$

$$\tau^w \bar{g} \partial_r w_n - Z w_n = \delta_{n,0} I_n^{(w)} + L_n^{\text{FE,in}}, \qquad\qquad r = \bar{g}, \qquad (2.12b)$$

$$\partial_r w_n - T^{(w)}\left[w_n\right] = 0, \qquad\qquad r = R_i, \qquad (2.12c)$$

and

$$
\begin{aligned}
L_n^{\text{FE,in}} =& \frac{f}{\bar{g}}\delta_{n,1} I_{n-1}^{(w)} - \tau^w \left\{ \bar{g}\sum_{m=0}^{n-1} \partial_r^{n-m+1} w_m F_{n-m} + 2f\sum_{m=0}^{n-1} \partial_r^{n-m} w_m F_{n-m-1} \right.\\
&\left. + \frac{f^2}{\bar{g}}\sum_{m=0}^{n-2} \partial_r^{n-m-1} w_m F_{n-m-2} - \frac{f'}{\bar{g}}\sum_{m=0}^{n-1} \partial_\theta \partial_r^{n-m-1} w_m F_{n-m-1} \right\}\\
&+ Z\sum_{m=0}^{n-1} \partial_r^{n-m} w_m F_{n-m} + \frac{f}{\bar{g}}Z\sum_{m=0}^{n-1} \partial_r^{n-m-1} w_m F_{n-m-1}.
\end{aligned}
$$

The exact solutions (Equation 2.6b) are

$$w_n(r,\theta) = \sum_{p=-\infty}^{\infty} \frac{\hat{w}_{n,p}}{\tau^w (k^w \bar{g}) J_p'(k^w \bar{g}) - \hat{Z}_p J_p(k^w \bar{g})} J_p(k^w r) e^{ip\theta},$$

and the $\hat{w}_{n,p}$ are determined recursively from the boundary conditions, (Equation 2.12b), beginning, at order zero, with

$$\hat{w}_{0,p} = \left(\widehat{I^{(w)}}\right)_p.$$

From this the interior IIO S, (Equation 1.15d), can be computed from

$$
S[I^{(w)}] = (\tau^u \partial_N w - Yw)(\bar{g} + g(\theta), \theta)
$$

$$
= \left\{ \tau^w (\bar{g} + \varepsilon f, -\varepsilon f') \cdot \left(\partial_r w, \frac{1}{\bar{g} + \varepsilon f} \partial_\theta w \right) - Yw \right\} (\bar{g} + \varepsilon f(\theta), \theta)
$$

$$
= \tau^w \sum_{n=0}^{\infty} \sum_{p=-\infty}^{\infty} \left\{ k^w (\bar{g} + \varepsilon f) \frac{J_p'(k^w(\bar{g} + \varepsilon f))}{\tau^w (k^w \bar{g}) J_p'(k^w \bar{g}) - \hat{Z}_p J_p(k^w \bar{g})} \right.
$$

$$
\left. - \frac{\varepsilon f'}{(\bar{g} + \varepsilon f)} (ip) \frac{J_p(k^w(\bar{g} + \varepsilon f))}{\tau^w (k^w \bar{g}) J_p'(k^w \bar{g}) - \hat{Z}_p J_p(k^w \bar{g})} \right\} \hat{w}_{n,p} e^{ip\theta} \varepsilon^n
$$

$$
- \sum_{n=0}^{\infty} \sum_{p=-\infty}^{\infty} \hat{Y}_p \frac{J_p(k^w(\bar{g} + \varepsilon f))}{\tau^w (k^w \bar{g}) J_p'(k^w \bar{g}) - \hat{Z}_p J_p(k^w \bar{g})} \hat{w}_{n,p} e^{ip\theta} \varepsilon^n.
$$

Expanding the Bessel functions $J_p'(k^w(\bar{g} + \varepsilon f))$ and $J_p(k^w(\bar{g} + \varepsilon f))$ in power series in ε, and equating at like powers of ε, this results in

$$
S_n(f)[I^{(w)}] = -\frac{f}{\bar{g}} S_{n-1}(f)[I^{(w)}]
$$

$$
+ \tau^w \left(k^w \bar{g} \sum_{\ell=0}^{n} \sum_{p=-\infty}^{\infty} \hat{w}_{\ell,p} \frac{(k^w f)^{n-\ell}}{(n-\ell)!} \frac{J_p^{(n+1-\ell)}(k^w \bar{g})}{\tau^w (k^w \bar{g}) J_p'(k^w \bar{g}) - \hat{Z}_p J_p(k^w \bar{g})} e^{ip\theta} \right.
$$

$$
+ 2k^w f \sum_{\ell=0}^{n-1} \sum_{p=-\infty}^{\infty} \hat{w}_{\ell,p} \frac{(k^w f)^{n-1-\ell}}{(n-1-\ell)!} \frac{J_p^{(n-\ell)}(k^w \bar{g})}{\tau^w (k^w \bar{g}) J_p'(k^w \bar{g}) - \hat{Z}_p J_p(k^w \bar{g})} e^{ip\theta}
$$

$$
+ \frac{k^w}{\bar{g}} f^2 \sum_{\ell=0}^{n-2} \sum_{p=-\infty}^{\infty} \hat{w}_{\ell,p} \frac{(k^w f)^{n-2-\ell}}{(n-2-\ell)!} \frac{J_p^{(n-1-\ell)}(k^u \bar{g})}{\tau^w (k^w \bar{g}) J_p'(k^w \bar{g}) - \hat{Z}_p J_p(k^w \bar{g})} e^{ip\theta}
$$

$$
\left. - \frac{f'}{\bar{g}} \sum_{\ell=0}^{n-1} \sum_{p=-\infty}^{\infty} \hat{w}_{\ell,p} \frac{(k^w f)^{n-1-\ell}}{(n-1-\ell)!} \frac{J_p^{(n-1-\ell)}(k^w \bar{g})}{\tau^w (k^w \bar{g}) J_p'(k^w \bar{g}) - \hat{Z}_p J_p(k^w \bar{g})} (ip) e^{ip\theta} \right)
$$

$$
- \sum_{\ell=0}^{n} \sum_{p=-\infty}^{\infty} \hat{Y}_p \hat{w}_{\ell,p} \frac{(k^w f)^{n-\ell}}{(n-\ell)!} \frac{J_p^{(n-\ell)}(k^u \bar{g})}{\tau^w (k^w \bar{g}) J_p'(k^w \bar{g}) - \hat{Z}_p J_p(k^w \bar{g})} e^{ip\theta}
$$

$$
- \frac{f}{\bar{g}} \sum_{\ell=0}^{n-1} \sum_{p=-\infty}^{\infty} \hat{Y}_p \hat{w}_{\ell,p} \frac{(k^w f)^{n-1-\ell}}{(n-1-\ell)!} \frac{J_p^{(n-1-\ell)}(k^w \bar{g})}{\tau^w (k^w \bar{g}) J_p'(k^w \bar{g}) - \hat{Z}_p J_p(k^w \bar{g})} e^{ip\theta}.
$$

2.4   The Method of Transformed Field Expansions

The method of Transformed Field Expansions (TFE) proceeds in much the same way as the FE approach, with a domain–flattening change prior to perturbation expansion. For definiteness we consider the TFE method applied to the exterior problem, (Equation 1.14), which we restate here for convenience,

$$\Delta u + (k^u)^2 \, u = 0, \qquad\qquad \bar{g} + g(\theta) < r < R^o,$$

$$-\tau^u \partial_N u + Y u = I^{(u)}, \qquad\qquad r = \bar{g} + g(\theta),$$

$$\partial_r u + T^{(u)} [u] = 0, \qquad\qquad r = R^o.$$

The change of variables we use is

$$r' = \frac{(R^o - \bar{g})r - R^o g(\theta)}{R^o - \bar{g} + g(\theta)}, \quad \theta' = \theta,$$

which maps the perturbed domain $\{\bar{g} + g(\theta) < r < R^o\}$ to the separable one $\Omega_{\bar{g}, R^o} = \{\bar{g} < r' < R^o\}$. This transformation changes the field u into

$$v(r', \theta') := u\left(\frac{(R^o - \bar{g} + g(\theta'))r' + R^o g(\theta')}{R^o - \bar{g}}, \theta' \right),$$

and modifies (Equation 1.14) to

$$\Delta v + (k^u)^2 \, v = F^{\text{ex}}(r, \theta; g), \qquad\qquad \bar{g} < r < R^o, \qquad\qquad (2.13\text{a})$$

$$- \tau^u \partial_N v + Y v = I^{(u)} + L^{\text{ex}}(\theta; g), \qquad\qquad r = \bar{g}, \qquad\qquad (2.13\text{b})$$

$$\partial_r v + T^{(u)} \, [v] = h^{\text{ex}}(\theta; g), \qquad\qquad r = R^o, \qquad\qquad (2.13\text{c})$$

where we have dropped the primed notation for clarity. After a precise calculation, it is not difficult to see that

$$F^{\text{ex}} = -\frac{1}{(R^o - \bar{g})^2} \left[F^{\text{ex},(0)} + \partial_r F^{\text{ex},(r)} + \partial_\theta F^{\text{ex},(\theta)} \right],$$

$$F^{\text{ex},(0)} = - (R^o - \bar{g})g(R^o - r)\partial_r v + (R^o - \bar{g})gr\partial_r v + g^2(R^o - r)\partial_r v + (R^o - \bar{g})g'\partial_\theta v - gg'\partial_\theta v$$

$$- (g')^2(R^o - r)\partial_r v + g[-2(R^o - \bar{g})r^2 + 2(R^o - \bar{g})(R^o - r)r](k^u)^2 v$$

$$+ g^2[r^2 - 4(R^o - r)r + (R^o - r)^2](k^u)^2 v + g^3 \frac{2(R^o - r)(2r - R^o)}{(R^o - \bar{g})}(k^u)^2 v$$

$$+ g^4 \frac{(R^o - r)^2}{(R^o - \bar{g})^2}(k^u)^2 v,$$

$$F^{\text{ex},(r)} = 2(R^o - \bar{g})gr(R^o - r)\partial_r v + g^2(R^o - r)^2\partial_r v - (R^o - \bar{g})g'(R^o - r)\partial_\theta v$$

$$+ gg'(R^o - r)\partial_\theta v + (g')^2(R^o - r)^2\partial_r v,$$

$$F^{\text{ex},(\theta)} = - 2(R^o - \bar{g})g\partial_\theta v - (R^o - \bar{g})g'(R^o - r)\partial_r v + g^2\partial_\theta v + gg'(R^o - r)\partial_r v,$$

and

$$\bar{g}(R^o - \bar{g})L^{\text{ex}} = \tau^u \left[2(R^o - \bar{g})\bar{g}g\partial_r v + g^2(R^o - \bar{g})\partial_r v \right.$$

$$+ (g')^2(R^o - \bar{g})\partial_r v - g'(R^o - \bar{g})\partial_\theta v + g'g\partial_\theta v \Big]$$

$$- [(R^o - \bar{g})g - \bar{g}g - g^2]Y v + [(R^o - \bar{g})g - \bar{g}g - g^2]I^{(u)},$$

and

$$h^{\text{ex}} = \frac{g}{R^o - \bar{g}} T^{(u)}[v].$$

Next, setting $g = \varepsilon f$ and expanding

$$v(r, \theta, \varepsilon) = \sum_{n=0}^{\infty} v_n(r, \theta)\varepsilon^n,$$

we show that

$$\Delta v_n + (k^u)^2 \, v_n = F_n^{\text{ex}}, \qquad\qquad \bar{g} < r < R^o, \qquad (2.14\text{a})$$

$$-\tau^u \partial_N v_n + Y v_n = \delta_{n,0} I^{(u)} + L_n^{\text{ex}}, \qquad\qquad r = \bar{g}, \qquad (2.14\text{b})$$

$$\partial_r v_n + T^{(u)}[v_n] = h_n^{\text{ex}}, \qquad\qquad r = R^o, \qquad (2.14\text{c})$$

where

$$F_n^{\text{ex}} = -\frac{1}{(R^o - \bar{g})^2} \left[F_n^{\text{ex},(0)} + \partial_r F_n^{\text{ex},(r)} + \partial_\theta F_n^{\text{ex},(\theta)} \right], \tag{2.15}$$

$$F_n^{\text{ex},(0)} = - (R^o - \bar{g})f(R^o - r)\partial_r v_{n-1} + (R^o - \bar{g})fr\partial_r v_{n-1} + f^2(R^o - r)\partial_r v_{n-2}$$

$$+ (R^o - \bar{g})f'\partial_\theta v_{n-1} - ff'\partial_\theta v_{n-2} - (f')^2(R^o - r)\partial_r v_{n-2}$$

$$+ f(R^o - \bar{g})[2r^2 + 2(R^o - r)r](k^u)^2 v_{n-1} + f^2[r^2 - 4(R^o - r)r + (R^o - r)^2](k^u)^2 v_{n-2}$$

$$+ f^3 \frac{2(R^o - r)(2r - R^o)}{(R^o - \bar{g})}(k^u)^2 v_{n-3} + f^4 \frac{(R^o - r)^2}{(R^o - \bar{g})^2}(k^u)^2 v_{n-4},$$

$$F_n^{\text{ex},(r)} = 2(R^o - \bar{g})fr(R^o - r)\partial_r v_{n-1} + f^2(R^o - r)^2\partial_r v_{n-2} - (R^o - \bar{g})f'(R^o - r)\partial_\theta v_{n-1}$$

$$+ ff'(R^o - r)\partial_\theta v_{n-2} + (f')^2(R^o - r)^2\partial_r v_{n-2},$$

$$F_n^{\text{ex},(\theta)} = - 2(R^o - \bar{g})f\partial_\theta v_{n-1} - (R^o - \bar{g})f'(R^o - r)\partial_r v_{n-1} + f^2\partial_\theta v_{n-2} + ff'(R^o - r)\partial_r v_{n-2},$$

and

$$\bar{g}(R^o - \bar{g})L_n^{\text{ex}} = -\bar{g}f\delta_{n,1}I^{(u)} + (R^o - \bar{g})f\delta_{n,1}I^{(u)} - f^2\delta_{n,2}I^{(u)} + \tau^u [2\bar{g}(R^o - \bar{g})f\partial_r v_{n-1}$$

$$+ (R^o - \bar{g})f^2\partial_r v_{n-2} + (R^o - \bar{g})(f')^2\partial_r v_{n-2} - (R^o - \bar{g})f'\partial_\theta v_{n-1} + ff'\partial_\theta v_{n-2}]$$

$$+ \bar{g}fY v_{n-1} - (R^o - \bar{g})fY v_{n-1} + f^2 Y v_{n-2}, \tag{2.16}$$

and

$$h_n^{\text{ex}} = \frac{f}{R^o - \bar{g}}T^{(u)}[v_{n-1}].$$

In addition, the IIO map, Q in (Equation 1.14d), is stated in transformed coordinates

$$Q[I^{(u)}] = -\tau^u \left\{ \frac{\bar{g} - R_i}{\bar{g} - R_i + g} \left[(\bar{g} + g) + \frac{(g')^2}{\bar{g} + g} \right] \partial_r v - \frac{g'}{\bar{g} + g} \partial_\theta v \right\} + Zv,$$

and then expanded in a Taylor series, (Equation 2.9). The nth term in the expansion can be expressed as

$$
\begin{aligned}
Q_n[I^{(u)}] = {} & -f \left(\frac{1}{\bar{g}} - \frac{1}{R^o - \bar{g}} \right) Q_{n-1}[I^{(u)}] + \frac{f^2}{\bar{g}(R^o - \bar{g})} Q_{n-2}[I^{(u)}] \\
& - \tau^u \left\{ \bar{g} \partial_r v_n + 2f \partial_r v_{n-1} + \frac{f^2 + (f')^2}{\bar{g}} \partial_r v_{n-2} - \frac{f'}{\bar{g}} \partial_\theta v_{n-1} + \frac{f(f')}{\bar{g}(R^o - \bar{g})} \partial_\theta v_{n-2} \right\} \\
& + Z v_n + f \left(\frac{1}{\bar{g}} - \frac{1}{R^o - \bar{g}} \right) Z v_{n-1} - \frac{f^2}{\bar{g}(R^o - \bar{g})} Z v_{n-2},
\end{aligned}
\tag{2.17}
$$

so that, provided with the $\{v_n\}$, we can estimate the terms, $\{Q_n\}$.

Last, we consider the TFE method applied to the Interior Problem via IIO (Equation 1.15),

$$\Delta w + (k^w)^2 \, w = 0, \qquad\qquad R_i < r < \bar{g} + g(\theta),$$

$$\tau^w \partial_N w - Zw = I^{(w)}, \qquad\qquad r = \bar{g} + g(\theta),$$

$$\partial_r w - T^{(w)}[w] = 0, \qquad\qquad r = R_i.$$

The relevant change of variables is

$$r' = \frac{(\bar{g} - R_i) r + R_i g(\theta)}{\bar{g} + g(\theta) - R_i}, \qquad \theta' = \theta,$$

which maps the perturbed domain $\{R_i < r < \bar{g} + g(\theta)\}$ to the separable one $\Omega_{R_i,\bar{g}} = \{R_i < r' < \bar{g}\}$. This transformation changes the field w into

$$v(r', \theta') := w\left(\frac{(\bar{g} + g(\theta') - R_i)r' - R_i g(\theta')}{\bar{g} - R_i}, \theta'\right),$$

and modifies (Equation 1.15) to

$$\Delta v + (k^w)^2\, v = F^{\text{in}}(r, \theta; g), \qquad\qquad R_i < r < \bar{g}, \qquad\qquad (2.18\text{a})$$

$$\tau^w \partial_N v - Zv = I^{(w)} + L^{\text{in}}(\theta; g), \qquad\qquad r = \bar{g}, \qquad\qquad (2.18\text{b})$$

$$\partial_r v - T^{(w)}\,[v] = h^{\text{in}}(\theta; g), \qquad\qquad r = R_i, \qquad\qquad (2.18\text{c})$$

with

$$F^{\text{in}} = -\frac{1}{(\bar{g} - R_i)^2} \left[F^{\text{in},(0)} + \partial_r F^{\text{in},(r)} + \partial_\theta F^{\text{in},(\theta)} \right], \tag{2.19}$$

$$\begin{aligned}
F^{\text{in},(0)} = & -(\bar{g} - R_i)g(r - R_i)\partial_r v - (\bar{g} - R_i)gr\partial_r v - g^2(r - R_i)\partial_r v - (\bar{g} - R_i)g'\partial_\theta v - gg'\partial_\theta v \\
& + (g')^2(r - R_i)\partial_r v + g[2(\bar{g} - R_i)r^2 + 2(\bar{g} - R_i)(r - R_i)r](k^w)^2 v \\
& + g^2[r^2 + 4(r - R_i)r + (r - R_i)^2](k^w)^2 v + g^3 \frac{2(r - R_i)(2r - R_i)}{(\bar{g} - R_i)}(k^w)^2 v \\
& + g^4 \frac{(r - R_i)^2}{(\bar{g} - R_i)^2}(k^w)^2 v,
\end{aligned} \tag{2.20}$$

$$\begin{aligned}
F^{\text{in},(r)} = & 2(\bar{g} - R_i)gr(r - R_i)\partial_r v + g^2(r - R_i)^2\partial_r v - (\bar{g} - R_i)g'(r - R_i)\partial_\theta v \\
& - gg'(r - R_i)\partial_\theta v + (g')^2(r - R_i)^2\partial_r v,
\end{aligned}$$

$$F^{\text{in},(\theta)} = 2(\bar{g} - R_i)g\partial_\theta v - (\bar{g} - R_i)g'(r - R_i)\partial_r v + g^2\partial_\theta v - gg'(r - R_i)\partial_r v,$$

and

$$\begin{aligned}
\bar{g}(\bar{g} - R_i)L^{\text{in}} = & -\tau^w \left[2(\bar{g} - R_i)\bar{g}g\partial_r v + g^2(\bar{g} - R_i)\partial_r v \right. \\
& \left. -(g')^2(\bar{g} - R_i)\partial_r v - g'(\bar{g} - R_i)\partial_\theta v - g'g\partial_\theta v \right] \\
& + [(\bar{g} - R_i)g + \bar{g}g + g^2]Zv + [(\bar{g} - R_i)g + \bar{g}g + g^2]W,
\end{aligned}$$

and

$$h^{\text{in}} = \frac{g}{\bar{g} - R_i} T^{(w)}[v], \tag{2.21}$$

where we have dropped the primed notation for clarity. Next we set $g = \varepsilon f$ and expand v in ε

$$v(r, \theta, \varepsilon) = \sum_{n=0}^{\infty} v_n(r, \theta)\varepsilon^n, \tag{2.22}$$

then we get

$$\Delta v_n + (k^w)^2 \, v_n = F_n^{\text{in}}, \qquad\qquad R_i < r < \bar{g}, \tag{2.23a}$$

$$\tau^w \bar{g} \partial_r v_n - Z v_n = \delta_{n,0} I^{(w)} + L_n^{\text{in}}, \qquad\qquad r = \bar{g}, \tag{2.23b}$$

$$\partial_r v_n - T^{(w)} [v_n] = h_n^{\text{in}}, \qquad\qquad r = R_i, \tag{2.23c}$$

where

$$F_n^{\text{in}} = -\frac{1}{(\bar{g} - R_i)^2} \left[F_n^{\text{in},(0)} + \partial_r F_n^{\text{in},(r)} + \partial_\theta F_n^{\text{in},(\theta)} \right], \tag{2.24}$$

$$F_n^{\text{in},(0)} = -(\bar{g} - R_i)f(r - R_i)\partial_r v_{n-1} - (\bar{g} - R_i)fr\partial_r v_{n-1} - f^2(r - R_i)\partial_r v_{n-2}$$

$$- (\bar{g} - R_i)f'\partial_\theta v_{n-1} - ff'\partial_\theta v_{n-2} + (f')^2(r - R_i)\partial_r v_{n-2}$$

$$+ f(\bar{g} - R_i)[2r^2 + 2(r - R_i)r](k^w)^2 v_{n-1} + f^2[r^2 + 4(r - R_i)r + (r - R_i)^2](k^w)^2 v_{n-2}$$

$$+ f^3 \frac{2(r - R_i)(2r - R_i)}{(\bar{g} - R_i)}(k^w)^2 v_{n-3} + f^4 \frac{(r - R_i)^2}{(\bar{g} - R_i)^2}(k^w)^2 v_{n-4},$$

$$F_n^{\text{in},(r)} = 2(\bar{g} - R_i)fr(r - R_i)\partial_r v_{n-1} + f^2(r - R_i)^2\partial_r v_{n-2} - (\bar{g} - R_i)f'(r - R_i)\partial_\theta v_{n-1}$$

$$- ff'(r - R_i)\partial_\theta v_{n-2} + (f')^2(r - R_i)^2\partial_r v_{n-2},$$

$$F_n^{\text{in},(\theta)} = 2(\bar{g} - R_i)f\partial_\theta v_{n-1} - (\bar{g} - R_i)f'(r - R_i)\partial_r v_{n-1} + f^2\partial_\theta v_{n-2} - ff'(r - R_i)\partial_r v_{n-2},$$

and

$$\bar{g}(\bar{g} - R_i)L_n^{\text{in}} = \bar{g}f\delta_{n,1}I^{(w)} + (\bar{g} - R_i)f\delta_{n,1}I^{(w)} + f^2\delta_{n,2}I^{(w)} - \tau^w \left[2\bar{g}(\bar{g} - R_i)f\partial_r v_{n-1}\right.$$

$$+ (\bar{g} - R_i)f^2\partial_r v_{n-2} + (\bar{g} - R_i)(f')^2\partial_r v_{n-2} - (\bar{g} - R_i)f'\partial_\theta v_{n-1} - ff'\partial_\theta v_{n-2}\big]$$

$$+ \bar{g}fZv_{n-1} + (\bar{g} - R_i)fZv_{n-1} + f^2Zv_{n-2}, \tag{2.25}$$

and

$$h_n^{\text{in}} = \frac{f}{\bar{g} - R_i}T^{(w)}\left[v_{n-1}\right]. \tag{2.26}$$

In addition we can recover that the IIO, S in (Equation 1.15d), changes to

$$S[I^{(w)}] = \tau^w \left\{ \frac{\bar{g} - R_i}{\bar{g} - R_i + g} \left[(\bar{g} + g) + \frac{(g')^2}{\bar{g} + g}\right]\partial_r v - \frac{g'}{\bar{g} + g}\partial_\theta v \right\} - Yv,$$

and

$$S_n[I^{(w)}] = -f\left(\frac{1}{\bar{g}} + \frac{1}{\bar{g} - R_i}\right)S_{n-1}[I^{(w)}] - \frac{f^2}{\bar{g}(\bar{g} - R_i)}S_{n-2}[I^{(w)}]$$

$$+ \tau^w \left\{\bar{g}\partial_r v_n + 2f\partial_r v_{n-1} + \frac{f^2 + (f')^2}{\bar{g}}\partial_r v_{n-2} - \frac{f'}{\bar{g}}\partial_\theta v_{n-1} - \frac{f(f')}{\bar{g}(\bar{g} - R_i)}\partial_\theta v_{n-2}\right\}$$

$$- Yv_n - f\left(\frac{1}{\bar{g}} + \frac{1}{\bar{g} - R_i}\right)Yv_{n-1} - \frac{f^2}{\bar{g}(\bar{g} - R_i)}Yv_{n-2}. \tag{2.27}$$

Again, provided with the $\{v_n\}$, we can readily approximate the terms, S_n, in the Taylor series expansion (Equation 2.9) of S.

CHAPTER 3

ANALYTICITY OF SOLUTIONS

Our approach to simulate solutions to (Equation 1.9) or (Equation 1.16) is based upon the assumption that $g(\theta) = \varepsilon f(\theta)$ where ε is sufficiently small. As we shall show in this chapter, provided that f is sufficiently smooth, then the IIOs, Q and S, are analytic in the perturbation parameter ε so that the following expansions are strongly convergent in an appropriate Sobolev space

$$Q(\varepsilon f) = \sum_{n=0}^{\infty} Q_n(f)\varepsilon^n, \tag{3.1a}$$

$$S(\varepsilon f) = \sum_{n=0}^{\infty} S_n(f)\varepsilon^n. \tag{3.1b}$$

Clearly, if this is the case then the operator $\mathbf{A}$ will also be analytic, as will $\mathbf{R}$ so that

$$\{\mathbf{A}(\varepsilon f), \mathbf{R}(\varepsilon f)\} = \sum_{n=0}^{\infty} \{\mathbf{A}_n(f), \mathbf{R}_n(f)\}\varepsilon^n. \tag{3.2}$$

We will shortly show that, under certain circumstances, there will be a unique solution, $\mathbf{V}$, of (Equation 1.17) which is also analytic in ε

$$\mathbf{V}(\varepsilon f) = \sum_{n=0}^{\infty} \mathbf{V}_n(f)\varepsilon^n. \tag{3.3}$$

Furthermore, it is clear that the $\mathbf{V}_n$ must satisfy

$$\mathbf{V}_n = \mathbf{A}_0^{-1} \left\{ \mathbf{R}_n - \sum_{\ell=0}^{n-1} \mathbf{A}_{n-\ell} \mathbf{V}_\ell \right\}, \tag{3.4}$$

and one key in the analysis is the invertibility of the operator $\mathbf{A}_0$ which we now investigate.

3.1 Interfacial Function Spaces

Before describing these rigorous results we specify the interfacial function spaces we require. For any real $s \geq 0$ the classical, periodic, L^2–based Sobolev norm (42) is

$$\|U\|_{H^s}^2 := \sum_{p=-\infty}^{\infty} \langle p \rangle^{2s} \left| \hat{U}_p \right|^2, \quad \langle p \rangle^2 := 1 + |p|^2, \quad \hat{U}_p := \frac{1}{2\pi} \int_0^{2\pi} U(\theta) e^{i\alpha_p x} \, d\theta, \tag{3.5}$$

which gives rise to the periodic Sobolev space (42)

$$H^s([0, 2\pi]) := \left\{ U(x) \in L^2([0, 2\pi]) \mid \|U\|_{H^s} < \infty \right\}.$$

We also require the dual space of $H^s([0, 2\pi])$, which is characterized by Theorem 8.10 of (42), that is typically denoted $H^{-s}([0, 2\pi])$. If $U' \in (H^s)' = H^{-s}$ then $\|U'\|_{H^{-s}}$ is defined by (Equation 3.5) where $\widehat{U'}_p = U'(\hat{U}_p)$.

With this definition we state the following Lemma.

Lemma 3.1.1. *For any $s \in \mathbf{R}$ there exist constants $C_Q, C_S > 0$ such that*

$$\left\| Q_0 I^{(u)} \right\|_{H^s} \leq C_Q \left\| I^{(u)} \right\|_{H^s}, \quad \left\| S_0 I^{(w)} \right\|_{H^s} \leq C_S \left\| I^{(w)} \right\|_{H^s},$$

for any $I^{(u)}, I^{(w)} \in H^s$.

We also recall, for any integer $s \geq 0$, the space of s–times continuously differentiable functions with the Hölder norm

$$|f|_{C^s} = \max_{0 \leq \ell \leq s} \left| \partial_x^\ell f \right|_{L^\infty}.$$

For later reference we recall the classical result.

Lemma 3.1.2. *For any integer $s \geq 0$, any $\delta > 0$, and any set $\Omega \subset \boldsymbol{R}^m$, if $f, u, g, \mu : \Omega \to \boldsymbol{C}$, $f \in C^s(\Omega)$, $u \in H^s(\Omega)$, $g \in C^{s+1/2+\delta}(\Omega)$, $\mu \in H^{s+1/2}(\Omega)$, then*

$$\|fu\|_{H^s} \leq \tilde{M}(m, s, \Omega) \, |f|_{C^s} \, \|u\|_{H^s} . \qquad \|g\mu\|_{H^{s+1/2}} \leq \tilde{M}(m, s, \Omega) \, |g|_{C^{s+1/2+\delta}} \, \|\mu\|_{H^{s+1/2}} ,$$

for some constant $\tilde{M}$.

In addition, we require the analogous result valid for any real value of s (43; 44).

Lemma 3.1.3. *For any $s \in \boldsymbol{R}$ and any set $\Omega \subset \boldsymbol{R}^m$, if $\varphi, \psi : \Omega \to \boldsymbol{C}$, $\varphi \in H^{|s|+m+2}(\Omega)$ and $\psi \in H^s(\Omega)$, then*

$$\|\varphi\psi\|_{H^s} \leq M(m, s, \Omega) \, \|\varphi\|_{H^{|s|+m+2}} \, \|\psi\|_{H^s} .$$

for some constant M.

Remark 3.1.4. Later in this chapter, we will be required to estimate terms of the form

$$\|(\partial_\theta f)u\|_{L^2(\Omega)} = \|(\partial_\theta f)u\|_{H^0(\Omega)} , \quad \|(\partial_\theta f)\mu\|_{H^{-1/2}([0,2\pi])} ,$$

where $\Omega \subset \mathbf{R}^2$, which feature Sobolev norms too weak for the standard algebra estimate, Lemma 3.1.2. For this reason we have introduced Lemma 3.1.3 which allows us to compute, for $m = 2$,

$$\|(\partial_\theta f)u\|_{L^2(\Omega)} = \|(\partial_\theta f)u\|_{H^0(\Omega)}$$

$$\leq M \, \|(\partial_\theta f)\|_{H^{|0|+2+2}([0,2\pi])} \, \|u\|_{H^0(\Omega)}$$

$$\leq M \, \|f\|_{H^5([0,2\pi])} \, \|u\|_{H^0(\Omega)} \,,$$

while, for $m = 1$,

$$\|(\partial_\theta f)\mu\|_{H^{-1/2}([0,2\pi])} \leq M \, \|(\partial_\theta f)\|_{H^{|-1/2|+1+2}([0,2\pi])} \, \|\mu\|_{H^{-1/2}([0,2\pi])}$$

$$\leq M \, \|f\|_{H^{4+1/2}([0,2\pi])} \, \|\mu\|_{H^{-1/2}([0,2\pi])} \,.$$

In this way, if we require $f \in H^5([0, 2\pi])$ then we can use the algebra property of Lemma 3.1.3 throughout our developments. We note that, by Sobolev embedding, if $f \in H^5([0, 2\pi])$ then $f \in C^4([0, 2\pi])$, and if $f \in C^5([0, 2\pi])$ then $f \in H^5([0, 2\pi])$.

3.2   Main Theorem: Analyticity of Solutions

We can now state the rigorous analysis of (Equation 3.3) for which we utilize the general theory of analyticity of solutions of linear systems of equations. We follow the developments found in (36) for the solution of (Equation 1.17). Given the expansions (Equation 3.2) we seek

the solution of the form (Equation 3.3) which satisfies (Equation 3.4). We restate the main result here.

Theorem 3.2.1 (Nicholls (36)). *Given two Banach spaces X and Y, suppose that:*

(H1) $\mathbf{R}_n \in Y$ *for all $n \geq 0$, and there exist constants $C_R > 0$, $B_R > 0$ such that*

$$\|\mathbf{R}_n\|_Y \leq C_R B_R^n, \quad n \geq 0.$$

(H2) $\mathbf{A}_n : X \to Y$ *for all $n \geq 0$, and there exists constants $C_A > 0$, $B_A > 0$ such that*

$$\|\mathbf{A}_n\|_{X \to Y} \leq C_A B_A^n, \quad n \geq 0.$$

(H3) $\mathbf{A}_0^{-1} : Y \to X$, *and there exists a constant $C_e > 0$ such that*

$$\left\|\mathbf{A}_0^{-1}\right\|_{Y \to X} \leq C_e.$$

Then the equation (Equation 1.17) *has a unique solution* (Equation 3.3), *and there exist constants $C_V > 0$ and $B_V > 0$ such that*

$$\|\mathbf{V}_n\|_X \leq C_V B_V^n, \quad n \geq 0,$$

for any

$$C_V \geq 2C_e C_R, \quad B_V \geq \max\{B_R, 2B_A, 4C_e C_A B_A\},$$

which implies that, for any $0 \leq \rho < 1$, (Equation 3.3) converges for all ε such that $B_V \varepsilon < \rho$,

i.e., $\varepsilon < \rho/B_V$.

All that remains is to find the forms (Equation 3.2), and establish Hypotheses (H1), (H2), and (H3). For the latter it is quite clear that

$$\mathbf{A}_0 = \begin{pmatrix} I & S_0 \\ Q_0 & I \end{pmatrix}, \quad \mathbf{A}_n = \begin{pmatrix} 0 & S_n \\ Q_n & 0 \end{pmatrix}, \quad n \geq 1; \quad \mathbf{V}_n = \begin{pmatrix} I_n^{(u)} \\ I_n^{(w)} \end{pmatrix}, \quad \mathbf{R}_n = \begin{pmatrix} \xi_n \\ \nu_n \end{pmatrix}.$$

For the spaces X and Y, the natural choices for the weak formulation we pursue here are

$$X = Y = H^{-1/2} \times H^{-1/2},$$

so that

$$\left\| \begin{pmatrix} I^{(u)} \\ I^{(w)} \end{pmatrix} \right\|_X^2 = \left\| I^{(u)} \right\|_{H^{-1/2}}^2 + \left\| I^{(w)} \right\|_{H^{-1/2}}^2.$$

Hypothesis (H1): We begin by noting that

$$\xi_n = -\tau^u \psi_n + Y \zeta_n, \quad \nu_n = -\tau^u \psi_n + Z \zeta_n,$$

where

$$\zeta_n = -e^{ik^u \bar{g} \sin(\phi - \theta)} \left[(ik^u) \sin(\phi - \theta) \right]^n F_n, \quad F_n := \frac{f^n}{n!},$$

and

$$\psi_n = \bar{g}\left[(ik^u)\sin(\phi - \theta)\right]\zeta_n + (ik^u)\left[f\sin(\phi - \theta) + (\partial_\theta f)\cos(\phi - \theta)\right]\zeta_{n-1}.$$

Now, if $Y : H^{1/2} \to H^{-1/2}$ and $Z : H^{1/2} \to H^{-1/2}$, then

$$\|\mathbf{R}_n\|_Y^2 = \|\xi_n\|_{H^{-1/2}}^2 + \|\nu_n\|_{H^{-1/2}}^2 = \|-\tau^u\psi_n + Y\zeta_n\|_{H^{-1/2}}^2 + \|-\tau^u\psi_n + Z\zeta_n\|_{H^{-1/2}}^2$$

$$\leq 2\left|\tau^u\right|^2 \|\nu_n\|_{H^{-1/2}}^2 + (C_Y + C_Z)\|\xi_n\|_{H^{1/2}}^2.$$

An induction is needed, while from the explanation given in Remark 3.1.4, this is bounded provided that $f \in H^5([0, 2\pi])$.

Hypothesis (H2): The analyticity estimates for the IIOs Q, Theorem 3.3.6, and S, Theorem 3.3.1, show rather directly that Hypothesis (H2) is verified provided that our configuration is δ–permissible, i.e.,

$$(k^u, \bar{g}, R^o, Y/(\tau^u\bar{g}), -T^{(u)}) \in \mathcal{C}_\delta(k^u, \bar{g}, R^o, Y/(\tau^u\bar{g}), -T^{(u)}), \qquad (3.6a)$$

$$(0, \bar{g}, R^o, Y/(\tau^u\bar{g}), -T^{(u)}) \in \mathcal{C}_\delta(0, \bar{g}, R^o, Y/(\tau^u\bar{g}), -T^{(u)}), \qquad (3.6b)$$

$$(k^w, R_i, \bar{g}, T^{(w)}, Z/(\tau^w\bar{g})) \in \mathcal{C}_\delta(k^w, R_i, \bar{g}, T^{(w)}, Z/(\tau^w\bar{g})), \qquad (3.6c)$$

$$(0, R_i, \bar{g}, T^{(w)}, Z/(\tau^w\bar{g})) \in \mathcal{C}_\delta(0, R_i, \bar{g}, T^{(w)}, Z/(\tau^w\bar{g})), \qquad (3.6d)$$

see Appendix B for details. Indeed, as we have

$$\left\|Q_n[I^{(u)}]\right\|_{H^{-1/2}} \leq C_Q B_Q^n, \quad \left\|S_n[I^{(w)}]\right\|_{H^{-1/2}} \leq C_S B_S^n,$$

it is a straightforward matter to show that

$$\|\mathbf{A}_n\|_{X \to Y} \le C_A B_A^n,$$

for $C_A = \max\{C_Q, C_S\}$ and $B_A = \max\{B_Q, B_S\}$.

Hypothesis (H3): We now address the existence and invertibility properties of the linearized operator $\mathbf{A}_0$ in the following Lemma.

Lemma 3.2.2. *If $\xi, \nu \in H^{-1/2}([0, 2\pi])$ then there exists a unique solution of*

$$\begin{pmatrix} I & S_0 \\ Q_0 & I \end{pmatrix} \begin{pmatrix} I^{(u)} \\ I^{(w)} \end{pmatrix} = \begin{pmatrix} \xi \\ \nu \end{pmatrix},$$

c.f. (Equation 2.5), satisfying

$$\left\| I^{(u)} \right\|_{H^{-1/2}} \le C_e \left\{ \|\xi\|_{H^{-1/2}} + \|\nu\|_{H^{-1/2}} \right\},$$

$$\left\| I^{(w)} \right\|_{H^{-1/2}} \le C_e \left\{ \|\xi\|_{H^{-1/2}} + \|\nu\|_{H^{-1/2}} \right\},$$

for some universal constant $C_e > 0$.

Proof. If we expand

$$\xi(\theta) = \sum_{p=-\infty}^{\infty} \hat{\xi}_p e^{ip\theta}, \quad \nu(\theta) = \sum_{p=-\infty}^{\infty} \hat{\nu}_p e^{ip\theta},$$

then we can find solutions of (Equation 2.5)

$$I^{(u)}(\theta) = \sum_{p=-\infty}^{\infty} \left(\widehat{I^{(u)}}\right)_p e^{ip\theta}, \quad I^{(w)}(\theta) = \sum_{p=-\infty}^{\infty} \left(\widehat{I^{(w)}}\right)_p e^{ip\theta},$$

where

$$\begin{pmatrix} \left(\widehat{I^{(u)}}\right)_p \\ \left(\widehat{I^{(w)}}\right)_p \end{pmatrix} = \frac{1}{1 - \widehat{(S_0)}_p \widehat{(Q_0)}_p} \begin{pmatrix} 1 & -\widehat{(S_0)}_p \\ -\widehat{(Q_0)}_p & 1 \end{pmatrix} \begin{pmatrix} \widehat{(\xi_0)}_p \\ \widehat{(\nu_0)}_p \end{pmatrix},$$

c.f. (Equation 2.8). The key is the analysis of the operators $\widehat{(S_0)}_p$, $\widehat{(Q_0)}_p$, and the determinant function

$$\Delta_p = 1 - \widehat{(S_0)}_p \widehat{(Q_0)}_p,$$

which is equivalent to $\tilde{\Delta}_p$ in (Equation 2.3). From their asymptotic properties, there exist constants $\tilde{K}_Q, \tilde{K}_S, \tilde{K}_\Delta > 0$ such that

$$\left|\widehat{(Q_0)}_p\right| < \tilde{K}_Q, \quad \left|\widehat{(S_0)}_p\right| < \tilde{K}_S, \quad \frac{1}{|\Delta_p|} < \tilde{K}_\Delta.$$

With this we can estimate

$$\begin{aligned} \left\|I^{(u)}\right\|_{H^{-1/2}}^2 &= \sum_{p=-\infty}^{\infty} \langle p \rangle^{-1} \left|\left(\widehat{I^{(u)}}\right)_p\right|^2 \\ &< \sum_{p=-\infty}^{\infty} \langle p \rangle^{-1} \tilde{K}_\Delta^2 \left(\left|\hat{\xi}_p\right|^2 + \tilde{K}_S^2 |\hat{\nu}_p|^2\right) \\ &= \tilde{K}\left(\|\xi\|_{H^{-1/2}}^2 + \|\nu\|_{H^{-1/2}}^2\right), \end{aligned}$$

for some $\tilde{K} > 0$. Proceeding similarly for W we complete the proof. □

Having established Hypotheses (H1), (H2), and (H3) we can invoke Theorem 3.2.1 to discover our final result.

Theorem 3.2.3. *If $f \in H^5([0, 2\pi])$ and the configuration is δ–permissible there exists a unique solution pair, (Equation 3.3), of the problem, (Equation 1.17), satisfying*

$$\left\| I_n^{(u)} \right\|_{H^{-1/2}} \leq C_U D^n, \quad \left\| I_n^{(w)} \right\|_{H^{-1/2}} \leq C_W D^n, \quad \forall n \geq 0,$$

for any $D > \|f\|_{H^5}$ where C_U and C_W are universal constants.

3.3 Analyticity of the Impedance–Impedance Operators

At this point, the only remaining task is to establish the analyticity of the IIOs, Q and S. This has been accomplished for the DNO $G^{(u)}$ in (44) so we consider the operator S on the interior domain. We focus on the dielectric case $\epsilon^{(w)} \in \mathbf{R}$ so that $k^w \in \mathbf{R}$. Given this assumption we prove the following result.

Theorem 3.3.1. *If $f \in H^5([0, 2\pi])$, the configuration is δ–permissible, (Equation 3.6), and $I^{(w)} \in H^{-1/2}([0, 2\pi])$ then the series (Equation 3.1b) converges strongly as an operator from $H^{-1/2}([0, 2\pi])$ to $H^{-1/2}([0, 2\pi])$. In other words there exist constants $K_S > 0$ and $B_S > 0$ such that*

$$\left\| S_n(f)[I^{(w)}] \right\|_{H^{-1/2}} \leq K_S B_S^n. \tag{3.7}$$

We present this result with the method of Transformed Field Expansions (TFE) (45; 46; 47) which has proven quite successful in establishing analyticity of the DNOs (28; 44). We establish analyticity of the field, then the IIO, S. We rewrite the (Equation 2.14) as

$$\Delta v_n + (k^w)^2 \, v_n = F_n^{\text{in}}, \qquad\qquad R_i < r < \bar{g}, \qquad (3.8\text{a})$$

$$\partial_r v_n - \frac{Z}{\tau^w \bar{g}} v_n = \frac{\delta_{n,0} I^{(w)}}{\tau^w \bar{g}} + \frac{L_n^{\text{in}}}{\tau^w \bar{g}}, \qquad r = \bar{g}, \qquad (3.8\text{b})$$

$$\partial_r v_n - T^{(w)} \, [v_n] = h_n^{\text{in}}, \qquad\qquad r = R_i. \qquad (3.8\text{c})$$

Our main result is the following analyticity theorem

Theorem 3.3.2. *If $f \in H^5([0, 2\pi])$, the configuration is δ–permissible, (Equation 3.6), and $I^{(w)} \in H^{-1/2}([0, 2\pi])$ then the series (Equation 2.22) converges strongly. In other words there exsit constants $K_v > 0$ and $B_S > 0$ such that*

$$\|v_n\|_{H^1(\Omega_{R_i, \bar{g}})} \le K_v B_S^n. \qquad (3.9)$$

The proof of Theorem 3.3.2 proceeds by applying an elliptic estimate Lemma (Lemma 3.3.3) to (Equation 3.8) and then a recursive Lemma (Lemma 3.3.5).

Lemma 3.3.3. *Suppose the configuration is δ–permissible, (Equation 3.6), $F_n^{in} \in (H^1(\Omega_{R_i,\bar{g}}))'$, $I^{(w)} \in H^{-1/2}([0, 2\pi])$, $L_n^{in} \in H^{-1/2}([0, 2\pi])$, and $h_n^{in} \in H^{-1/2}([0, 2\pi])$. Then there is a unique solution of* (Equation 3.8) *satisfying*

$$\|v_n\|_{H^1} \leq C_e \big\{ \|F_n^{in}\|_{(H^1)'} + \delta_{n,0} \|I^{(w)}\|_{H^{-1/2}} + \|L_n^{in}\|_{H^{-1/2}} + \|h_n^{in}\|_{H^{-1/2}} \big\}, \qquad (3.10)$$

for some universal constant C_e.

Proof. We apply the elliptic estimate Theorem B.3.1 and for this we only need to show

$$\mathrm{Re}\left\{ \left(\widehat{T^{(w)}}\right)_p \right\} \geq 0, \quad \mathrm{Re}\left\{ \frac{\hat{Z}_p}{\tau^w \bar{g}} \right\} \leq 0, \quad \left|\mathrm{Im}\left\{ \left(\widehat{T^{(w)}}\right)_p \right\}\right| < \infty, \quad \left|\mathrm{Im}\left\{ \frac{\hat{Z}_p}{\tau^w \bar{g}} \right\}\right| < \infty, \quad (3.11)$$

for $p \neq 0$. Note that Z is free to be chosen, and in the work of Despres (39; 40) it was selected to be $-i\eta$ for a constant $\eta \in \mathbf{R}^+$. With this choice the second and fourth conditions in (Equation 3.11) are automatically satisfied if we assume k^w (and thus τ^w) is real and positive.

Recall that

$$\left(\widehat{T^{(w)}}\right)_p = k^w \frac{J_p'(k^w R_i)}{J_p(k^w R_i)}.$$

The identity $J_{-n}(z) = (-1)^n J_n(z)$ implies that

$$\left(\widehat{T^{(w)}}\right)_{-p} = k^w \frac{J_{-p}'(k^w R_i)}{J_{-p}(k^w R_i)} = k^w \frac{(-1)^p J_p'(k^w R_i)}{(-1)^p J_p(k^w R_i)} = \left(\widehat{T^{(w)}}\right)_p,$$

hence it suffices to consider $\left(\widehat{T^{(w)}}\right)_p$ with $p > 0$. We notice that both $J_p(k^w R_i)$ and $J_p'(k^w R_i)$

are real-valued for real arguments $k^w R_i$, which shows that

$$\left| \text{Im} \left\{ \left(\widehat{T^{(w)}}\right)_p \right\} \right| = \left| \text{Im} \left\{ k^w \frac{J_p'(k^w R_i)}{J_p(k^w R_i)} \right\} \right| = 0 < \infty.$$

Let $\{j_p\}_{p=1}^{\infty} = \{j_1, j_2, \dots\}$ be the first (smallest) zero of Bessel's function of order p, $\{J_p(z)\}$,

and $\{j_p'\}_{p=1}^{\infty} = \{j_1', j_2', \dots\}$ be the first (smallest) zero of the first order derivative of Bessel's

function of order p, $\{J_p'(z)\}$. From (48, Eq. 10.21.3 and Eq. 10.14.2), we have

$$p \leq j_p, \quad \text{and} \quad J_p(p) > 0, \quad \forall p \geq 1.$$

Additionally, we notice that $J_p(0) = 0, \forall p \geq 1$. Thus, for a fixed p, $J_p(z)$ is positive over the

interval $(0, j_p)$ which contains $(0, p)$.

Next we apply the Mean Value Theorem over the interval $(0, p)$: There exists an x in $(0, p)$

such that

$$J_p'(x) = \frac{J_p(p) - J_p(0)}{p - 0} = \frac{J_p(p)}{p} > 0.$$

From (48, Eq. 10.21.3) we have $p \leq j_p'$ and $J_p'(0) = 0$ for all $p \geq 1$, thus we can conclude that

$J_p'(z)$ is positive over the interval $(0, j_p')$ which contains $(0, p)$.

We finish the proof by taking the interval $(0, 1)$, which is contained in the interval $(0, p)$ for all $p \geq 1$, and choosing R_i such that $0 < k^w R_i < 1$. Then we have

$$\mathrm{Re}\left\{\left(\widehat{T^{(w)}}\right)_p\right\} = \left(\widehat{T^{(w)}}\right)_p = k^w \frac{J_p'(k^w R_i)}{J_p(k^w R_i)} \geq 0.$$

$\square$

Remark 3.3.4. We note that the first condition in (Equation 3.11) is false at $p = 0$ as $J_0'(z) = -J_1(z)$ which necessitates the condition $p \neq 0$.

To control the right-hand side of (Equation 3.8) we prove the following.

Lemma 3.3.5. *Suppose $f \in H^5([0, 2\pi])$ and the configuration is δ–permissible, (Equation 3.6). Assume that*

$$\|v_n\|_{H^1(\Omega_{R_i, \bar{g}})} \leq K_v B_S^n, \quad \forall n < N, \tag{3.12}$$

for constants $K_v > 0$ and $B_S > 0$, then there exists a constant $C_v > 0$ such that

$$\left\|F_N^{in}\right\|_{(H^1(\Omega_{R_i, \bar{g}}))'} \leq K_v \|f\|_{H^5} C_v B_S^{N-1},$$

$$\left\|h_N^{in}\right\|_{H^{-1/2}([0, 2\pi])} \leq K_v \|f\|_{H^5} C_v B_S^{N-1},$$

$$\left\|L_N^{in}\right\|_{H^{-1/2}([0, 2\pi])} \leq K_v \|f\|_{H^5} C_v B_S^{N-1}.$$

Proof. Note that from (Equation 2.24) and Appendix B.1

$$\left\|F_N^{in}\right\|_{(H^1)'} \leq \left\|F_n^{in,(0)}\right\|_{L^2} + \left\|F_n^{in,(r)}\right\|_{L^2} + \left\|F_n^{in,(\theta)}\right\|_{L^2},$$

and, for conciseness, we consider the third term only; the other cases follow in an identical manner. For this estimate, using the Lemma 3.1.3

$$
\begin{aligned}
\left\|F_n^{\text{in},(\theta)}\right\|_{L^2} &\leq \|2(\bar{g}-R_i)f\partial_\theta v_{N-1}\|_{L^2} + \left\|(\bar{g}-R_i)f'(r-R_i)\partial_r v_{N-1}\right\|_{L^2} \\
&\quad + \left\|f^2\partial_\theta v_{N-2}\right\|_{L^2} + \left\|ff'(r-R_i)\partial_r v_{N-2}\right\|_{L^2} \\
&\leq 2(\bar{g}-R_i)M\|f\|_{H^4}\|v_{N-1}\|_{H^1} + (\bar{g}-R_i)M\|f\|_{H^5}\mathcal{R}\|v_{N-1}\|_{H^1} \\
&\quad + M^2\|f\|_{H^4}^2\|v_{N-2}\|_{H^1} + M^2\|f\|_{H^4}\|f\|_{H^5}\mathcal{R}\|v_{N-2}\|_{H^1} \\
&\leq K_v\|f\|_{H^5}(C_v/3)B_S^{N-1},
\end{aligned}
$$

where $\mathcal{R}$ is defined by

$$
\|(r-R_i)v\|_{H^0} \leq \mathcal{R}\|v\|_{H^0},
$$

and we are done if C_v is chosen appropriately and $B_S > \|f\|_{H^5}$.

For h_N^{in} (Equation 2.26) we conduct the following sequence of steps

$$
\begin{aligned}
\left\|h_N^{\text{in}}\right\|_{H^{-1/2}} &\leq \left\|\frac{f}{\bar{g}-R_i}T^{(w)}[v_{N-1}]\right\|_{H^{-1/2}} \leq \frac{M}{\bar{g}-R_i}\|f\|_{H^{4+1/2}}\left\|T^{(w)}v_{N-1}\right\|_{H^{-1/2}} \\
&\leq \frac{M}{\bar{g}-R_i}\|f\|_{H^5}C_{T^{(w)}}\|v_{N-1}\|_{H^{1/2}} \\
&\leq \frac{MC_{T^{(w)}}}{\bar{g}-R_i}\|f\|_{H^5}C_t\|v_{N-1}\|_{H^1(\Omega_{R_i,\bar{g}})} \leq \frac{MC_{T^{(w)}}}{\bar{g}-R_i}\|f\|_{H^5}C_tK_vB_S^{N-1},
\end{aligned}
$$

where $C_{T^{(w)}}$ is the bounding constant for the operator $T^{(w)}$, and C_t is the bounding constant

for the trace operator

$$\|v\|_{H^{s+1/2}([0,2\pi])} \leq C_t \|v\|_{H^{s+1}(\Omega_{R_i,\bar{g}})} .$$

We are done if we select C_v large enough.

Regarding the terms L_N^{in} (Equation 2.25) we focus on a single term

$$\mathcal{L} := \frac{1}{\bar{g}(\bar{g} - R_i)(\tau^w \bar{g})} \left\{ -\tau^w(\bar{g} - R_i)(f')^2 \partial_r v_{N-2} \right\} = -\frac{1}{\bar{g}^2}(f')^2 \partial_r v_{N-2},$$

and make the estimate

$$
\begin{aligned}
\|\mathcal{L}\|_{H^{-1/2}} &= \left\| -\frac{1}{\bar{g}^2}(f')^2 \partial_r v_{N-2} \right\|_{H^{-1/2}} \\
&\leq \frac{M^2}{\bar{g}^2} \|f\|^2_{H^{4+1/2}} \|\partial_r v_{N-2}\|_{H^{-1/2}} \\
&\leq \frac{M^2}{\bar{g}^2} \|f\|^2_{H^{4+1/2}} C_t \|v_{N-2}\|_{H^1} \\
&\leq \frac{M^2 C_t}{\bar{g}^2} \|f\|^2_{H^5} K_v B_S^{N-2},
\end{aligned}
$$

and we are done if C_v is chosen well and $B_S > \|f\|_{H^5}$. □

We can now present the proof of Theorem 3.3.2

Proof. (Theorem 3.3.2). We work by induction and begin with $n = 0$. The estimate on v_0 follows directly from Lemma 3.3.3 with F and L identically zero. We new assume that (Equation 3.9) holds for all $n < N$ and apply Lemma 3.3.3 which implies that

$$\|v_N\|_{H^1} \leq C_e \big\{ \big\|F_N^{\text{in}}\big\|_{(H^1)'} + \big\|L_N^{\text{in}}\big\|_{H^{-1/2}} + \big\|h_N^{\text{in}}\big\|_{H^{-1/2}} \big\}.$$

Using Lemma 3.3.5 we have

$$\|v_N\|_{H^1} \leq C_e 3 K_v C_v \|f\|_{H^5} B_S^{N-1} \leq K_v B_S^N,$$

provided that we choose

$$3 C_e C_v \|f\|_{H^5} < B_S.$$

$\square$

Finally, we establish Theorem 3.3.1.

Proof. (Theorem 3.3.1). From (Equation 2.27) and applying Lemma 3.3.2, it is straightforward to demonstrate that

$$\left\|S_0(f)[I^{(w)}]\right\|_{H^{-1/2}} \leq \|\tau^w \bar{g} \partial_r v_0 - Y v_0\|_{H^{s-1/2}} \leq \|\tau^w \bar{g} \partial_r v_0\|_{H^{-1/2}} + \|Y v_0\|_{H^{-1/2}}$$

$$\leq |\tau^w| \bar{g} \|v_0\|_{H^{1/2}} + C_Y \|v_0\|_{H^{1/2}}$$

$$\leq (|\tau^w| \bar{g} + C_Y) C_t \|v_0\|_{H^1}$$

$$\leq (|\tau^w| \bar{g} + C_Y) C_t K_v \leq K_S,$$

if $K_S > 0$ is chosen appropriately.

Assuming that (Equation 3.7) holds for all $n < N$ we now investigate an estimate of S_N. For simplicity we consider consider the single term

$$\mathcal{S} := \tau^w \left(\frac{-f(f')}{\bar{g}(\bar{g} - R_i)} \right) \partial_\theta v_{N-2},$$

and we measure

$$\|\mathcal{S}\|_{H^{-1/2}} \left\| \tau^w \left(\frac{-f(f')}{\bar{g}(\bar{g} - R_i)} \right) \partial_\theta v_{N-2} \right\|_{H^{-1/2}}$$

$$\leq |\tau^w| \frac{M^2}{\bar{g}(\bar{g} - R_i)} \|f\|_{H^{4+1/2}}^2 \|v_{N-2}\|_{H^{-1/2}}$$

$$\leq |\tau^w| \frac{M^2}{\bar{g}(\bar{g} - R_i)} \|f\|_{H^5}^2 C_t \|v_{N-2}\|_{H^1}$$

$$\leq |\tau^w| \frac{M^2}{\bar{g}(\bar{g} - R_i)} \|f\|_{H^5}^2 C_t K_v B_S^{N-2}.$$

We are done provided that

$$K_S > |\tau^w| \frac{M^2}{\bar{g}(\bar{g} - R_i)} C_t K_v, \quad B_S > \|f\|_{H^5}.$$

$\square$

In an analogous manner, the analyticity of Q is stated in the following theorem.

Theorem 3.3.6. *If $f \in H^5([0, 2\pi])$, the configuration is δ–permissible, (Equation 3.6), and $I^{(u)} \in H^{-1/2}([0, 2\pi])$ then the series (Equation 3.1a) converges strongly as an operator from $H^{-1/2}([0, 2\pi])$ to $H^{-1/2}([0, 2\pi])$. In other words there exist constants $K_Q > 0$ and $B_Q > 0$ such that*

$$\left\| Q_n(f)[I^{(u)}] \right\|_{H^{-1/2}} \leq K_Q B_Q^n.$$

The proof proceeds in a similar fashion to that of Theorem 3.3.1. The crucial difference lies in the elliptic estimate, c.f. Lemma 3.3.3, which in this case requires

$$\mathrm{Re}\left\{ \frac{\hat{Y}_p}{\tau^u \bar{g}} \right\} \geq 0, \quad \mathrm{Re}\left\{ \left(-\widehat{T^{(u)}} \right)_p \right\} \leq 0, \quad \left| \mathrm{Im}\left\{ \frac{\hat{Y}_p}{\tau^u \bar{g}} \right\} \right| < \infty, \quad \left| \mathrm{Im}\left\{ \left(-\widehat{T^{(u)}} \right)_p \right\} \right| < \infty.$$

As before, the operator Y is free to be chosen and we again follow Despres (39; 40) who selected $i\eta$ for a constant $\eta \in \mathbf{R}^+$. As k^u, and therefore τ^u, are real and positive, the first and third conditions are satisfied. For the other conditions we note that

$$\left(\widehat{T^{(u)}} \right)_p = -k^u \frac{H_p'(k^u R^o)}{H_p(k^u R^o)},$$

and recall that Shen and Wang (49) established

$$0 < \mathrm{Im} \left\{ \frac{H'_p(k^u R^o)}{H_p(k^u R^o)} \right\} < 1, \quad p \neq 0,$$

c.f. (2.34a) and (2.34c) in (49). So for a fixed R^o we have

$$\left| \mathrm{Im} \left\{ \left(-\widehat{T^{(u)}} \right)_p \right\} \right| < \infty, \quad \forall p,$$

while (2.34b) of (49) delivers

$$\frac{p}{R^o} \geq \mathrm{Re} \left\{ -k^u \frac{H'_p(k^u R^o)}{H_p(k^u R^o)} \right\} \geq \frac{1}{2R^o} > 0, \quad p \neq 0.$$

Therefore

$$\mathrm{Re} \left\{ \left(-\widehat{T^{(u)}} \right)_p \right\} \leq 0, \quad p \neq 0.$$

CHAPTER 4

NUMERICAL SIMULATIONS

In this chapter, we present results of simulations of our implementations of the algorithms stated above. The schemes are essentially High–Order Spectral (HOS) approaches (14; 15; 13) with products approximated by convolutions implemented by the Fast Fourier Transform.

4.1 Implementation Details

The numerical approaches we describe in this chapter utilize either the Dirichlet–Neumann operator (DNO) formulation of the problem (Equation 1.7 and Equation 1.8) or the Impedance–Impedance operator (IIO) formulation (Equation 1.14 and Equation 1.15). To simulate these DNO and IIO we use either the FE method § 2.3 or the TFE method § 2.4 which are Fourier collocation/Taylor methods (46; 27) enhanced by Padé summation (50). In more detail we approximate $\{U, W\}$ by

$$
U_{N_\theta, N}(r, \theta) := \sum_{n=0}^{N} \sum_{p=-N_\theta/2}^{N_\theta/2-1} \hat{U}_{n,p} e^{ip\theta} \varepsilon^n, \quad W_{N_\theta, N}(r, \theta) := \sum_{n=0}^{N} \sum_{p=-N_\theta/2}^{N_\theta/2-1} \hat{W}_{n,p} e^{ip\theta} \varepsilon^n,
$$

and $\{I^{(u)}, I^{(w)}\}$ by

$$
\left\{ I^{(u)}, I^{(w)} \right\} \approx \left\{ \left[I^{(u)} \right]_{N_\theta, N}, \left[I^{(w)} \right]_{N_\theta, N} \right\} := \sum_{n=0}^{N} \sum_{p=-N_\theta/2}^{N_\theta/2-1} \left\{ \left(\widehat{I^{(u)}} \right)_{n,p}, \left(\widehat{I^{(w)}} \right)_{n,p} \right\} e^{ip\theta} \varepsilon^n.
$$

The TFE approach requires an additional discretization in the radial direction which we achieve by a Chebyshev collocation scheme. An important consideration is how the series in ε are summed. The classical numerical analytic continuation technique of Padé approximation (50) has been successfully brought to bear upon HOPS methods in the past (see, e.g., (23; 47)), and we will use it here.

4.2   The Method of Manufactured Solutions

Before proceeding to our numerically simulations, we validate our code using the Method of Manufactured Solutions (MMS) (51; 52; 53). To summarize the MMS, when solving a system of partial differential equations subject to boundary conditions for an unknown, v, say

$$\mathcal{P}v = 0, \qquad\qquad \text{in } \Omega, \qquad\qquad (4.1a)$$

$$\mathcal{B}v = 0, \qquad\qquad \text{at } \partial\Omega, \qquad\qquad (4.1b)$$

it is typically just as easy to implement an algorithm to solve the "inhomogenous" versions of the above,

$$\mathcal{P}v = \mathcal{F}, \qquad\qquad \text{in } \Omega, \qquad\qquad (4.2a)$$

$$\mathcal{B}v = \mathcal{J}, \qquad\qquad \text{at } \partial\Omega. \qquad\qquad (4.2b)$$

In order to test an implementation, one begins with the "manufactured solution", $\tilde{v}$, and sets

$$\mathcal{F}_{\tilde{v}} := \mathcal{P}\tilde{v}, \quad \mathcal{J}_{\tilde{v}} := \mathcal{B}\tilde{v}.$$

Now, given this pair $\{\mathcal{F}_{\tilde{v}}, \mathcal{J}_{\tilde{v}}\}$ we have an *exact* solution to (Equation 4.2) against which we can compare our numerically simulated solution. While this provides no guarantee of a correct implementation, with a careful choice of $\tilde{v}$, e.g. one which displays the same qualitative behavior as solutions of (Equation 4.1), the approach can give great confidence in the accuracy of a scheme.

For the implementation in question we consider the 2π–periodic, outgoing solutions of the Helmholtz equation, (Equation 1.1a),

$$u^q(r,\theta) = A_u^q H_q(k^u r) e^{iq\theta}, \quad q \in \mathbf{Z}, \quad A_u^q \in \mathbf{C},$$

and the bounded counterpart for (Equation 1.1b)

$$w^q(r,\theta) = A_w^q J_q(k^w r) e^{iq\theta}, \quad q \in \mathbf{Z}, \quad A_w^q \in \mathbf{C}.$$

The parameters, q, A_u^q, and A_w^q are all arbitrary. For any choice of the radius of the interface $\bar{g}$, we define the Dirichlet and Neumann traces

$$U^{\text{exact}}(\theta) := u^q(\bar{g} + g(\theta), \theta), \quad \tilde{U}^{\text{exact}}(\theta) := (-\partial_N u^q)(\bar{g} + g(\theta), \theta),$$

and

$$W^{\text{exact}}(\theta) := w^q(\bar{g} + g(\theta), \theta), \quad \tilde{W}^{\text{exact}}(\theta) := (\partial_N w^q)(\bar{g} + g(\theta), \theta).$$

From these we define, for any real $\eta > 0$ with $Y = i\eta$ and $Z = -i\eta$, the impedances

$$I^{(u),\text{exact}}(\theta) := \tau^u \tilde{U}^{\text{exact}} + i\eta U^{\text{exact}}, \quad \tilde{I}^{(u),\text{exact}}(\theta) := \tau^u \tilde{U}^{\text{exact}} - i\eta U^{\text{exact}},$$

and

$$I^{(w),\text{exact}}(\theta) := \tau^w \tilde{W}^{\text{exact}} + i\eta W^{\text{exact}}, \quad \tilde{I}^{(w),\text{exact}}(\theta) := \tau^w \tilde{W}^{\text{exact}} - i\eta W^{\text{exact}}.$$

4.3 <u>Convergence Study</u>

For our convergence study we select the 2π–periodic and analytic profile

$$f(\theta) = e^{\cos(\theta)}, \tag{4.3}$$

see Figure 3, and with this we first compute the exact surface current, $\tilde{U}^{\text{exact}}$. We make the physical parameter choices

$$q = 2, \quad A_u^q = 2, \quad A_w^q = 1, \quad \bar{g} = 0.025, \quad \varepsilon = 0.002, \tag{4.4a}$$

and numerical parameter choices

$$N_\theta = 64, \quad N = 16, \tag{4.4b}$$
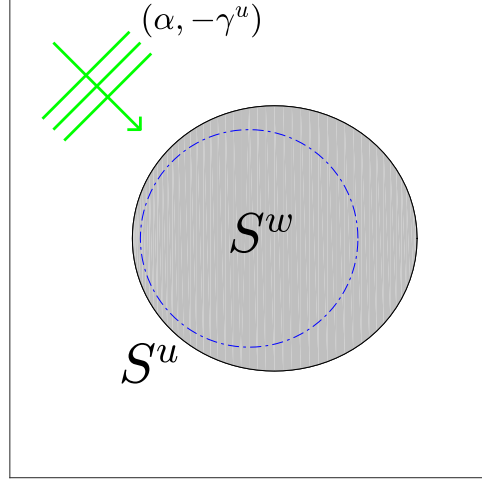
Figure 3. Plot of the cross–section of a dielectric nanorod (occupying S^w) shaped by $r = \bar{g} + \varepsilon \exp(\cos(\theta))$ ($\varepsilon = \bar{g}/5$) housed in a dielectric (occupying S^u) under plane–wave illumination with wavenumber $(\alpha, -\gamma^u)$. The dash–dot blue line depicts the unperturbed geometry, the circle $r = \bar{g}$.

and compute approximations to $\tilde{U}^{\text{exact}}$ by the FE algorithm delivering $\tilde{U}^{\text{FE}}$ and the TFE algorithm delivering $\tilde{U}^{\text{TFE}}$. We measure the relative errors by

$$\text{Error}_{\text{DNO}}^{\text{FE}} = \frac{\left|\tilde{U}^{\text{exact}} - \tilde{U}_{N_\theta,N}^{\text{FE}}\right|_{L^\infty}}{\left|\tilde{U}^{\text{exact}}\right|_{L^\infty}}, \quad \text{Error}_{\text{DNO}}^{\text{TFE}} = \frac{\left|\tilde{U}^{\text{exact}} - \tilde{U}_{N_\theta,N_r,N}^{\text{TFE}}\right|_{L^\infty}}{\left|\tilde{U}^{\text{exact}}\right|_{L^\infty}}. \tag{4.5}$$

We display results of the convergence study in Figure 4 using Taylor and Padé summation, respectively. In these we see not only the reliability and robustness of our approach, but also the extremely rapid, spectral, accuracy of our simulations. Notice that the method using Padé

summation converges faster than Taylor summation. We take the Padé summation results for the rest of our calculations and simulations.
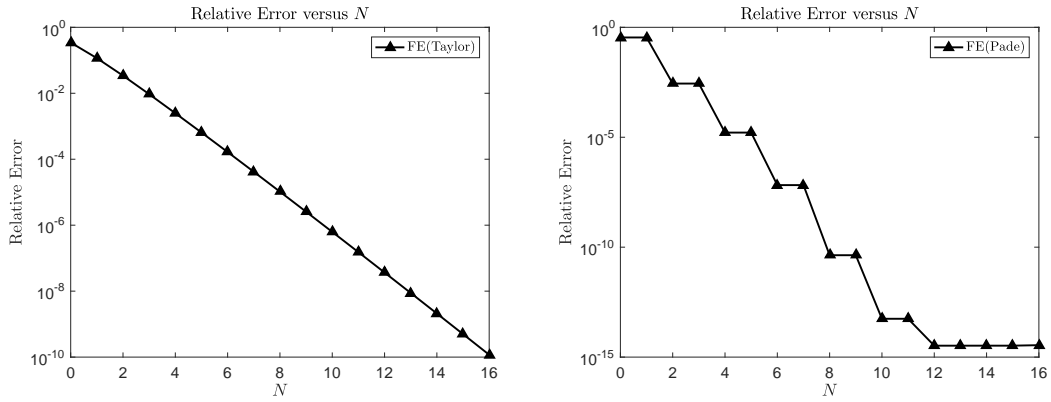
Figure 4. Relative error (Equation 4.5) versus perturbation order for configuration (Equation 4.4a); FE with Taylor and Padé summation .

Next, we reprise the calculation with larger choices of the perturbation parameter, $\varepsilon = 0.02$ and $\varepsilon = 0.05$. We use both the FE and TFE algorithms with the same choice of $f(\theta)$, (Equation 4.3), physical parameters, (Equation 4.4a), and numerical parameters, (Equation 4.4b), supplemented with

$$R_i = \bar{g}/10, \quad R^o = 10\bar{g}, \quad N_r = 64, \quad N = 24.$$

We compute approximations $\{\tilde{U}^{\mathrm{FE}}, \tilde{U}^{\mathrm{TFE}}\}$ and report results in Figure 5, for $\varepsilon = 0.02$ and $\varepsilon = 0.05$, respectively. Again, the fidelity and utility of both approaches is clearly visible in each, but we note the added accuracy and stability which TFE can provide.
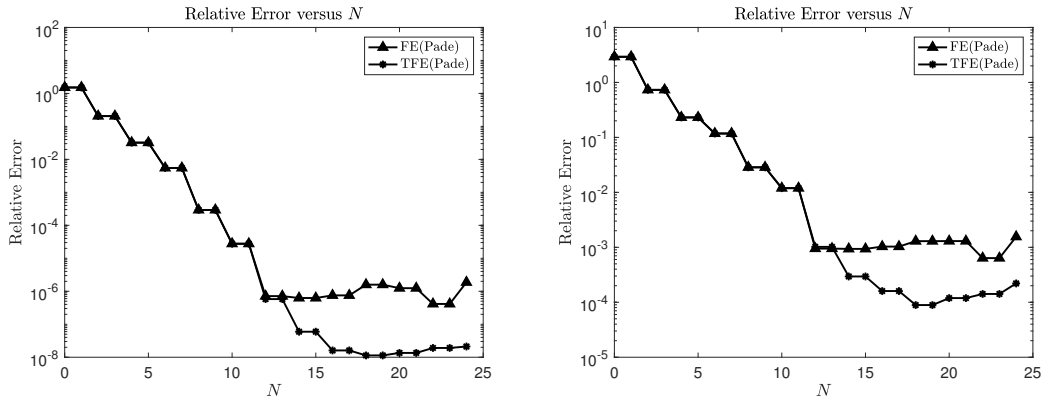
Figure 5. Relative error (Equation 4.5) versus perturbation order; FE and TFE with Padé summation, $\varepsilon = 0.02$ and $\varepsilon = 0.05$.

4.4   Robust Comparison: DNOs versus IIOs

In this section, we demonstrate and compare the behaviors of IIOs and DNOs at, and near, their Dirichlet eigenvalues. We select the following physical parameters

$$q = 2, \quad A_u^q = 2, \quad A_w^q = 1, \quad \eta = 3.4, \quad k^u = 13.9626, \quad k^w = 5.13562230, \tag{4.6}$$

and numerical parameter choices

$$N_\theta = 64, \quad N = 16, \quad N_r = 32. \tag{4.7}$$

We supply the data $\{U^{\text{exact}}, W^{\text{exact}}\}$ to our TFE algorithm to simulate DNOs producing, $\tilde{W}_{N_\theta, N_r, N}$, and $\{I^{(u),\text{exact}}, I^{(w),\text{exact}}\}$ to simulate IIOs producing, $\tilde{I}^{(w)}_{N_\theta, N_r, N}$. Here we also compute the relative error

$$\text{Error}^{\text{DNO}} = \frac{\left| \tilde{W}^{\text{exact}} - \tilde{W}_{N_\theta, N_r, N} \right|_{L^\infty}}{\left| \tilde{W}^{\text{exact}} \right|_{L^\infty}}, \quad \text{Error}^{\text{IIO}} = \frac{\left| \tilde{I}^{(w),\text{exact}} - \tilde{I}^{(w)}_{N_\theta, N_r, N} \right|_{L^\infty}}{\left| \tilde{I}^{(w),\text{exact}} \right|_{L^\infty}}.$$

To begin our study, we choose $\bar{g} = 0.5$, carried out the MMS simulations with our IIO method, (Equation 1.16), and display our results in Figures 6(a) and 6(b). We repeat this with our DNO approach and report the outcomes in Figures 7(a) and 7(b). We see in this generic, non-resonant, configuration that both algorithms display a spectral rate of convergence as N is refined (up to the conditioning of the algorithm) which improves as ε is decreased.

Before proceeding, we note that the choice of radius

$$\bar{g} = 1,$$

(a) Error versus perturbation order, N.　　(b) Error versus perturbation sizer, ε.
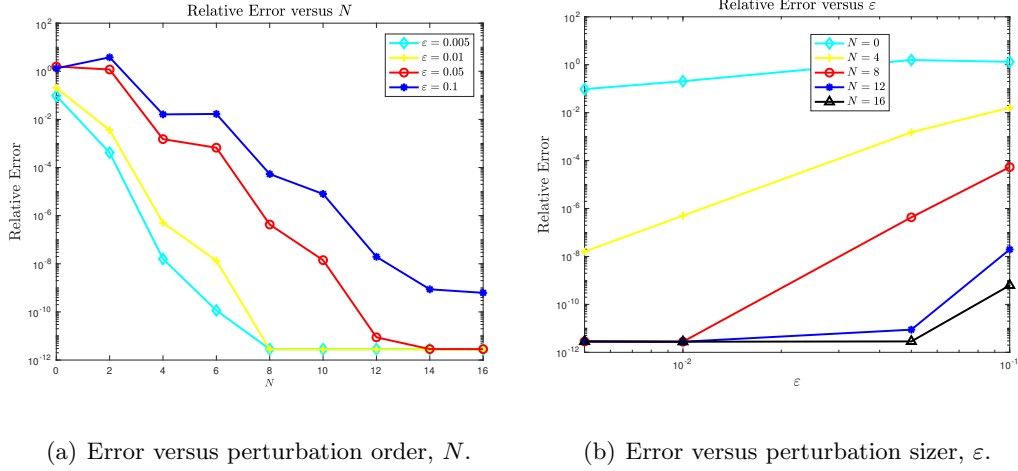
Figure 6. Plot of relative error with $\varepsilon = 0.005, 0.01, 0.05, 0.1$ and $N = 0, 4, 8, 12, 16$ for a

non-resonant configuration using the IIO formulation.

induces a singularity in the interior DNO resulting in a lack of uniqueness. To test the performance of our methods near this scenario, we first take

$$\bar{g} = 1 - 10^{-12}.$$

With the same choice of physical, (Equation 4.6), and numerical, (Equation 4.7), parameters as before, we conduct simulations with the IIO method, (Equation 1.16), and display our results in Figures 8(a) and 8(b). We revisit these computations with our DNO approach and show our results in Figures 9(a) and 9(b). We see in this nearly resonant configuration, that while the IIO methodology continues to display a spectral rate of convergence as N is refined (improving as ε is decreased), the DNO approach does *not* provide results of the same quality.
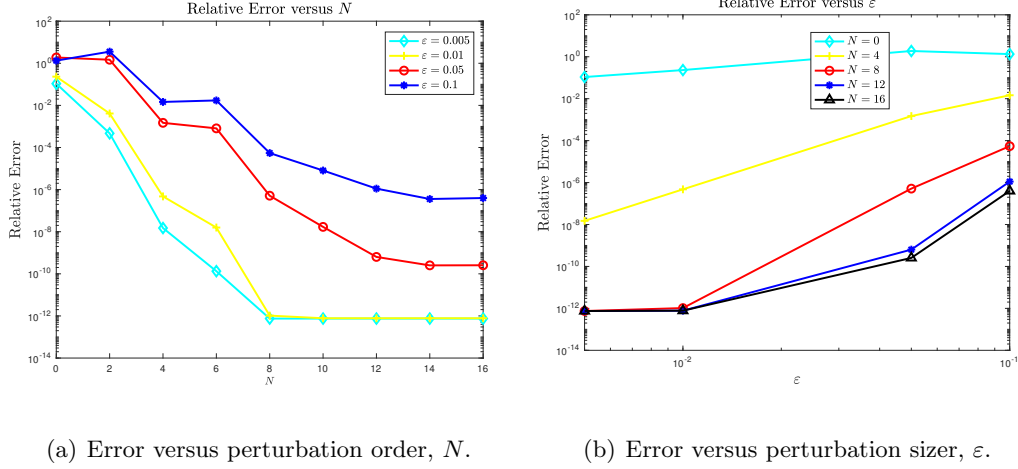
(a) Error versus perturbation order, N.   (b) Error versus perturbation sizer, ε.

Figure 7. Plot of relative error with $\varepsilon = 0.005, 0.01, 0.05, 0.1$ and $N = 0, 4, 8, 12, 16$ for a

non-resonant configuration using the DNO formulation.

To close this section, we choose

$$\bar{g} = 1 - 10^{-16}.$$

The simulation with the IIO method is displayed in Figures 10(a) and 10(b), while the DNO

approach are shown in Figures 11(a) and 11(b). We see in this resonant (to machine precision)

configuration, the IIO again displays a spectral rate of convergence as N is refined (improving

as ε is decreased), while the DNO approach delivers completely unacceptable results.

4.5   Simulation of Nanorods

We return to the problem of scattering of plane–wave incident radiation $u^{\mathrm{inc}} = \exp(i\alpha x -$

$i\gamma^u z)$ by a nanorod which demands the Dirichlet and Neumann conditions, (Equation 1.1c)

(a) Error versus perturbation order, N.   (b) Error versus perturbation sizer, ε.
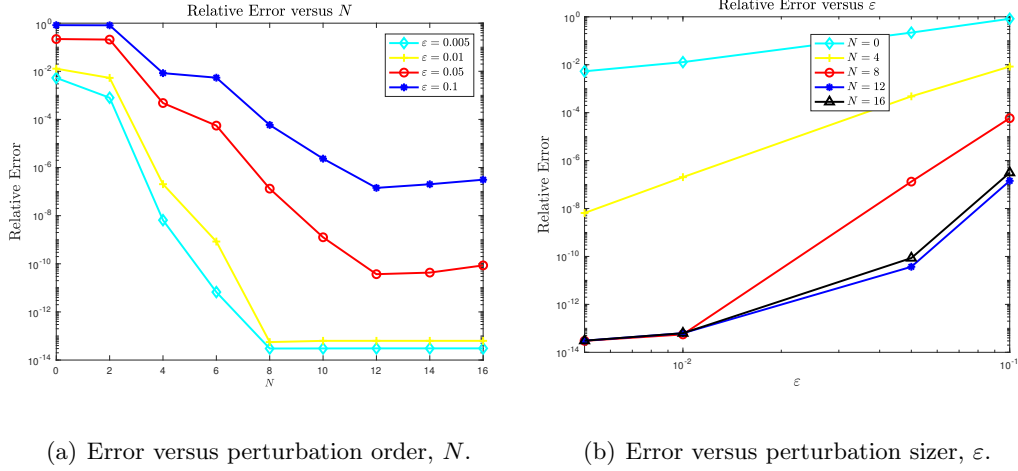
Figure 8. Plot of relative error with $\varepsilon = 0.005, 0.01, 0.05, 0.1$ and $N = 0, 4, 8, 12, 16$ for a nearly resonant configuration using the IIO formulation.

and (Equation 1.1d) respectively. More specifically, we consider metallic nanorods housed in a dielectric with outer interface shaped by

$$r = \bar{g} + g(\theta) = \bar{g} + \varepsilon f(\theta).$$

We illuminate this structure over a range of incident wavelengths $\lambda_{min} \leq \lambda \leq \lambda_{max}$ and perturbation sizes $\varepsilon_{min} \leq \varepsilon \leq \varepsilon_{max}$, and compute the magnitudes of the reflected and transmitted surface currents, $\tilde{U}$ and $\tilde{W}$. These we term the "Reflection Map" (RM) and "Transmission Map" (TM) in analogy with similar quantities of interest in the study of metallic gratings (1; 2; 3; 4). Our study of the Fröhlich condition, (Equation 2.4), indicates that there should be a sizable enhancement in each at an LSPR. In the case of a nanorod with a perfectly circular
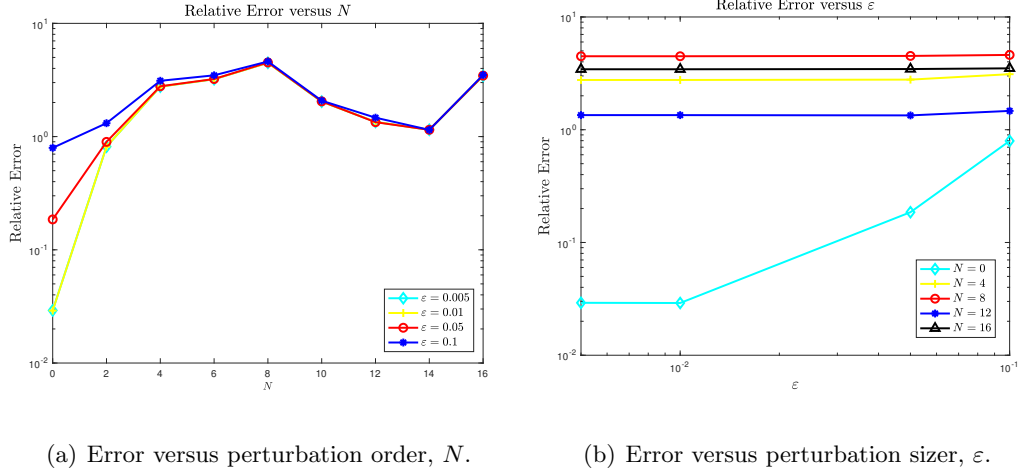
(a) Error versus perturbation order, N.
(b) Error versus perturbation sizer, ε.

Figure 9. Plot of relative error with $\varepsilon = 0.005, 0.01, 0.05, 0.1$ and $N = 0, 4, 8, 12, 16$ for a nearly resonant configuration using the DNO formulation.

cross–section we computed the value as the λ_C satisfying (Equation 2.4), and in subsequent plots this is depicted with a dashed red line.

4.5.1   An Analytic Deformation

Using the FE approach to compute the DNOs, we begin our study with the 2π–periodic and analytic profile (Equation 4.3) from § 4.3

$$f(\theta) = e^{\cos(\theta)},$$

(a) Error versus perturbation order, N.   (b) Error versus perturbation sizer, ε.
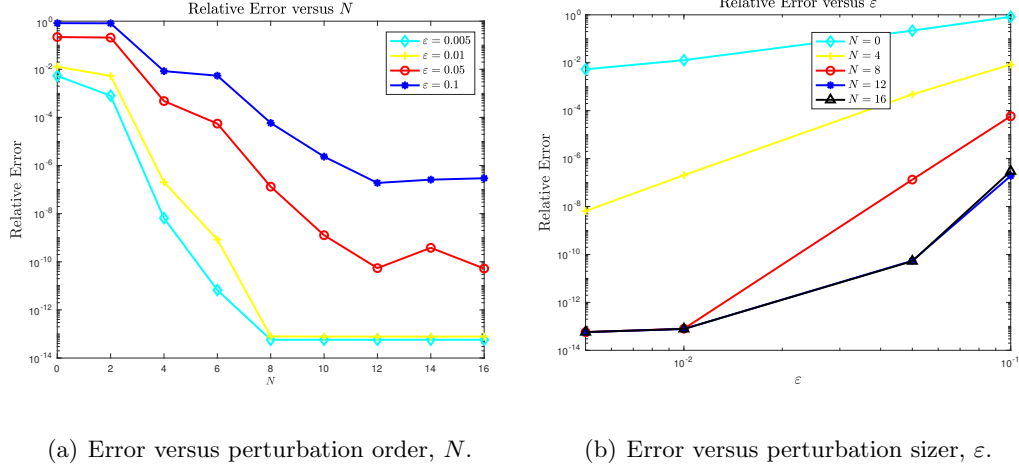
Figure 10. Plot of relative error with $\varepsilon = 0.005, 0.01, 0.05, 0.1$ and $N = 0, 4, 8, 12, 16$ for a

resonant configuration using the IIO formulation.

see Figure 3. With this we consider the following physical configuration

$$\bar{g} = 0.025, \quad n^u = 1, \quad n^w = n^{\mathrm{Ag}},$$

$$\lambda_{min} = 0.300, \quad \lambda_{max} = 0.800, \quad \varepsilon_{min} = 0, \quad \varepsilon_{max} = \bar{g}/10, \tag{4.8}$$

so that a silver (Ag) nanorod sits in vacuum, with numerical parameters

$$N_\lambda = 201, \quad N_\varepsilon = 201, \quad N_\theta = 64, \quad N = 16. \tag{4.9}$$

(a) Error versus perturbation order, N.　　(b) Error versus perturbation sizer, ε.
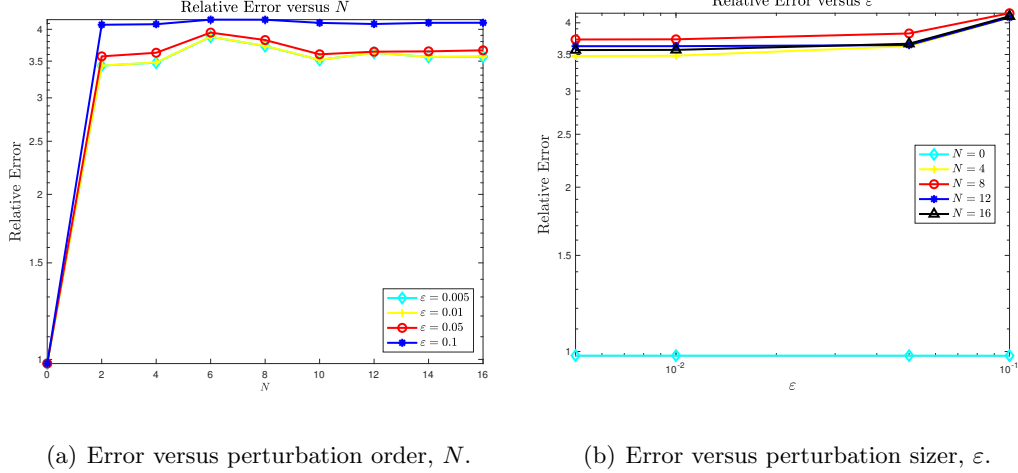
Figure 11. Plot of relative error with $\varepsilon = 0.005, 0.01, 0.05, 0.1$ and $N = 0, 4, 8, 12, 16$ for a

resonant configuration using the DNO formulation.

To compute the RM and TM we measure the magnitudes by

$$|\tilde{U}|_2 = \left\| \tilde{U}_{N_\theta, N} \right\|_2, \quad |\tilde{W}|_2 = \left\| \tilde{W}_{N_\theta, N} \right\|_2.$$

Plots of the RM and TM are displayed in Figure 12. In Figure 13 we show the final slice at

$\varepsilon = \varepsilon_{max}$, together with the Fröhlich value of the LSPR, (Equation 2.4), as a dashed red line.

We see how even a relatively moderate value of the deformation parameter ε (one tenth of the

rod radius) can produce a sizable shift in the LSPR location.

We revisit these calculations with two fundamental changes to the configuration (Equation 4.8):

(1) boundary perturbation of twice the size ($\varepsilon_{max} = \bar{g}/5$), (2) water as the host dielectric

($n^u = n^{\text{water}}$). To summarize the effects of these changes, we present a collection of the final
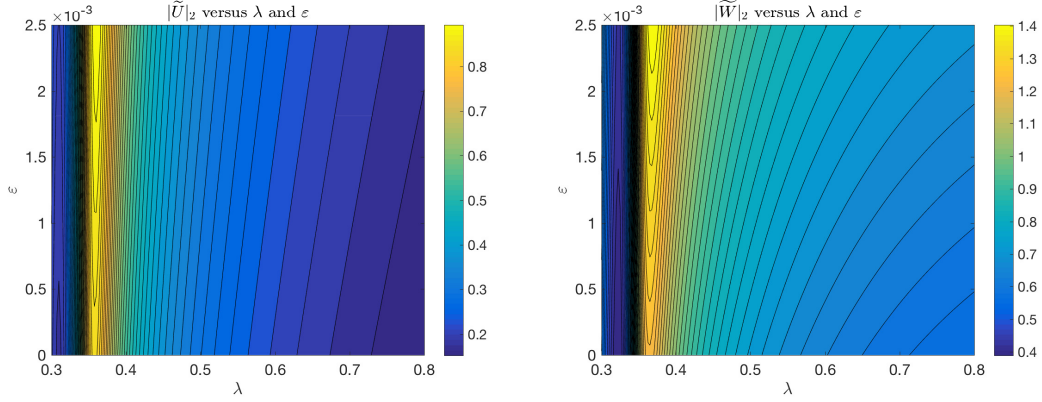
Figure 12. Reflection Map and Transmission Map for a silver nanorod shaped by the analytic profile, (Equation 4.3), in vacuum. $\varepsilon_{max} = \bar{g}/10$, $\bar{g} = 0.025$, $\lambda_{min} = 0.300$, and $\lambda_{max} = 0.800$.

slices of RM and TM at $\varepsilon = \varepsilon_{max}$ in Figure 14. Not only does an increase in the deformation size move the LSPR further away from the Fröhlich value, but also placing the nanorod in water spreads out the LSPR response in a significant way. Importantly, these results are easily generated with our method and show how useful our approach can be in the evaluation and design of nanorod structures.

4.5.2   A Low–Frequency Cosine Deformation

Continuing with the FE recursions, we consider the 2π–periodic, low–frequency ellipsoidal profile

$$f(\theta) = \cos(2\theta), \tag{4.10}$$
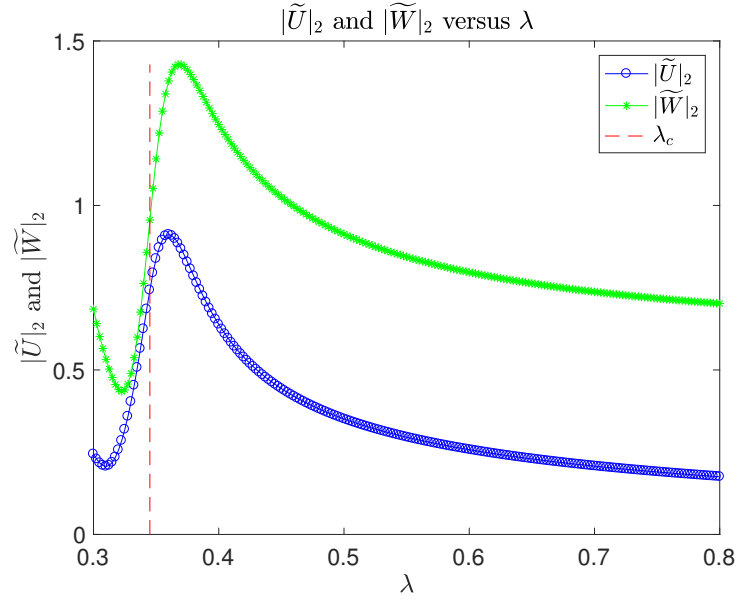
Figure 13. Final Slice of Reflection and Transmission Maps at $\varepsilon = \varepsilon_{max}$ for a silver nanorod shaped by the analytic profile, (Equation 4.3), in vacuum.

see Figure 15. Again we consider the physical configuration (Equation 4.8) with numerical parameters (Equation 4.9).

Plots of the RM and TM are displayed in Figure 16. In Figure 17, we show the final slice at $\varepsilon = \varepsilon_{max}$, with two perturbation sizes, $\varepsilon_{max} = \bar{g}/10$ and $\varepsilon_{max} = \bar{g}/5$, and two dielectrics, vacuum and water. The Fröhlich value of the LSPR, (Equation 2.4), is plotted as a dashed red line. As before, even a small perturbation in the deformation can move the LSPR shift in a noticeable way. Not only does an increase in the deformation size move the LSPR further away from the Fröhlich value, but also placing the nanorod in water spreads out the LSPR response.

Note that the LSPR response rises to a "double–peak" in water, though not as severely as for

the analytic profile.

4.5.3   A Higher–Frequency Cosine Deformation

Once again with the FE approach, we conclude with clover shaped cross–sections of the

form

$$f(\theta) = \cos(4\theta), \tag{4.11}$$

see Figure 18. Once again we consider the physical configuration (Equation 4.8) with numerical

parameters (Equation 4.9). Plots of the RM and TM are displayed in Figure 19. In Figure 20,

we show the final slice at $\varepsilon = \varepsilon_{max}$, with two perturbation sizes, $\varepsilon_{max} = \bar{g}/10, \bar{g}/5$, and two

dielectrics, vacuum and water. Again, the Fröhlich value of the LSPR, (Equation 2.4), is plotted

as a dashed red line.

Unsurprisingly, we notice how even a moderate value of the deformation parameter delivers

a sizable shift in the LSPR location. In this case we see that an increase in the deformation

size moves the LSPR further away from the Fröhlich value, and placing the nanorod in water

not only spreads out the LSPR response, but also creates a "bifurcation" in the response.

4.5.4   A TFE approach with IIOs

We close by studing the clover shaped profile, (Equation 4.11), using the TFE approach

with IIOs. We compute the magnitudes of the reflected and transmitted surface currents, $\tilde{I}^{(u)}$

and $\tilde{I}^{(w)}$,

$$|\tilde{I}^{(u)}|_2 = \left\| \tilde{I}^{(u)}_{N_\theta, N_r, N} \right\|_2, \quad |\tilde{I}^{(w)}|_2 = \left\| \tilde{I}^{(w)}_{N_\theta, N_r, N} \right\|_2,$$

which should also be enhanced at an LSPR. We consider the following physical configuration

$$\bar{g} = 0.025, \quad n^u = 1, \quad n^w = n^{\mathrm{Ag}},$$

$$\lambda_{min} = 0.300, \quad \lambda_{max} = 0.800, \quad \varepsilon_{min} = 0, \quad \varepsilon_{max} = \bar{g}/5,$$

so that a silver (Ag) nanorod sits in vacuum, with numerical parameters

$$N_\lambda = 201, \quad N_\varepsilon = 201, \quad N_\theta = 32, \quad N_r = 16, \quad N = 8.$$

Plots of the RM and TM are displayed in Figure 21. In Figure 22 we show the final slice $(\varepsilon = \varepsilon_{max})$ of each of these, together with the Fröhlich value of the LSPR, (Equation 2.4), as a dashed red line. Here we draw the same conclusion that a relatively moderate value of the deformation parameter (one fifth of the rod radius) can produce a sizable shift in the LSPR location which our novel approach can accurately capture.

(a) $\varepsilon = \bar{g}/10$ in vacuum.

(b) $\varepsilon = \bar{g}/5$ in vacuum.

(c) $\varepsilon = \bar{g}/10$ in water.

(d) $\varepsilon = \bar{g}/5$ in water.
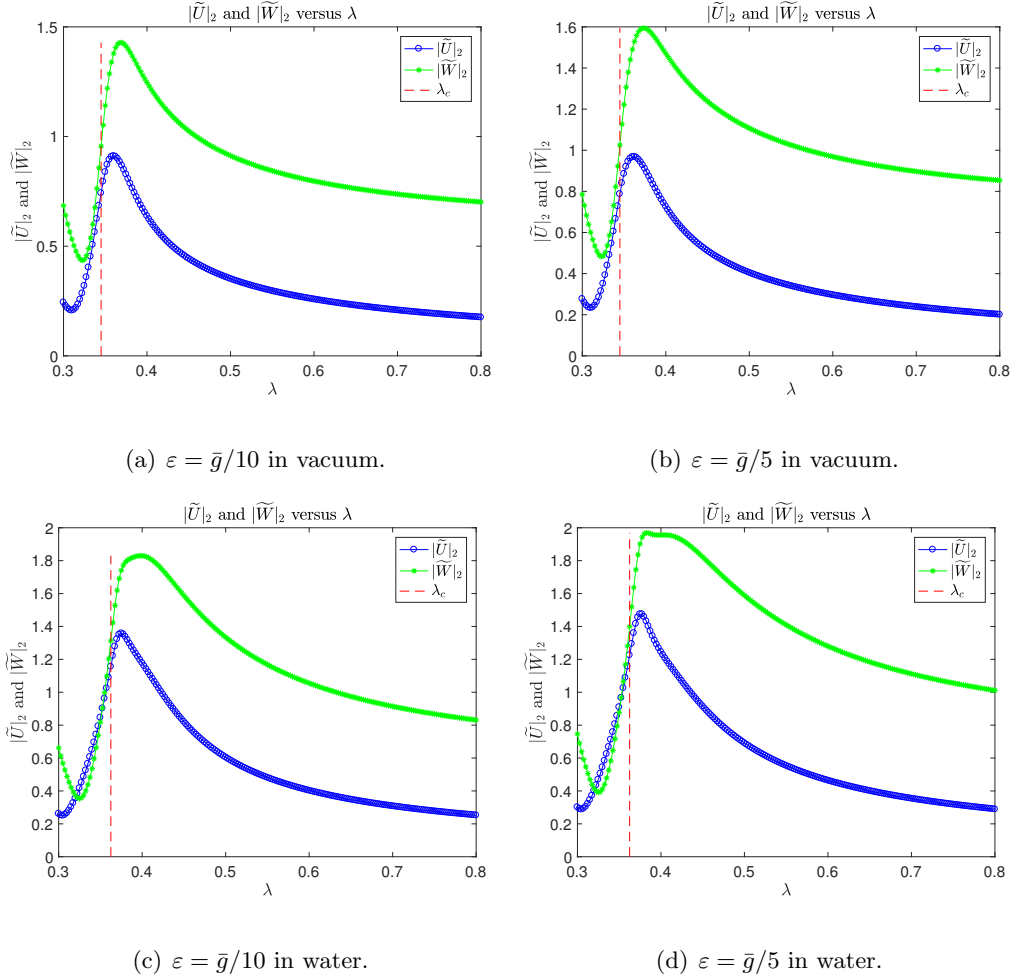
Figure 14. Final slices of Reflection Maps and Transmission Maps for a silver nanorod shaped by the analytic profile, (Equation 4.3).
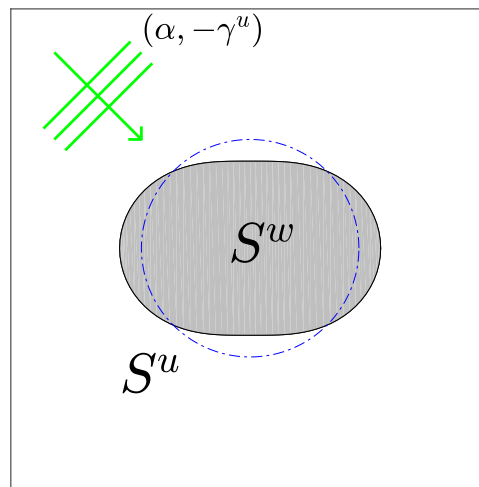
Figure 15. Plot of the cross–section of a metallic nanorod (occupying S^w) shaped by

$r = \bar{g} + \varepsilon \cos(2\theta)$ ($\varepsilon = \bar{g}/5$) housed in a dielectric (occupying S^u) under plane–wave

illumination with wavenumber $(\alpha, -\gamma^u)$. The dash–dot blue line depicts the unperturbed

geometry, the circle $r = \bar{g}$.
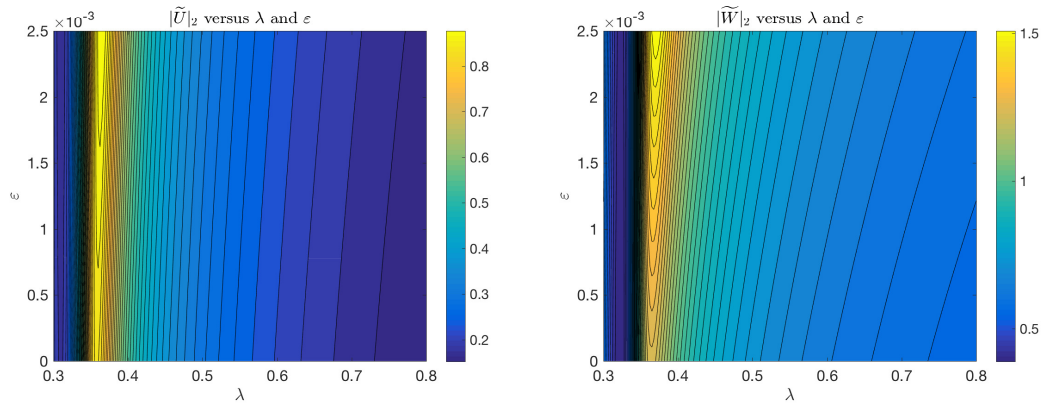
Figure 16. Reflection Map and Transmission Map for a silver nanorod shaped by an ellipsoidal profile, (Equation 4.10), in vacuum. $\varepsilon_{max} = \bar{g}/10$, $\bar{g} = 0.025$, $\lambda_{min} = 0.3$, $\lambda_{max} = 0.8$.

(a) $\varepsilon = \bar{g}/10$ in vacuum.

(b) $\varepsilon = \bar{g}/5$ in vacuum.

(c) $\varepsilon = \bar{g}/10$ in water.

(d) $\varepsilon = \bar{g}/5$ in water.
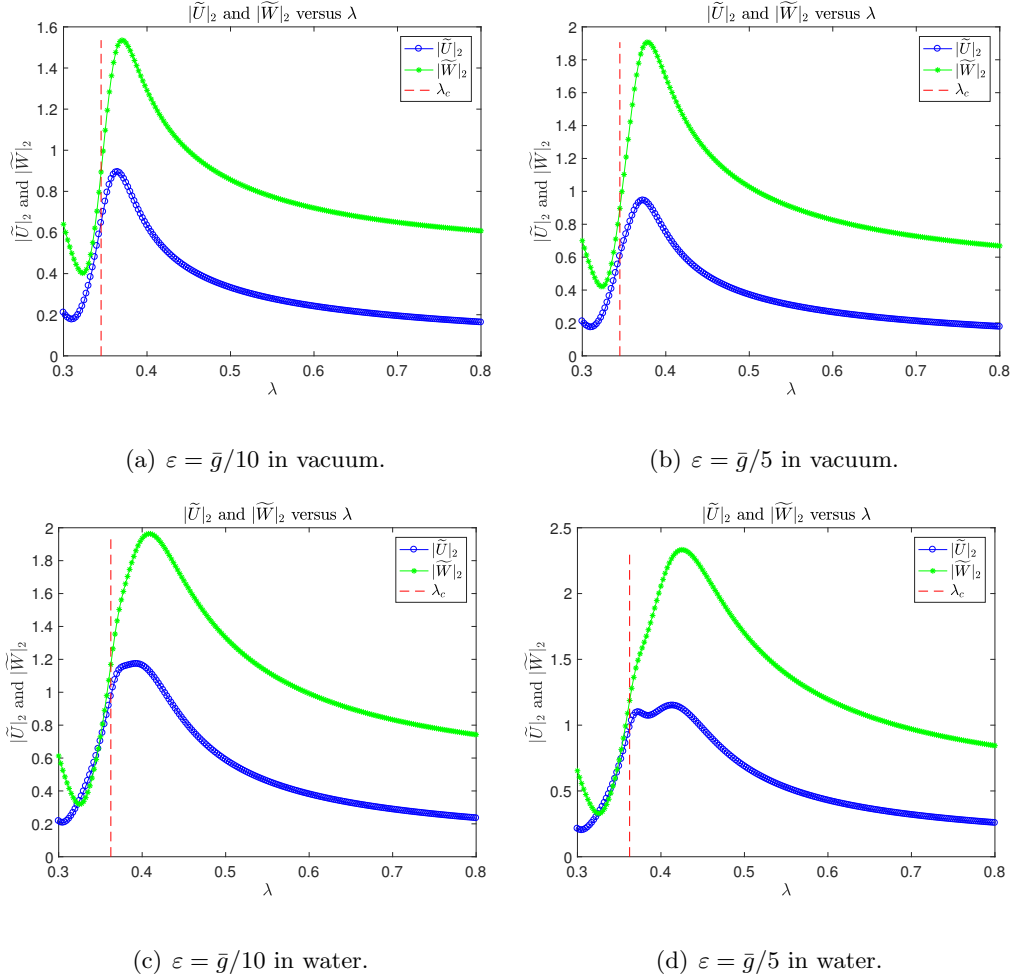
Figure 17. Final slices of Reflection Maps and Transmission Maps for a silver nanorod shaped by the ellipsoidal profile, (Equation 4.10).
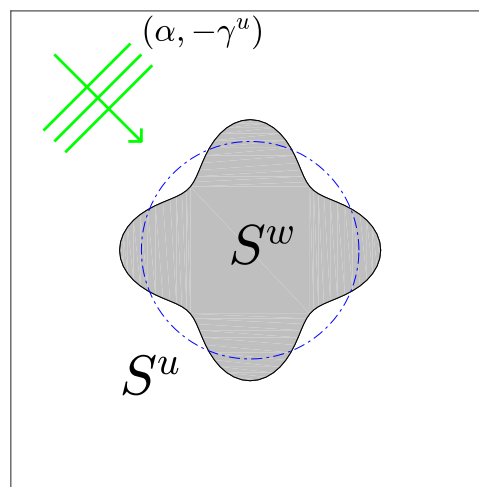
Figure 18. Plot of the cross–section of a metallic nanorod (occupying S^w) shaped by $r = \bar{g} + \varepsilon \cos(4\theta)$ ($\varepsilon = \bar{g}/5$) housed in a dielectric (occupying S^u) under plane–wave illumination with wavenumber $(\alpha, -\gamma^u)$. The dash–dot blue line depicts the unperturbed geometry, the circle $r = \bar{g}$.
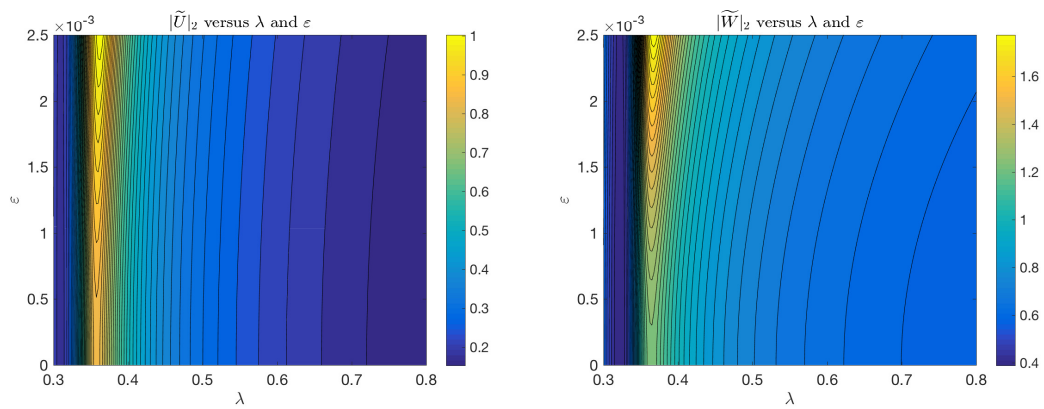
Figure 19. Reflection Map and Transmission Map for a silver nanorod shaped by a clover shaped profile, (Equation 4.11), in vacuum. $\varepsilon_{max} = \bar{g}/10$, $\bar{g} = 0.025$, $\lambda_{min} = 0.3$, $\lambda_{max} = 0.8$.

(a) $\varepsilon = \bar{g}/10$ in vacuum.

(b) $\varepsilon = \bar{g}/5$ in vacuum.

(c) $\varepsilon = \bar{g}/10$ in water.

(d) $\varepsilon = \bar{g}/5$ in water.
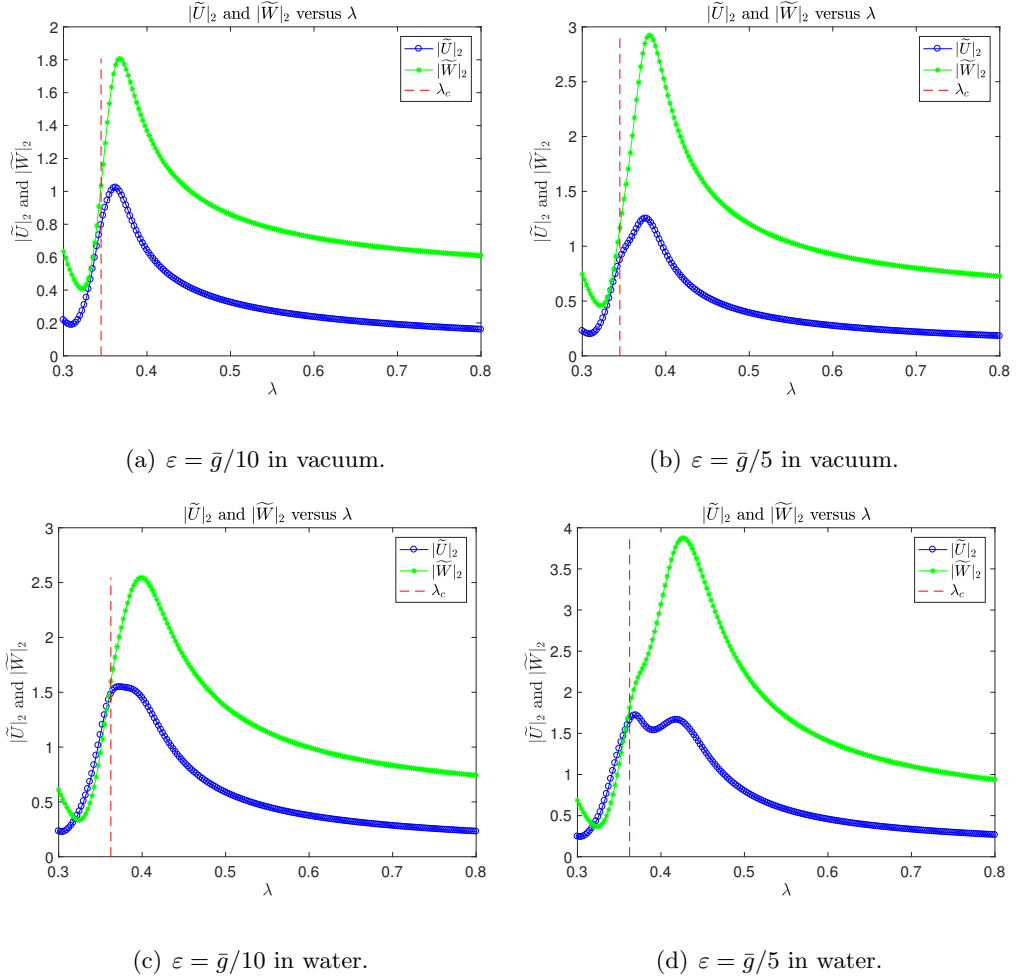
Figure 20. Final slices of Reflection Maps and Transmission Maps for a silver nanorod shaped by the clover shaped profile, (Equation 4.11).
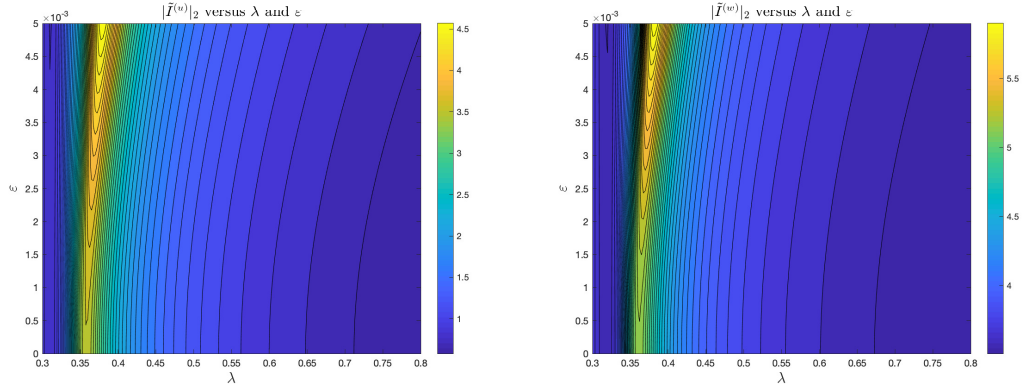
Figure 21. Reflection Map and Transmission Map for a silver nanorod shaped by the the clover shaped profile, (Equation 4.11), in vacuum, using IIO and TFE. $\varepsilon_{max} = \bar{g}/5$, $\bar{g} = 0.025$, $\lambda_{min} = 0.3$, $\lambda_{max} = 0.8$.
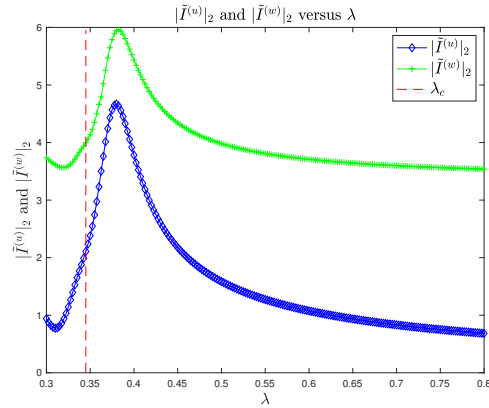
Figure 22. Final Slice of Reflection and Transmission Maps at $\varepsilon = \varepsilon_{max}$ for a silver nanorod shaped by the clover shaped profile, (Equation 4.11), in vacuum, using IIO and TFE.

CHAPTER 5

CONCLUSION

In this thesis we have investigated High–Order Perturbation of Surfaces (HOPS) algorithms for the numerical simulation of the problem of scattering of linear waves by a nanorod in terms of Dirichlet–Neumann Operators (DNO) and Impedance–Impedance Operator (IIO). We have also studied the Localized Surface Plasmon Resonances (LSPRs) which can be induced in silver nanorods with visible light, and how they change as the shapes of these rods are varied analytically away from perfectly cylindrical.

We build the *Double–Layered* Penetrable obstacle scattering problem based upon the work in (28; 44). In the contribution we provide HOPS algorithms with boundary formulation not only in terms of the Dirichlet–Neumann Operator, but also the Impedance–Impedance Operator, which does not suffer from the artificial "Dirichlet eigenvalues" issue. In addition, we establish and prove the analyticity of solutions to the problem via IIO formulation. The numerical experiments and simulations demonstrate the remarkable efficiency, fidelity, and high–order accuracy of our algorithms.

APPENDICES

Appendix A

DIRICHLET–NEUMANN OPERATORS FORMULATION

A.1 The Non–Trivial Configurations

For ε sufficiently small and f sufficiently smooth, the operators, $\{G^{(u)}, G^{(w)}\}$, and data, $\{\zeta, \psi\}$, can be shown to be analytic in ε so that the following Taylor series are strongly convergent

$$\{G^{(u)}, G^{(w)}, \zeta, \psi\} = \{G^{(u)}, G^{(w)}, \zeta, \psi\}(\varepsilon f) = \sum_{n=0}^{\infty} \{G_n^{(u)}, G_n^{(w)}, \zeta_n, \psi_n\}\varepsilon^n,$$

as well as the resulting scattered fields

$$U = U(\varepsilon f) = \sum_{n=0}^{\infty} U_n \varepsilon^n, \quad W = W(\varepsilon f) = \sum_{n=0}^{\infty} W_n \varepsilon^n.$$

Furthermore, it is straightforward to identify a recursive formula for U_n. Using $W_n = U_n - \zeta_n$ we can write (Equation 1.9) as

$$\left(\sum_{n=0}^{\infty} \left(G_n^{(u)} + \tau^2 G_n^{(w)}\right) \varepsilon^n\right) \left[\sum_{m=0}^{\infty} U_m \varepsilon^m\right] = -\sum_{n=0}^{\infty} \psi_n \varepsilon^n + \tau^2 \left(\sum_{n=0}^{\infty} G_n^{(w)} \varepsilon^n\right) \left[\sum_{m=0}^{\infty} \zeta_m \varepsilon^m\right],$$

then equating at order $\mathcal{O}(\varepsilon^n)$, we find

$$(G_0^{(u)} + \tau^2 G_0^{(w)})U_n = -\psi_n + \sum_{m=0}^{n} G_{n-m}^{(w)} [\zeta_m] - \sum_{m=0}^{n-1} (G_{n-m}^{(u)} + \tau^2 G_{n-m}^{(w)}) [U_m]. \tag{A.1}$$

At order zero we recover the trivial configuration calculation, (Equation 2.1), in Chapter 2. The higher order corrections are recovered from (Equation A.1). The forms of the data, $\{\zeta_n, \psi_n\}$, are also stated in Section 2.1. All that remains is to specify expressions for operators, $\{G_n^{(u)}, G_n^{(w)}\}$. Detailed calculations for the operator $G_n^{(u)}$ was presented in (28; 44). Here we apply FE and TFE methods to approximate the DNO $G_n^{(w)}$.

A.2 The Method of Field Expansions

Focusing upon the Interior Problem via DNO (Equation 1.8), the field w in the inner domain, $\{r < \bar{g} + \varepsilon f(\theta)\}$, is written as

$$w = w(r, \theta; \varepsilon) = \sum_{n=0}^{\infty} w_n(r, \theta)\varepsilon^n.$$

Upon insertion of this into (Equation 1.8) we find that the w_n must be solutions of the boundary value problem

$$\Delta w_n + (k^u)^2 w_n = 0, \qquad R_i < r < \bar{g}, \qquad \text{(A.2a)}$$

$$w_n(\bar{g}, \theta) = \delta_{n,0}W - \sum_{m=0}^{n-1} \frac{f^{n-m}}{(n-m)!}\partial_r^{n-m}w_m(\bar{g}, \theta), \qquad r = \bar{g}, \qquad \text{(A.2b)}$$

$$\partial_r w_n - T^{(w)}[w_n] = 0, \qquad r = R_i. \qquad \text{(A.2c)}$$

The exact solutions (Equation 2.2) are

$$w_n(r, \theta) = \sum_{p=-\infty}^{\infty} \hat{w}_{n,p} \frac{J_p(k^w r)}{J_p(k^w \bar{g})}e^{ip\theta},$$

Appendix A (Continued)

and the $\hat{w}_{n,p}$ are determined recursively from the boundary conditions, (Equation A.2b), be-

ginning, at order zero, with

$$\hat{w}_{0,p} = \hat{W}_p.$$

From this the DNO, (Equation 1.8d), can be computed from

$$G^{(w)}[W] = (\partial_N w)(\bar{g} + g(\theta), \theta)$$

$$= \sum_{n=0}^{\infty} \sum_{p=-\infty}^{\infty} \left\{ k^w(\bar{g} + \varepsilon f) \frac{J_p'(k^w(\bar{g} + \varepsilon f))}{J_p(k^w \bar{g})} \right.$$

$$\left. - \frac{\varepsilon f'}{(\bar{g} + \varepsilon f)}(ip) \frac{J_p(k^w(\bar{g} + \varepsilon f))}{J_p(k^w \bar{g})} \right\} \hat{w}_{n,p} e^{ip\theta} \varepsilon^n,$$

expanding the Bessel functions $J_p'(k^w(\bar{g} + \varepsilon f))$ and $J_p(k^w(\bar{g} + \varepsilon f))$ in power series in ε, and

equating like powers of ε. This results in

$$G_n^{(w)}(f)[W] = -\frac{f}{\bar{g}} G_{n-1}^{(w)}(f)[W] k^w \bar{g} + \sum_{\ell=0}^{n} \sum_{p=-\infty}^{\infty} \hat{w}_{\ell,p} \frac{(k^w f)^{n-\ell}}{(n-\ell)!} \frac{J_p^{(n+1-\ell)}(k^w \bar{g})}{J_p(k^w \bar{g})} e^{ip\theta}$$

$$+ 2k^w f \sum_{\ell=0}^{n-1} \sum_{p=-\infty}^{\infty} \hat{w}_{\ell,p} \frac{(k^w f)^{n-1-\ell}}{(n-1-\ell)!} \frac{J_p^{(n-\ell)}(k^w \bar{g})}{J_p(k^w \bar{g})} e^{ip\theta}$$

$$+ \frac{k^w}{\bar{g}} f^2 \sum_{\ell=0}^{n-2} \sum_{p=-\infty}^{\infty} \hat{w}_{\ell,p} \frac{(k^w f)^{n-2-\ell}}{(n-2-\ell)!} \frac{J_p^{(n-1-\ell)}(k^w \bar{g})}{J_p(k^w \bar{g})} e^{ip\theta}$$

$$- \frac{1}{\bar{g}}(f') \sum_{\ell=0}^{n-1} \sum_{p=-\infty}^{\infty} \hat{w}_{\ell,p} \frac{(k^w f)^{n-1-\ell}}{(n-1-\ell)!} \frac{J_p^{(n-1-\ell)}(k^w \bar{g})}{J_p(k^w \bar{g})} (ip) e^{ip\theta}.$$

Appendix A (Continued)

A.3   The Method of Transformed Field Expansions

As always, the TFE method begins with a change of variables which is the same as the one

for the interior problem

$$r' = \frac{(\bar{g} - R_i)r + R_i g(\theta)}{\bar{g} + g(\theta) - R_i}, \quad \theta' = \theta,$$

which maps the perturbed domain $\{R_i < r < \bar{g} + g(\theta)\}$ to the separable one $\{R_i < r' < \bar{g}\}$.

The field w is changed into

$$v(r', \theta') = w\left(\frac{(\bar{g} + g(\theta') - R_i)r' - R_i g(\theta')}{\bar{g} - R_i}, \theta'\right),$$

and modifies (Equation 1.8) to

$$\Delta v + (k^w)^2 v = F^{\text{in}}(r, \theta; g), \qquad R_i < r < \bar{g}, \qquad \text{(A.3a)}$$

$$v = W, \qquad r = \bar{g}, \qquad \text{(A.3b)}$$

$$\partial_r v - T^{(w)}[v] = h^{\text{in}}(\theta; g), \qquad r = R_i, \qquad \text{(A.3c)}$$

where F^{in} is presented in (Equation 2.19) and h^{in} in (Equation 2.21). In addition, the (Equation 1.8d)

changes to

$$G^{(w)}[W] = \frac{\bar{g} - R_i}{\bar{g} - R_i + g}\left[(\bar{g} + g) + \frac{(g')^2}{\bar{g} + g}\right]\partial_r v - \frac{g'}{\bar{g} + g}\partial_\theta v.$$

Appendix A (Continued)

Upon setting $g = \varepsilon f$ and expanding

$$v(r, \theta, \varepsilon) = \sum_{n=0}^{\infty} v_n(r, \theta)\varepsilon^n,$$

we can show that

$$\Delta v_n + (k^w)^2 \, v_n = F_n^{\text{in}}, \qquad\qquad R_i < r < \bar{g}, \qquad\qquad \text{(A.4a)}$$

$$v_n = \delta_{n,0} W, \qquad\qquad r = \bar{g}, \qquad\qquad \text{(A.4b)}$$

$$\partial_r v_n - T^{(w)}[v_n] = h_n^{\text{in}}, \qquad\qquad r = R_i, \qquad\qquad \text{(A.4c)}$$

where F_n^{in} is presented in (Equation 2.24) and h_n^{in} in (Equation 2.26). Then it is not difficult to see that

$$G_n^{(w)}[W] = - f \left(\frac{1}{\bar{g}} + \frac{1}{\bar{g} - R_i} \right) G_{n-1}^{(w)}[W] - \frac{f^2}{\bar{g}(\bar{g} - R_i)} G_{n-2}^{(w)}[W] + \bar{g}\partial_r v_n$$

$$+ 2f\partial_r v_{n-1} + \frac{f^2 + (f')^2}{\bar{g}} \partial_r v_{n-2} - \frac{f'}{\bar{g}} \partial_\theta v_{n-1} - \frac{f(f')}{\bar{g}(\bar{g} - R_i)} \partial_\theta v_{n-2}.$$

Provided with the $\{v_n\}$, we can readily approximate the terms, $G_n^{(w)}$, in the Taylor series expansion of $G^{(w)}$.

Appendix B

THE ELLIPTIC ESTIMATE

B.1   Volumetric Function Spaces

With the goal of establishing analyticity results, we discuss necessary volumetric function spaces in addition to the interfacial spaces we described above. For this we consider the domain $\Omega_{a,b} := \{a < r < b\}$ with inner and outer boundaries $\Gamma_a := \{r = a\}$ and $\Gamma_b := \{r = b\}$, respectively. For clarity of presentation we use the following notation for the classical θ–periodic volumetric and surface Sobolev spaces

$$H^1(\Omega_{a,b}), \quad H^{1/2}(\Gamma_a), \quad H^{1/2}(\Gamma_b).$$

The precise nature of the spaces $H^{1/2}(\Gamma_a)$ and $H^{1/2}(\Gamma_b)$ has already been made precise, and the details of the space $H^1(\Omega_{a,b})$ can be made clear by the following considerations. If $v \in H^1(\Omega_{a,b})$ then

$$v(r, \theta) = \sum_{p=-\infty}^{\infty} \hat{v}_p(r)e^{ip\theta}, \quad \hat{v}_p(r) = \frac{1}{2\pi} \int_0^{2\pi} v(r,\theta)e^{-ip\theta} \, d\theta,$$

and $\|v\|_{H^1(\Omega_{a,b})} < \infty$ where

$$\|v\|^2_{H^1(\Omega_{a,b})} := \sum_{p=-\infty}^{\infty} \left(\langle p \rangle^2 \|\hat{v}_p\|^2_{L^2(dr)} + \|\partial_r \hat{v}_p\|^2_{L^2(dr)} \right), \quad \|\hat{v}_p\|^2_{L^2(dr)} := \int_a^b |\hat{v}_p(r)|^2 \, r \, dr.$$

Appendix B (Continued)

The existence, uniqueness, and elliptic regularity results demand an understanding of the duals of $H^1(\Omega_{a,b})$, $H^{1/2}(\Gamma_a)$ and $H^{1/2}(\Gamma_b)$. As we have seen, the latter are simply the spaces $H^{-1/2}(\Gamma_a)$ and $H^{-1/2}(\Gamma_b)$. However, the former require a little more work to characterize. Following Evans (38) (Section 5.9.1) we use the Riesz Representation Theorem to identify any $F \in (H^1(\Omega_{a,b}))'$ with an element $u_F \in H^1(\Omega_{a,b})$ such that

$$\langle F, v \rangle = (u_F, v)_{H^1(\Omega_{a,b})}, \quad \forall v \in H^1(\Omega_{a,b}),$$

where $\langle \cdot, \cdot \rangle$ is the duality pairing between $H^1(\Omega_{a,b})$ and $(H^1(\Omega_{a,b}))'$, and $(\cdot, \cdot)_{H^1(\Omega_{a,b})}$ is the $H^1(\Omega_{a,b})$ inner product

$$(u, v)_{H^1(\Omega_{a,b})} = \int_{\Omega_{a,b}} \nabla u \cdot \overline{\nabla v} + u\overline{v} \, dV.$$

As $u_F \in H^1(\Omega_{a,b})$ we can identify $F^0, F^r, F^\theta \in L^2(\Omega_{a,b})$ such that, in the weak sense

$$F = F^0 + (\partial_r F^r)\hat{r} + \frac{(\partial_\theta F^\theta)}{r}\hat{\theta},$$

and

$$\|F\|_{(H^1(\Omega_{a,b}))'}^2 = \|F^0\|_{L^2(\Omega_{a,b})}^2 + \|F^r\|_{L^2(\Omega_{a,b})}^2 + \left\|\frac{F^\theta}{r}\right\|_{L^2(\Omega_{a,b})}^2$$

gives the norm of $(H^1(\Omega_{a,b}))'$. We note that since $0 < a < b < \infty$ this is equivalent to

$$\|F^0\|_{L^2(\Omega_{a,b})}^2 + \|F^r\|_{L^2(\Omega_{a,b})}^2 + \left\|F^\theta\right\|_{L^2(\Omega_{a,b})}^2.$$

Appendix B (Continued)

Remark B.1.1. We note, for later use, the important fact that $H^1(\Omega_{a,b})$ embeds compactly into $L^2(\Omega_{a,b})$ while $H^{1/2}(\Gamma_a)$ embed compactly into $L^2(\Gamma_a)$ and $H^{1/2}(\Gamma_b)$ embed compactly into $L^2(\Gamma_b)$ (54).

B.2 Uniqueness

We now present the fundamental result which enables the proof of our analyticity theorems. For this we consider the generic Helmholtz problem

$$\Delta v + k^2 v = F, \qquad \text{in } \Omega_{a,b}, \qquad \text{(B.1a)}$$

$$\partial_r v - Av = K, \qquad \text{at } \Gamma_a, \qquad \text{(B.1b)}$$

$$\partial_r v - Bv = L, \qquad \text{at } \Gamma_b, \qquad \text{(B.1c)}$$

where A and B can be order–one Fourier multipliers

$$A : H^{1/2}(\Gamma_a) \to H^{-1/2}(\Gamma_a), \quad B : H^{1/2}(\Gamma_b) \to H^{-1/2}(\Gamma_b),$$

though they can also be constants, e.g., the choice of Despres (39; 40) $A = i\eta_a$, $B = i\eta_b$, where $\eta_a, \eta_b \in \mathbf{R}$.

Appendix B (Continued)

We can decide decisively upon uniqueness of solutions to (Equation B.1) by considering this problem with $F \equiv K \equiv L \equiv 0$ and writing the exact solution via separation of variables. The solution of (Equation B.1a) with $F \equiv 0$ is

$$v(r,\theta) = \sum_{p=-\infty}^{\infty} \left\{ c_p J_p(kr) + d_p Y_p(kr) \right\} e^{ip\theta}, \tag{B.2}$$

with derivative

$$\partial_r v(r,\theta) = \sum_{p=-\infty}^{\infty} \left\{ c_p k J_p'(kr) + d_p k Y_p'(kr) \right\} e^{ip\theta}, \tag{B.3}$$

while the boundary conditions, (Equation B.1b)–(Equation B.1c), in the case $K \equiv L \equiv 0$ deliver

$$\begin{pmatrix} k J_p'(ka) - \hat{A}_p J_p(ka) & k Y_p'(ka) - \hat{A}_p Y_p(ka) \\ k J_p'(kb) - \hat{B}_p J_p(kb) & k Y_p'(kb) - \hat{B}_p Y_p(kb) \end{pmatrix} \begin{pmatrix} c_p \\ d_p \end{pmatrix} = \begin{pmatrix} 0 \\ 0 \end{pmatrix}. \tag{B.4}$$

Clearly, this has only the zero solution provided that the determinant function is non–zero

$$\Lambda_p(k,a,b,\hat{A}_p,\hat{B}_p) := \left(k J_p'(ka) - \hat{A}_p J_p(ka) \right) \left(k Y_p'(kb) - \hat{B}_p Y_p(kb) \right)$$
$$- \left(k Y_p'(ka) - \hat{A}_p Y_p(ka) \right) \left(k J_p'(kb) - \hat{B}_p J_p(kb) \right).$$

If we define a "configuration" (k,a,b,A,B) then we can specify a δ–permissible configuration set

$$\mathcal{C}_\delta(k,a,b,A,B) := \left\{ (k,a,b,A,B) \mid \left| \Lambda_p(k,a,b,\hat{A}_p,\hat{B}_p) \right|^2 > \delta^2, \forall p \in \mathbf{Z} \right\}, \tag{B.5}$$

for some $\delta > 0$.

Appendix B (Continued)

For later reference we explicitly mention the case $k = 0$ which corresponds to Laplace's equation. We consider the problem

$$\Delta v = F, \qquad \text{in } \Omega_{a,b}, \qquad \text{(B.6a)}$$

$$\partial_r v - Av = K, \qquad \text{at } \Gamma_a, \qquad \text{(B.6b)}$$

$$\partial_r v - Bv = L, \qquad \text{at } \Gamma_b. \qquad \text{(B.6c)}$$

The exact solution of (Equation B.6a) is, in the case $F \equiv 0$,

$$v(r, \theta) = c_0 \log(r) + d_0 + \sum_{|p|=1}^{\infty} \left\{ c_p \left(\frac{r}{b} \right)^{|p|} + d_p \left(\frac{r}{a} \right)^{-|p|} \right\} e^{ip\theta}, \qquad \text{(B.7)}$$

with derivative

$$\partial_r v(r, \theta) = \frac{c_0}{r} + \sum_{|p|=1}^{\infty} |p| \left\{ \frac{c_p}{b} \left(\frac{r}{b} \right)^{|p|-1} - \frac{d_p}{a} \left(\frac{r}{a} \right)^{-|p|-1} \right\} e^{ip\theta}. \qquad \text{(B.8)}$$

The boundary conditions (Equation B.6b)–(Equation B.6c), for $K \equiv L \equiv 0$, demand, for $p \neq 0$,

$$\begin{pmatrix} q^{|p|} \left(|p|/(bq) - \hat{A}_p \right) & \left(-|p|/a - \hat{A}_p \right) \\ \left(|p|/b - \hat{B}_p \right) & q^{|p|} \left(-(|p|\,q)/a - \hat{B}_p \right) \end{pmatrix} \begin{pmatrix} c_p \\ d_p \end{pmatrix} = \begin{pmatrix} 0 \\ 0 \end{pmatrix}, \qquad \text{(B.9)}$$

Appendix B (Continued)

where $q := a/b$ (note that $0 < q < 1$), and, for $p = 0$,

$$\begin{pmatrix} 1/a - \hat{A}_0 \log(a) & -\hat{A}_0 \\ 1/b - \hat{B}_0 \log(b) & -\hat{B}_0 \end{pmatrix} \begin{pmatrix} c_0 \\ d_0 \end{pmatrix} = \begin{pmatrix} 0 \\ 0 \end{pmatrix}. \tag{B.10}$$

Once again, the uniqueness of solutions to this problem is determined by the vanishing of the determinant function

$$\Lambda_p(0, a, b, \hat{A}_p, \hat{B}_p) = \left(\frac{|p|}{a} + \hat{A}_p \right) \left(\frac{|p|}{b} - \hat{B}_p \right) - q^{2|p|} \left(\frac{|p|}{bq} - \hat{A}_p \right) \left(\frac{|p| q}{a} + \hat{B}_p \right), \tag{B.11}$$

for $p \neq 0$, and

$$\Lambda_0(0, a, b, \hat{A}_0, \hat{B}_0) = \frac{a\hat{A}_0 - b\hat{B}_0}{ab} + \hat{A}_0 \hat{B}_0 \log(q), \tag{B.12}$$

for $p = 0$. Again, we specify a δ–permissible configuration set

$$\mathcal{C}_\delta(0, a, b, A, B) := \left\{ (0, a, b, A, B) \mid \left| \Lambda_p(0, a, b, \hat{A}_p, \hat{B}_p) \right|^2 > \delta^2, \forall p \in \mathbf{Z} \right\}, \tag{B.13}$$

for some $\delta > 0$.

Remark B.2.1. Regarding the possibility of Λ_p being zero, general statements are more difficult to make. However, if we make the choice of Despres (39; 40), $\hat{A}_p = \hat{B}_p = i\eta$, then

$$\Lambda_p = \left(1 - q^{2|p|} \right) \left(|p|^2 + \eta^2 \right) + i\, |p|\, q^{2|p|} \eta\, (q - 1/q) = \mathcal{O}(p^2),$$

and both the real and imaginary parts of Λ_p are non–zero.

Appendix B (Continued)

B.3 Existence

We now establish existence and estimates for permissible configurations satisfying (Equation B.5) and (Equation B.13).

Theorem B.3.1. *If $F \in (H^1(\Omega_{a,b}))'$, $K \in H^{-1/2}(\Gamma_a)$, $L \in H^{-1/2}(\Gamma_b)$, the configurations satisfy*

$$\{k, a, b, A, B\} \in \mathcal{C}_\delta(k, a, b, A, B), \quad \{0, a, b, A, B\} \in \mathcal{C}_\delta(0, a, b, A, B)$$

for some $\delta > 0$, and the Fourier multiplier operators satisfy the conditions

$$\mathrm{Re}\left\{\hat{A}_p\right\} \geq 0, \quad \mathrm{Re}\left\{\hat{B}_p\right\} \leq 0, \quad \left|\mathrm{Im}\left\{\hat{A}_p\right\}\right| < \infty, \quad \left|\mathrm{Im}\left\{\hat{B}_p\right\}\right| < \infty, \qquad \text{(B.14)}$$

then there exists a unique solution of the Helmholtz problem, (Equation B.1), which satisfies the estimate

$$\|v\|_{H^1(\Omega_{a,b})} \leq C_e \left\{\|F\|_{(H^1(\Omega_{a,b}))'} + \|K\|_{H^{-1/2}(\Gamma_a)} + \|L\|_{H^{-1/2}(\Gamma_b)}\right\}, \qquad \text{(B.15)}$$

for some universal constant $C_e > 0$.

Appendix B (Continued)

Proof. To establish this result we write the solution $v = v_0 + v_1$ where the first function satisfies

(Equation B.1) with homogeneous boundary conditions and slightly modified inhomogeneity

$$\Delta v_0 + k^2 v_0 = G, \qquad \text{in } \Omega_{a,b}, \qquad\qquad \text{(B.16a)}$$

$$\partial_r v_0 - A v_0 = 0, \qquad \text{at } \Gamma_a, \qquad\qquad \text{(B.16b)}$$

$$\partial_r v_0 - B v_0 = 0, \qquad \text{at } \Gamma_b, \qquad\qquad \text{(B.16c)}$$

and the second resolves a harmonic equation with boundary conditions

$$\Delta v_1 = 0, \qquad \text{in } \Omega_{a,b}, \qquad\qquad \text{(B.17a)}$$

$$\partial_r v_1 - A v_1 = K, \qquad \text{at } \Gamma_a, \qquad\qquad \text{(B.17b)}$$

$$\partial_r v_1 - B v_1 = L, \qquad \text{at } \Gamma_b. \qquad\qquad \text{(B.17c)}$$

Since the configuration is in the set $\mathcal{C}_\delta(k, a, b, A, B)$, we will show in Theorem B.3.2 that

(Equation B.16) has a unique solution satisfying the estimate

$$\|v_0\|_{H^1(\Omega_{a,b})} \leq C_0 \|G\|_{(H^1(\Omega_{a,b}))'}, \qquad\qquad \text{(B.18)}$$

and, since the configuration is in the set $\mathcal{C}_\delta(0, a, b, A, B)$, we will show in Theorem B.3.3 that

(Equation B.17) has a unique solution such that

$$\|v_1\|_{H^1(\Omega_{a,b})} \leq C_1 \left\{ \|K\|_{H^{-1/2}(\Gamma_a)} + \|L\|_{H^{-1/2}(\Gamma_b)} \right\}. \qquad\qquad \text{(B.19)}$$

Appendix B (Continued)

Inserting $v = v_0 + v_1$ into (Equation B.1) we find that v_0 satisfies (Equation B.16) with $G = F - k^2 v_1$ so that

$$\|v\|_{H^1(\Omega_{a,b})} \leq \|v_0\|_{H^1(\Omega_{a,b})} + \|v_1\|_{H^1(\Omega_{a,b})}$$

$$\leq C_0 \left\|F - k^2 v_1\right\|_{(H^1(\Omega_{a,b}))'} + \|v_1\|_{H^1(\Omega_{a,b})}$$

$$\leq C_0 \left\{ \|F\|_{(H^1(\Omega_{a,b}))'} + k^2 \|v_1\|_{(H^1(\Omega_{a,b}))'} \right\} + \|v_1\|_{H^1(\Omega_{a,b})}$$

$$\leq C_0 \left\{ \|F\|_{(H^1(\Omega_{a,b}))'} + k^2 \|v_1\|_{H^1(\Omega_{a,b})} \right\} + \|v_1\|_{H^1(\Omega_{a,b})}$$

$$\leq C_0 \|F\|_{(H^1(\Omega_{a,b}))'} + (C_0 k^2 + 1) C_1 \left\{ \|K\|_{H^{-1/2}(\Gamma_a)} + \|L\|_{H^{-1/2}(\Gamma_b)} \right\},$$

and we are done provided

$$C_e = \max \left\{ 2C_0, 2C_1(C_0 k^2 + 1) \right\}.$$

$\square$

The next theorem states the estimate for v_0.

Theorem B.3.2. *If $G \in (H^1(\Omega_{a,b}))'$, the configuration $\{k, a, b, A, B\} \in \mathcal{C}_\delta$ for some $\delta > 0$, and the Fourier multiplier operators satisfy the conditions (Equation B.14), then there exists a unique solution of the Helmholtz problem, (Equation B.16), which satisfies the estimate (Equation B.18) for some universal constant $C_0 > 0$.*

Proof. We follow very closely the work of Harari and Hughes (55) and Demkowicz and Ihlenburg (56), which was later enhanced (44) for use on domains with perturbed interface shape. Here we modify this approach to address a related but significantly different problem.

Appendix B (Continued)

We define the zero–mode Fourier multiplier operators A_0 and B_0 by

$$A_0[\psi(\theta)] := \sum_{p=-\infty}^{\infty} \hat{A}_{0p} \hat{\psi}_p \varepsilon^{ip\theta} \delta_{p,0} = \hat{A}_0 \hat{\psi}_0, \quad B_0[\psi(\theta)] := \sum_{p=-\infty}^{\infty} \hat{B}_{0p} \hat{\psi}_p \varepsilon^{ip\theta} \delta_{p,0} = \hat{B}_0 \hat{\psi}_0.$$

It is easy to show that A_0 and B_0 each map L^2 to L^2. A weak formulation of (Equation B.16) is:

Find $v_0 \in H^1(\Omega_{a,b})$ such that $\mathcal{A}(v_0, \phi) + \mathcal{D}_1(v_0, \phi) + \mathcal{D}_2(v_0, \phi) = \mathcal{L}(\phi), \quad \forall \phi \in H^1(\Omega_{a,b}),$

where

$$\mathcal{A}(v, \phi) := \int_{\Omega_{a,b}} \nabla v \cdot \overline{\nabla \phi} \, dV + \int_{\Omega_{a,b}} v \overline{\phi} \, dV$$
$$+ \mathrm{Re}\left\{ \int_{\Gamma_a} ((A - A_0)v)\overline{\phi} \, ds \right\} - \mathrm{Re}\left\{ \int_{\Gamma_b} ((B - B_0)v)\overline{\phi} \, ds \right\},$$

$$\mathcal{D}_1(v, \phi) := -(k^2 + 1) \int_{\Omega_{a,b}} v \overline{\phi} \, dV,$$

$$\mathcal{D}_2(v, \phi) := \mathrm{Im}\left\{ \int_{\Gamma_a} ((A - A_0)v)\overline{\phi} \, ds \right\} - \mathrm{Im}\left\{ \int_{\Gamma_b} ((B - B_0)v)\overline{\phi} \, ds \right\}$$
$$+ \int_{\Gamma_a} (A_0 v)\overline{\phi} \, ds - \int_{\Gamma_b} (B_0 v)\overline{\phi} \, ds,$$

$$\mathcal{L}(\phi) := - \int_{\Omega_{a,b}} G \overline{\phi} \, dV.$$

Following (55; 56; 44) it is not difficult to show that $\mathcal{A}$ is a continuous, sesquilinear form from $H^1(\Omega_{a,b}) \times H^1(\Omega_{a,b})$ to $\mathbf{C}$ which induces a bounded operator $\mathbf{A} : H^1(\Omega_{a,b}) \to (H^1(\Omega_{a,b}))'$ (see

Appendix B (Continued)

Lemma 2.1.38 of (54)). The first two terms are "standard" while the latter two require that A

and B be at most order–one Fourier multipliers, e.g.,

$$\left| \text{Re} \left\{ \int_{\Gamma_a} A[v_{r=a}] \overline{\phi_{r=a}} \, ds \right\} \right| \leq |\langle A[v_{r=a}], \phi_{r=a} \rangle| \leq \|A[v_{r=a}]\|_{H^{-1/2}(\Gamma_a)} \|\phi_{r=a}\|_{H^{1/2}(\Gamma_a)},$$

which are bounded as $v, \phi \in H^1(\Omega_{a,b})$, the trace operator maps each to $H^{1/2}(\Gamma_a)$, and $A :$

$H^{1/2}(\Gamma_a) \rightarrow H^{-1/2}(\Gamma_a)$.

Furthermore, $\mathcal{A}$ is $H^1(\Omega_{a,b})$–elliptic (54), i.e., there is a $\gamma > 0$ such that

$$\text{Re} \left\{ \mathcal{A}(v,v) \right\} \geq \gamma \|v\|_{H^1(\Omega_{a,b})}^2.$$

The first two terms do not cause any problem as they are the $H^1(\Omega_{a,b})$–norm, however the

second two must be handled by estimates such as

$$\text{Re} \left\{ \int_{\Gamma_a} (A - A_0)[v_{r=a}] \overline{v_{r=a}} \, ds \right\} = \sum_{p=-\infty, p \neq 0}^{\infty} \text{Re} \left\{ \hat{A}_p \right\} |\hat{v}_p(a)|^2 \geq \sum_{p=-\infty, p \neq 0}^{\infty} |\hat{v}_p(a)|^2 \geq 0,$$

$$- \text{Re} \left\{ \int_{\Gamma_b} (B - B_0)[v_{r=a}] \overline{v_{r=b}} \, ds \right\} = \sum_{p=-\infty, p \neq 0}^{\infty} \text{Re} \left\{ -\hat{B}_p \right\} |\hat{v}_p(b)|^2 \geq \sum_{p=-\infty, p \neq 0}^{\infty} |\hat{v}_p(b)|^2 \geq 0.$$

By the Lax–Milgram Lemma (see Lemma 2.1.51 of (54)) the operator $\mathbf{A}$ satisfies

$$\left\| \mathbf{A}^{-1} \right\|_{H^1(\Omega_{a,b}) \leftarrow (H^1(\Omega_{a,b}))'} \leq \frac{1}{\gamma},$$

(see Theorem 2.1.44 of (54)).

Appendix B (Continued)

Again, as shown in (55; 56; 44) it is not hard to show that $\mathcal{D}_1$ is a continuous sesquilinear from $L^2(\Omega_{a,b}) \times L^2(\Omega_{a,b})$ to $\mathbf{C}$ which induces another bounded operator $\mathbf{D}_1 : L^2(\Omega_{a,b}) \rightarrow L^2(\Omega_{a,b})$. Since $H^1(\Omega_{a,b})$ embeds compactly into $L^2(\Omega_{a,b})$ we have that $\mathbf{D}_1$ is a compact operator.

It is a little more difficult to show that $\mathcal{D}_2$ is a continuous sesquilinear form from $L^2 \times L^2$ to $\mathbf{C}$. For instance, we calculate

$$\mathrm{Im}\left\{ \int_{\Gamma_a} (A - A_0)[v_{r=a}]\overline{\phi_{r=a}} \, ds \right\} = \sum_{p=-\infty, p \neq 0}^{\infty} \mathrm{Im}\left\{ \hat{A}_p \hat{v}_p(a)\overline{\hat{\phi}_p(a)} \right\},$$

which is bounded by the boundedness of $\mathrm{Im}\left\{ \hat{A}_p \right\}$ and the Cauchy–Schwartz inequality. In addition $A_0 : L^2(\Gamma_a) \rightarrow L^2(\Gamma_a)$ so

$$\int_{\Gamma_a} A_0[v_{r=a}]\overline{\phi_{r=a}} \, ds \leq \|A_0[v_{r=a}]\|_{L^2(\Gamma_a)} \|\phi_{r=a}\|_{L^2(\Gamma_a)}.$$

So since $H^{1/2}(\Gamma_a)$ embeds compactly into $L^2(\Gamma_a)$, with a similar result for B, we have that the induced operator $\mathbf{D}_2$ is a compact operator.

Thus, the governing equations can be written as

$$(\mathbf{A} + \mathbf{D}_1 + \mathbf{D}_2)v_0 = G \quad \implies \quad (I + \mathbf{A}^{-1}(\mathbf{D}_1 + \mathbf{D}_2))v_0 = \mathbf{A}^{-1}G,$$

Appendix B (Continued)

where $\mathbf{A}^{-1}(\mathbf{D}_1 + \mathbf{D}_2)$ is a compact map from $H^1(\Omega_{a,b})$ to $H^1(\Omega_{a,b})$. Thus, by Fredholm's theory (55; 56; 44), provided the null space of $(\mathbf{A} + \mathbf{D}_1 + \mathbf{D}_2)$ is trivial (which we are guaranteed by our choice of configuration), there exists a (unique) solution satisfying

$$\|v_0\|_{H^1(\Omega_{a,b})} \leq \left\|(I + \mathbf{A}^{-1}(\mathbf{D}_1 + \mathbf{D}_2))\mathbf{A}^{-1}G\right\|_{H^1(\Omega_{a,b})}$$

$$\leq \left\|I + \mathbf{A}^{-1}(\mathbf{D}_1 + \mathbf{D}_2)\right\|_{H^1(\Omega_{a,b}) \leftarrow H^1(\Omega_{a,b})} \left\|\mathbf{A}^{-1}\right\|_{H^1(\Omega_{a,b}) \leftarrow (H^1(\Omega_{a,b}))'} \|G\|_{(H^1(\Omega_{a,b}))'},$$

and we are done. $\qquad\qquad\square$

The last theorem states the estimate for v_1.

Theorem B.3.3. *If $K \in H^{-1/2}(\Gamma_a)$, $L \in H^{-1/2}(\Gamma_b)$, the configuration $\{k = 0, a, b, A, B\} \in \mathcal{C}_\delta$ for some $\delta > 0$, then there exists a harmonic function satisfying* (Equation B.17) *which verifies the estimate* (Equation B.19).

Proof. The solution of (Equation B.17a) is given by (Equation B.7) with r–derivative specified in (Equation B.8). To satisify the boundary conditions we use the Fourier series representations

$$K(\theta) = \sum_{p=-\infty}^{\infty} \hat{K}_p e^{ip\theta}, \quad L(\theta) = \sum_{p=-\infty}^{\infty} \hat{L}_p e^{ip\theta},$$

Appendix B (Continued)

and generate (Equation B.9) and (Equation B.10) with right–hand–side $(\hat{K}_p, \hat{L}_p)^T$. More specifically, for $p \neq 0$,

$$
\begin{pmatrix} q^{|p|} \left(|p|/(bq) - \hat{A}_p \right) & \left(-|p|/a - \hat{A}_p \right) \\ \left(|p|/b - \hat{B}_p \right) & q^{|p|} \left(-(|p|\,q)/a - \hat{B}_p \right) \end{pmatrix} \begin{pmatrix} c_p \\ d_p \end{pmatrix} = \begin{pmatrix} \hat{K}_p \\ \hat{L}_p \end{pmatrix},
$$

and, for $p = 0$,

$$
\begin{pmatrix} 1/a - \hat{A}_0 \log(a) & -\hat{A}_0 \\ 1/b - \hat{B}_0 \log(b) & -\hat{B}_0 \end{pmatrix} \begin{pmatrix} c_0 \\ d_0 \end{pmatrix} = \begin{pmatrix} \hat{K}_0 \\ \hat{L}_0 \end{pmatrix}.
$$

Using the definition of the determinant function, (Equation B.11), for $p \neq 0$, and, (Equation B.12), we can write the solution as

$$
\begin{pmatrix} c_p \\ d_p \end{pmatrix} = \frac{1}{\Lambda_p} \left\{ \begin{pmatrix} \left(|p|/a + \hat{A}_p \right) \hat{L}_p \\ \left(-|p|/b + \hat{B}_p \right) \hat{K}_p \end{pmatrix} + q^{|p|} \begin{pmatrix} \left(-(|p|\,q)/a - \hat{B}_p \right) \hat{K}_p \\ \left(|p|/(bq) - \hat{A}_p \right) \hat{L}_p \end{pmatrix} \right\},
$$

for $p \neq 0$, and

$$
\begin{pmatrix} c_0 \\ d_0 \end{pmatrix} = \frac{1}{\Lambda_0} \begin{pmatrix} -\hat{B}_0 \hat{K}_0 + \hat{A}_0 \hat{L}_0 \\ \left(-1/b + \hat{B}_0 \log(b) \right) \hat{K}_0 + \left(1/a - \hat{A}_0 \log(a) \right) \hat{L}_0 \end{pmatrix}.
$$

Appendix B (Continued)

We have already assumed that we are in a δ–permissible configuration so we know that $\Lambda_p > \delta$ and all of these solutions are well–defined. To investigate the regularity results which we claim, we must study the asmptotics of (Equation B.11). As $0 < q < 1$ we can see that

$$\Lambda_p(0, a, b, \hat{A}_p, \hat{B}_p) \sim \left(\frac{|p|}{a} + \hat{A}_p \right) \left(\frac{|p|}{b} - \hat{B}_p \right),$$

and since A and B are at most order–one Fourier multipliers, i.e., there exist $\tilde{C}_A > 0$ and $\tilde{C}_B > 0$ such that

$$\left| \hat{A}_p \right| < \tilde{C}_A \langle p \rangle, \quad \left| \hat{B}_p \right| < \tilde{C}_B \langle p \rangle,$$

it is clear that there is a constant $\tilde{C}_\Lambda > 0$, such that

$$\frac{1}{\tilde{C}_\Lambda} < \frac{|\Lambda_p|}{\langle p \rangle^2} < \tilde{C}_\Lambda.$$

Thus, we find, as $p \to \infty$,

$$c_p \sim \left(\frac{|p|/a + \hat{A}_p}{\Lambda_p} \right) \hat{K}_p, \quad d_p \sim \left(\frac{-|p|/b + \hat{B}_p}{\Lambda_p} \right) \hat{L}_p,$$

so that

$$|c_p|^2 \le C_c \langle p \rangle^{-2} \left| \hat{K}_p \right|^2, \quad |d_p|^2 \le C_d \langle p \rangle^{-2} \left| \hat{L}_p \right|^2,$$

for constants $C_c, C_d > 0$.

Appendix B (Continued)

Regarding the $H^1(\Omega_{a,b})$ norm of v_1 we note that, from Parseval's relation,

$$\|v_1\|^2_{H^1(\Omega_{a,b})} = \sum_{p=-\infty}^{\infty} \langle p \rangle^2 \left\| \widehat{(v_1)}_p \right\|^2_{L^2(dr)} + \left\| \partial_r \widehat{(v_1)}_p \right\|^2_{L^2(dr)} .$$

From (Equation B.7) we have

$$\left\| \widehat{(v_1)}_p \right\|^2_{L^2(dr)} \leq |c_p|^2 \left\| \left(\frac{r}{b}\right)^{|p|} \right\|^2_{L^2(dr)} + |d_p|^2 \left\| \left(\frac{r}{a}\right)^{-|p|} \right\|^2_{L^2(dr)},$$

and from (Equation B.8)

$$\left\| \partial_r \widehat{(v_1)}_p \right\|^2_{L^2(dr)} \leq |p|^2 \left|\frac{c_p}{b}\right|^2 \left\| \left(\frac{r}{b}\right)^{|p|-1} \right\|^2_{L^2(dr)} + |p|^2 \left|\frac{d_p}{a}\right|^2 \left\| \left(\frac{r}{a}\right)^{-|p|-1} \right\|^2_{L^2(dr)} .$$

For $p \neq -1$ it is an elementary Calculus exercise to deduce that

$$\|r^p\|^2_{L^2(dr)} = \int_a^b r^{2p+1} \, dr = \frac{b^{2p+2} - a^{2p+2}}{2p+2} < C\langle p \rangle^{-1},$$

while $\left\| r^{-1} \right\|_{L^2(dr)} = \log(b/a) < \infty$. With this it is not difficult to show that

$$\|v_1\|^2_{H^1(\Omega_{a,b})} \leq C_0 \sum_{p=-\infty}^{\infty} \langle p \rangle^2 \langle p \rangle^{-1} \left(|c_p|^2 + |d_p|^2 \right) + C_1 \sum_{p=-\infty}^{\infty} \langle p \rangle^{-1} |p|^2 \left(|c_p|^2 + |d_p|^2 \right)$$

$$\leq C \sum_{p=-\infty}^{\infty} \langle p \rangle^1 \langle p \rangle^{-2} \left(\left|\hat{K}_p\right|^2 + \left|\hat{L}_p\right|^2 \right) \leq C \left\{ \|K\|_{H^{-1/2}} + \|L\|_{H^{-1/2}} \right\},$$

and we are done. $\qquad\qquad\qquad\square$

Appendix C

PERMISSIONS FOR THE INCLUSION OF PUBLISHED WORKS

The boundary formulation via Dirichlet–Neumann Operator, and its related algorithms and numerical experiments, were previously published by Springer, which allows authors to use their articles in their thesis. Their policy states "Authors have the right to reuse their articles Version of Record, in whole or in part, in their own thesis." and is available at https://www.springer.com/gp/rights-permissions/obtaining-permissions/882.

CITED LITERATURE

1. Raether, H.: <u>Surface plasmons on smooth and rough surfaces and on gratings</u>. Berlin, Springer, 1988.

2. Maier, S. A.: <u>Plasmonics: Fundamentals and Applications</u>. New York, Springer, 2007.

3. Novotny, L. and Hecht, B.: <u>Principles of Nano–Optics</u>. Cambridge, Cambridge University Press, second edition, 2012.

4. Enoch, S. and Bonod, N.: <u>Plasmonics: From Basics to Advanced Topics</u>. Springer Series in Optical Sciences. New York, Springer, 2012.

5. Xu, H., Bjerneld, E., Käll, M., and Börjesson, L.: Spectroscopy of single hemoglobin molecules by surface enhanced raman scattering. <u>Phys. Rev. Lett.</u>, 83:4357–4360, 1999.

6. Loo, C., Lowery, A., Halas, N., West, J., and Drezek, R.: Immunotargeted nanoshells for integrated cancer imaging and therapy. <u>Nano Letters</u>, 5(4):709–711, 2005.

7. El-Sayed, I., Huang, X., and El-Sayed, M.: Selective laser photo-thermal therapy of epithelial carcinoma using anti-egfr antibody conjugated gold nanoparticles. <u>Cancer Lett.</u>, 239(1):129–135, 2006.

8. Strikwerda, J. C.: <u>Finite difference schemes and partial differential equations</u>. Society for Industrial and Applied Mathematics (SIAM), Philadelphia, PA, second edition, 2004.

9. LeVeque, R. J.: <u>Finite difference methods for ordinary and partial differential equations</u>. Society for Industrial and Applied Mathematics (SIAM), Philadelphia, PA, 2007. Steady-state and time-dependent problems.

10. Johnson, C.: <u>Numerical solution of partial differential equations by the finite element method</u>. Cambridge, Cambridge University Press, 1987.

11. Ihlenburg, F.: <u>Finite element analysis of acoustic scattering</u>. New York, Springer-Verlag, 1998.

12. Hesthaven, J. S. and Warburton, T.: Nodal discontinuous Galerkin methods, volume 54 of Texts in Applied Mathematics. New York, Springer, 2008. Algorithms, analysis, and applications.

13. Deville, M. O., Fischer, P. F., and Mund, E. H.: High-order methods for incompressible fluid flow, volume 9 of Cambridge Monographs on Applied and Computational Mathematics. Cambridge, Cambridge University Press, 2002.

14. Gottlieb, D. and Orszag, S. A.: Numerical analysis of spectral methods: theory and applications. Philadelphia, Pa., Society for Industrial and Applied Mathematics, 1977. CBMS-NSF Regional Conference Series in Applied Mathematics, No. 26.

15. Canuto, C., Hussaini, M. Y., Quarteroni, A., and Zang, T. A.: Spectral methods in fluid dynamics. New York, Springer-Verlag, 1988.

16. Boyd, J. P.: Chebyshev and Fourier spectral methods. Mineola, NY, Dover Publications Inc., second edition, 2001.

17. Nicholls, D. P.: A method of field expansions for vector electromagnetic scattering by layered periodic crossed gratings. Journal of the Optical Society of America, A, 32(5):701–709, 2015.

18. Nicholls, D. P., Oh, S.-H., Johnson, T. W., and Reitich, F.: Launching surface plasmon waves via vanishingly small periodic gratings. Journal of Optical Society of America, A, 33(3):276–285, 2016.

19. Colton, D. and Kress, R.: Inverse acoustic and electromagnetic scattering theory. Berlin, Springer-Verlag, second edition, 1998.

20. Rayleigh, L.: On the dynamical theory of gratings. Proc. Roy. Soc. London, A79:399–416, 1907.

21. Rice, S. O.: Reflection of electromagnetic waves from slightly rough surfaces. Comm. Pure Appl. Math., 4:351–378, 1951.

22. Bruno, O. and Reitich, F.: Numerical solution of diffraction problems: A method of variation of boundaries. J. Opt. Soc. Am. A, 10(6):1168–1175, 1993.

23. Bruno, O. and Reitich, F.: Numerical solution of diffraction problems: A method of variation of boundaries. II. Finitely conducting gratings, Padé approximants, and singularities. J. Opt. Soc. Am. A, 10(11):2307–2316, 1993.

24. Bruno, O. and Reitich, F.: Numerical solution of diffraction problems: A method of variation of boundaries. III. Doubly periodic gratings. J. Opt. Soc. Am. A, 10(12):2551–2562, 1993.

25. Bruno, O. P. and Reitich, F.: Boundary–variation solutions for bounded–obstacle scattering problems in three dimensions. J. Acoust. Soc. Am., 104(5):2579–2583, 1998.

26. Nicholls, D. P. and Reitich, F.: Shape deformations in rough surface scattering: Cancellations, conditioning, and convergence. J. Opt. Soc. Am. A, 21(4):590–605, 2004.

27. Nicholls, D. P. and Reitich, F.: Shape deformations in rough surface scattering: Improved algorithms. J. Opt. Soc. Am. A, 21(4):606–621, 2004.

28. Nicholls, D. P. and Nigam, N.: Exact non-reflecting boundary conditions on general domains. J. Comput. Phys., 194(1):278–303, 2004.

29. Nicholls, D. P.: Three–dimensional acoustic scattering by layered media: A novel surface formulation with operator expansions implementation. Proceedings of the Royal Society of London, A, 468:731–758, 2012.

30. Nicholls, D. P. and Shen, J.: A stable, high–order method for two–dimensional bounded–obstacle scattering. SIAM J. Sci. Comput., 28(4):1398–1419, 2006.

31. Gillman, A., Barnett, A., and Martinsson, P.: A spectrally accurate direct solution technique for frequency-domain scattering problems with variable media. BIT Numer. Math., 55(1):141–170, 2015.

32. Nicholls, D. P. and Tammali, V.: A high–order perturbation of surfaces (hops) approach to Fokas integral equations: Vector electromagnetic scattering by periodic crossed gratings. Applied Numerical Methods, 101:1–17, 2016.

33. Petit, R.: Electromagnetic theory of gratings. Berlin, Springer-Verlag, 1980.

34. Nicholls, D. P.: Stable, high-order computation of impedance–impedance operators for three-dimensional layered medium simulations. Proceedings of the Royal Society of London A: Mathematical, Physical and Engineering Sciences, 474(2212), 2018.

35. Prez-Arancibia, C., Shipman, S., Turc, C., and Venakides, S.: Domain decomposition for quasi-periodic scattering by layered media via robust boundary-integral equations at all frequencies. Communications in Computational Physics, 26:265–310, 02 2019.

36. Nicholls, D. P.: On analyticity of linear waves scattered by a layered medium. Journal of Differential Equations, 263(8):5042–5089, 2017.

37. Nicholls, D. P. and Tong, X.: High-order perturbation of surfaces algorithms for the simulation of localized surface plasmon resonances in two dimensions. J. Sci. Comput., Feb 2018.

38. Evans, L. C.: Partial differential equations. Providence, RI, American Mathematical Society, second edition, 2010.

39. Després, B.: Méthodes de décomposition de domaine pour les problèmes de propagation d'ondes en régime harmonique. Le théorème de Borg pour l'équation de Hill vectorielle. Institut National de Recherche en Informatique et en Automatique (INRIA), Rocquencourt, 1991. Thèse, Université de Paris IX (Dauphine), Paris, 1991.

40. Després, B.: Domain decomposition method and the Helmholtz problem. In Mathematical and numerical aspects of wave propagation phenomena (Strasbourg, 1991), pages 44–52. SIAM, Philadelphia, PA, 1991.

41. Colton, D. and Kress, R.: Inverse acoustic and electromagnetic scattering theory, volume 93 of Applied Mathematical Sciences. Springer, New York, third edition, 2013.

42. Kress, R.: Linear integral equations. New York, Springer-Verlag, third edition, 2014.

43. Folland, G. B.: Introduction to partial differential equations. Princeton, N.J., Princeton University Press, 1976. Preliminary informal notes of university courses and seminars in mathematics, Mathematical Notes.

44. Nicholls, D. P. and Nigam, N.: Error analysis of an enhanced DtN–fe method for exterior scattering problems. Numer. Math., 105(2):267–298, 2006.

45. Nicholls, D. P. and Reitich, F.: A new approach to analyticity of Dirichlet-Neumann operators. Proc. Roy. Soc. Edinburgh Sect. A, 131(6):1411–1433, 2001.

46. Nicholls, D. P. and Reitich, F.: Stability of high-order perturbative methods for the computation of Dirichlet-Neumann operators. J. Comput. Phys., 170(1):276–298, 2001.

47. Nicholls, D. P. and Reitich, F.: Analytic continuation of Dirichlet-Neumann operators. Numer. Math., 94(1):107–146, 2003.

48. NIST Digital Library of Mathematical Functions. http://dlmf.nist.gov/, Release 1.0.22 of 2019-03-15. F. W. J. Olver, A. B. Olde Daalhuis, D. W. Lozier, B. I. Schneider, R. F. Boisvert, C. W. Clark, B. R. Miller and B. V. Saunders, eds.

49. Shen, J. and Wang, L.-L.: Analysis of a spectral-Galerkin approximation to the Helmholtz equation in exterior domains. SIAM J. Numer. Anal., 45(5):1954–1978, 2007.

50. Baker, Jr., G. A. and Graves-Morris, P.: Padé approximants. Cambridge, Cambridge University Press, second edition, 1996.

51. Burggraf, O. R.: Analytical and numerical studies of the structure of steady separated flows. J. Fluid Mech., 24:113–151, 1966.

52. Roache, P. J.: Code verification by the method of manufactured solutions. J. Fluids Eng., 124(1):4–10, 2002.

53. Roy, C. J.: Review of code and solution verification procedures for computational simulation. J. Comp. Phys., 205(1):131–156, 2005.

54. Sauter, S. A. and Schwab, C.: Boundary element methods, volume 39 of Springer Series in Computational Mathematics. Springer-Verlag, Berlin, 2011. Translated and expanded from the 2004 German original.

55. Harari, I. and Hughes, T. J. R.: Analysis of continuous formulations underlying the computation of time-harmonic acoustics in exterior domains. Comput. Methods Appl. Mech. Engrg., 97(1):103–124, 1992.

56. Demkowicz, L. and Ihlenburg, F.: Analysis of a coupled finite-infinite element method for exterior Helmholtz problems. Numer. Math., 88(1):43–73, 2001.

57. Nicholls, D. P. and Shen, J.: A stable high-order method for two-dimensional bounded-obstacle scattering. SIAM Journal Scientific Computing, 28:1398–1419, 2006.

58. Billingham, J. and King, A.: Wave Motion. Cambridge Texts in Applied Mathematics. Cambridge University Press, 2000.

59. Shen, J., Tang, T., and Wang, L.: Spectral Methods: Algorithms, Analysis and Applications. Springer Series in Computational Mathematics. Springer Berlin Heidelberg, 2011.

60. Trefethen, L. N.: Spectral methods in MATLAB, volume 10 of Software, Environments, and Tools. Society for Industrial and Applied Mathematics (SIAM), Philadelphia, PA, 2000.

VITA

Xin Tong

☎ *312-613-0664*
✉ *xtong20@uic.edu*
🖰 *homepages.math.uic.edu/~xtong20/*

Education

- **Ph.D. in Mathematics**, *University of Illinois at Chicago (UIC)*
  - Advisor: David Nicholls
  - Research topic: Numerical Analysis on Differential Equations, Spectral Methods
  - Dissertation: Simulation of Localized Surface Plasmon Resonances
- **M.S. in Applied Mathematics**, *Illinois Institute of Technology (IIT)*, August 2014
  - Advisor: Fred Hickernell and Co-Advisor: Sou-Cheng Terrya Choi
  - Thesis: A Guaranteed, Adaptive, Automatic Algorithm for Univariate Function Minimization
- **B.S. in Mathematics and Applied Mathematics**, *Central University of Finance and Economics (CUFE)*, China, July 2011
  - Minor: Bachelor of Economics in Finance

Publications and Papers

- D. P. Nicholls and X. Tong, *High-Order Perturbation of Surfaces Algorithms for the Simulation of Localized Surface Plasmon Resonances in Graphene Nanotubes* (2020), Under review.
- D. P. Nicholls and X. Tong, *Simulation of Localized Surface Plasmon Resonances in Two Dimensions via Impedance–Impedance Operators* (2019), Under review.
- D. P. Nicholls and X. Tong, *High–Order Perturbation of Surfaces Algorithms for the Simulation of Localized Surface Plasmon Resonances in Two Dimensions*, Volume 76, Issue 3, 1370-1395 (2018), Journal of Scientific Computing.
- S-C. T. Choi, Y. Ding, F. J. Hickernell, X. Tong, *Local Adaption for Approximation and Minimization of Univariate Functions*, Volume 40, June 2017, Pages 17-33, Journal of Complexity.
- S-C. T. Choi, Y. Ding, F. J. Hickernell, L. Jiang, Ll. A. Jiménez Rugama, X. Tong, Y. Zhang, X. Zhou, *GAIL: Guaranteed Automatic Integration Library (versions 1.0-2.3)*, MATLAB software, 2013–2019.

Research Experience

- **High–Order Perturbation of Surface (HOPS) Project**, *PhD research*
  - Established High-Order Perturbation of Surfaces Algorithms for the simulation of Localized Surface Plasmon Resonances of Nonarods and Graphene Ribbons
  - Analyzed the existence and uniqueness using elliptic estimates
  - Designed the numerical experiments and implemented using programming softwares
- **Guaranteed Automatic Integration Library (GAIL)**, *Ongoing*
  - Constructed a guaranteed, adaptive automatic algorithm (MIN) of univariate function minimization
  - Created funmin_g for MIN and polished it as a function in the software package GAIL v2.0-2.3
  - Documentation lead: maintained the architecture, API, and produced HTML files of demos and help-pages, `http://gailgithub.github.io/GAIL_Dev/`
- **Machine Learning Project**, *2017-2018*
  - Used the FashionMNIST dataset for image classification on PyTorch
  - Applied CNN model, with different optimizers, activation functions, and adding regularization
- **Supercomputing Project**, *2016*
  - Implemented HOPS algorithm for Bounded–Obstacle Scattering problem using MPI and OpenMP
  - Provided a 1.7 speedup over the Serial processing
- **Beijing Scientific Research Projects of University Students**, *2008–2010*
  - Project *Research on blood collection and storage of Beijing and draw up a contingency plan*
  - Granted 10,000RMB (about 1,500 USD) research funding by the Ministry of Education of Beijing

Presentations

- *A Brief Introduction to GAIL (Guaranteed Automatic Integration Library) Version 2.3*, Practice and Experience in Advanced Research Computing (PEARC19), Chicago, IL, July 2019.

- *Simulation of Localized Surface Plasmon Resonances via Dirichlet–Neumann Operators and Impedance–Impedance Operators*, The Mathematics of Finite Elements and Applications 2019 (MAFE-LAP 2019), London, UK, June 2019.

- *A Non-Overlapping Domain Decomposition Method for Simulating Localized Surface Plasmon Resonances: High Accuracy Numerical Simulation*, SIAM Conference on Computational Science and Engineering (CSE19), Spokane, Washington, March 2019.

- *High-order Perturbation of Surfaces Algorithms for the Simulation of Localized Surface Plasmon Resonances*, 2018 Society for Industrial and Applied Mathematics (SIAM) Annual Meeting (AN18), Portland, Oregon, July 2018.

- *A Locally Adaptive Algorithm for Global Minimization of Univariate Functions*, 2018 SIAM Annual Meeting (AN18), Portland, Oregon, July 2018.

- *High-Order Perturbation of Surfaces Algorithms for the Simulation of localized Surface Plasmon Resonances*, Chicago Area SIAM Student Conference (CASSC) 2018, Illinois Institute of Technology, April 2018.

- *High-Order Perturbation of Surfaces Method for Bounded-Obstacle Scattering in Polar Coordinates*, Hybrid Numerical Methods Meeting, Lawrence Berkeley National Laboratory, June 2016.

- *A Guaranteed, Adaptive, Automatic Algorithm for Univariate Function Minimization*, ACNW Optimization Workshop, Northwestern University, June 2015.

Advanced Academic Background

- Harmonic Analysis, Linear and Nonlinear Waves, Finite Element Method, Supercomputing/Parallel Computing, Probability, Applied Statistics, Stochastic Analysis, Computational Finance, Econometric

Additional Experience

- **Teaching Assistant**, *UIC*, 2014–2019
  - Led discussion sessions on Pre-calculus, Calculus and Introduction to Differential Equations
  - Lecturer of Introduction to Differential Equations in Summer 2016
  - Instructor of Summer Enrichment Math Workshop in Summer 2018
  - Instructor of UIC Global students workshops in Summer 2019
- **Treasurer of SIAM Student Chapter**, *UIC*, 2016-2017
  - Recorded the expense and applied the annual Fundding
  - Organizer in CASSC (Chicago Area SIAM Student Conference) 2017
  - Student Representitive of the UIC Chapter in SIAM Annual Metting 2018
- **Manager of Weekly Problem Team**, *IIT*, 2013–2014
  - Graded answers and uploaded the problems and contest results every week

Awards and Honors

- Student Presenters Award, UIC, Oct 2018, Oct 2016
- SIAM Student Travel Award, SIAM, Sept 2018, March 2018
- 2018 Victor Twersky Memorial Scholarship, UIC, April 2018
- Excellent Graduate of Beijing, CUFE, China, June 2011
- National Scholarship, CUFE, China, Nov 2010

Skills

- Scientific computing: Matlab, Maple, Mathematica
- Programming: C/C++, Python
- Machine learning: SVM, Neural Networks/CNN, Clustering
- Additional: GitHub, Parallel Computing